

AD-A136 219

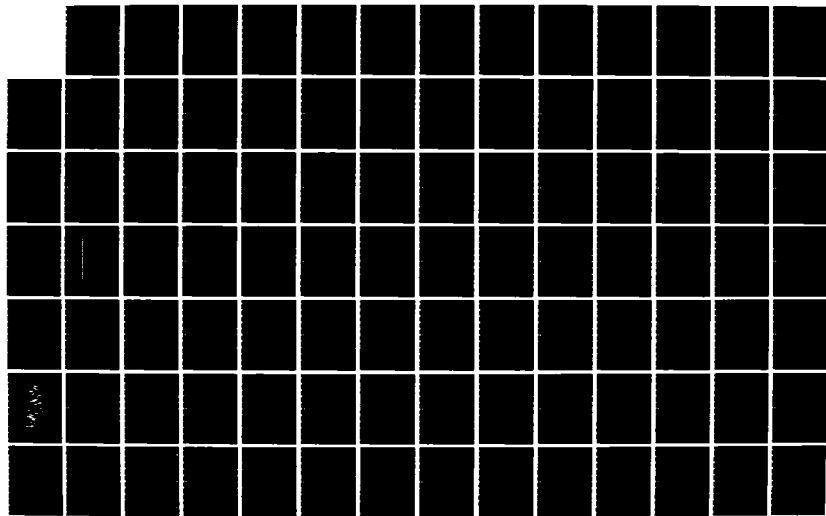
TARGET TRACK AND STABILIZATION FOR MANPORTABLE DIRECT  
FIRE MISSILES(U) MCDONNELL DOUGLAS ASTRONAUTICS CO-HB  
HUNTINGTON BEACH CA F GENTILE ET AL. NOV 81 MDC-69941  
DAAH01-80-C-1618

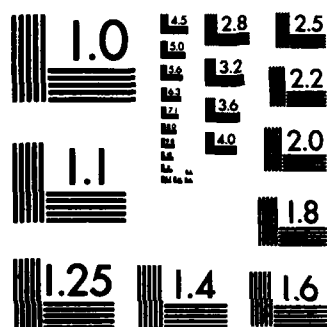
1/2

UNCLASSIFIED

F/G 17/5

NL





MICROCOPY RESOLUTION TEST CHART  
NATIONAL BUREAU OF STANDARDS-1963-A

MDC G9941

219

## FINAL REPORT - VOLUME 1

AD-A136

### Target Track and Stabilization for Manportable Direct Fire Missiles

McDonnell Douglas Astronautics Company  
5301 Bolsa Avenue  
Huntington Beach, CA 92647

November 1981

Prepared for  
U.S. ARMY MISSILE R&D COMMAND  
Redstone Arsenal, AL 35809

DTIC FILE COPY

DISPATCHED TO DTIC
Approved for release by
Distribution Statement

DTIC  
ELECTE  
DEC 22 1983  
D

UNCLASSIFIED

SECURITY CLASSIFICATION OF THIS PAGE (When Data Entered)

REPORT DOCUMENTATION PAGE		READ INSTRUCTIONS BEFORE COMPLETING FORM
1. REPORT NUMBER MDC G9941	2. GOVT ACCESSION NO.	3. RECIPIENT'S CATALOG NUMBER
4. TITLE (and Subtitle) Final Report, Vol. I Target Track and Stabilization for Manportable Direct Fire Missiles		5. TYPE OF REPORT & PERIOD COVERED Final Technical 9/30/80 to 11/30/81
7. AUTHOR(s) F. Gentile G. Tutt		6. PERFORMING ORG. REPORT NUMBER MDC G9941
9. PERFORMING ORGANIZATION NAME AND ADDRESS MDAC-Huntington Beach 5301 Bolsa Avenue Huntington Beach, California 92647		8. CONTRACT OR GRANT NUMBER(s) DAAH01-80-C-1618
11. CONTROLLING OFFICE NAME AND ADDRESS Headquarters U.S. Army Missile R&D Command Redstone Arsenal, Alabama 35809		10. PROGRAM ELEMENT, PROJECT, TASK AREA & WORK UNIT NUMBERS CLIN 0002
14. MONITORING AGENCY NAME & ADDRESS (if different from Controlling Office) DCASPRO-MDAC Huntington Beach 5301 Bolsa Avenue Huntington Beach, California 92647		12. REPORT DATE November, 1981
		13. NUMBER OF PAGES 170
		15. SECURITY CLASS. (of this report) Unclassified
16. DISTRIBUTION STATEMENT (of this Report)		15a. DECLASSIFICATION DOWNGRADING SCHEDULE
<div style="border: 1px solid black; padding: 5px; text-align: center;">             DISTRIBUTION STATEMENT A              Approved for public release;              Distribution Unlimited           </div>		
17. DISTRIBUTION STATEMENT (of the abstract entered in Block 20, if different from Report)		
18. SUPPLEMENTARY NOTES		
19. KEY WORDS (Continue on reverse side if necessary and identify by block number)		
Guidance                      Beam-rider Tracking                      Infantry Stabilization                  Image Processing Anti-Armor		
20. ABSTRACT (Continue on reverse side if necessary and identify by block number)		
Tradeoff analyses were conducted to select an optimum method for tracking armored vehicles and stabilizing a laser beam for beamrider missile guidance, for a manportable infantry weapon. The optimum approach was found to be a two-axis gimbal-mounted infrared sensor and laser projector, with IR image autotrack and gyro stabilization. A breadboard example was built and tested, demonstrating the practicality and indicating expected performance of the recommended method.		

## CONTENTS

Section I	INTRODUCTION	1
Section II	PHASE I, TRADEOFF STUDY	3
	1. Introduction	3
	2. Summary	3
	3. Initial Screening	6
	4. Evaluation of Candidates	16
	5. Evaluation Summary	91
Section III	PHASE II, TEST PROGRAM	97
	1. Introduction and Summary	97
	2. Test Objectives	99
	3. Test Article Description	100
	4. Test Equipment Description	118
	5. Table Mounted Tests	125
	6. Shoulder Mounted Tests	152
	7. Results and Conclusions	159
Section IV	RECOMMENDATIONS	161
Appendix	BIBLIOGRAPHY	163

Accession For		
NTIS GRA&I	<input checked="" type="checkbox"/>	
DTIC TAB	<input type="checkbox"/>	
Unannounced	<input type="checkbox"/>	
Justification		
By <i>Tex Ltr. on File</i>		
Distribution/		
Availability Codes		
Dist	Avail and/or	Special
<i>A/1</i>		

RE: Classified References, Distribution  
 Unlimited  
 No change in distribution statement per Mr.  
 W. E. Miller, Army Missile Comd, Advanced  
 Sensors Directorate

## SECTION I

### Introduction

This document comprises the final report in accordance with CLIN 0002 of MICOM Labs Contract DAAH01-80-C-1618. The report is bound in two volumes: Volume I covers Phase I (CLIN 0001) and that part of Phase II (CLIN 0003) which was contained in the original contract dated 30 September 1980. Volume II covers that part of Phase II which was added on 15 September 1981 (sometimes called "Task 3"), which involved image processing of missile flight and target imagery from a live TOW missile firing. The scope of this study was governed by Technical Requirement No. R-0034 (statement of work) contained in the Contract and by the funding and schedule limitations of that contract. Section 1.0 (Scope) of R-0034 is as follows:

#### 1.1 Objective

The purpose of this effort is to conduct the various tradeoff analyses and evaluations necessary to provide an optimum solution(s) to the problems of stabilizing and/or tracking targets for manportable, direct fire guided missiles. The effort will consist of technology survey, evaluation, ranking, and critical component test validation. The missile application toward which this effort is directed, is a future infantry anti-tank/assault guided missile.

#### 1.2 Requirements Description

1.2.1 During Phase I, the contractor shall collect technology status data, perform analytical tradeoff studies, evaluate alternatives, and establish a matrix of technical alternatives. This matrix will provide the government with the contractor's estimate of performance (range, accuracy, countermeasures hardness), size, weight, development costs and unit production costs.

1.2.2 During Phase I, the contractor shall furnish (a) the tradeoff matrix, with supporting rationale, and (b) a test plan for an economical series of experiments to implement and conduct initial evaluation of

critical components using breadboard hardware.

1.2.3 During Phase II, the contractor shall conduct these critical component evaluation tests after Army approval of the test plan.

In accordance with these objectives and requirements, a tradeoff study was performed, a recommended configuration selected, and a brassboard tracker system designed and built. The system was then tested in the laboratory and in the field.

The engineering effort funded by the contract for Phase I was based on 404 man hours. The performance period of Phase I was from award (30 September 1980) to 30 November 1980. Phase II funding was based on 2359 man hours for the original scope, and 589 additional hours for the image processing task. The performance period of Phase II was from 7 January 1981 to 30 November 1981.

Section II  
PHASE I - TRADEOFF STUDY

1. Introduction

Experience has shown that gunner aiming error and tracking jitter are the limiting factors in the accuracy of manportable direct fire guided missiles. To improve the performance of such weapons it is necessary to aid the gunner in target tracking and stabilization so that an accurate line-of-sight can be provided to the missile guidance system. Phase I of this study was performed to define the best technical approach to the tracking and stabilization problem.

The study consisted of four principal tasks:

1. Concept definition
2. Prescreening
3. Final evaluation & selection
4. Phase II Test Plan development

2. Summary


Thirty-one alternative approaches were defined for Task 1. These approaches consisted of various combinations of scene stabilization, target tracking and line-of-sight stabilization methods ranging from a totally unaided and completely manual system to fully automated and totally independent target tracking and line-of-sight stabilization systems using mechanical, optical and electro-optical techniques.



The prescreening process was a qualitative evaluation of the 31 candidates based upon engineering judgement and past experience with similar systems. The 4 most promising candidates were selected for a more detailed and quantitative evaluation. The four candidates selected for final evaluation were:

- A. DUAL GIMBAL - Independently gimballed IR sensor and Laser Projector.
- B. COMMON GIMBAL - Sensor and projector mounted on a common 2 axis gimbal system.
- C. COMMON MIRROR - Sensor and projector optical line-of-sight controlled by a single 2 axis mirror.
- D. FIXED SENSOR - Scene stabilized electro-optically; projector line-of-sight controlled by a 2 axis mirror.

Figure 2.0-1 is a summary of the final evaluation. The common gimbal achieved the highest score and was recommended for the testing during Phase II of this study. A test plan for the implementation and evaluation of the selected approach was developed for Phase II, and is published separately as MDC Report G9296 (see Bibliography, item #37 in the Appendix).

Alternative Stabilization/ Tracking Approaches	Evaluation Factors										Sum/10
	Accuracy	Weight	Risk	Unit Production Cost	Crossing Target Accuracy	Adverse Environment	Reliability Maintainability	Target Mix	Training Ease	Development Cost	
Weighting 	20	19	13	12	9	8	7	5	4	3	
A (Dual Gimbal)	8	5	7	8	9	8	6	7	10	8	73
B (Common Gimbal)	9	7	8	9	4	8	8	7	9	9	78
C (Common Mirror)	8	2	6	8	4	8	7	7	8	7	61
D (Fixed Sensor)	3	8	2	5	9	8	6	7	7	3	58

Grading: 10 - Best; 1 - Worst

Figure 2.0-1. Final Evaluation Results

### 3. Initial Screening

In the initial screening, a general ranking of candidate methods, with respect to each evaluation factor, was based upon engineering judgment using past experience with similar systems. The alternative conceptual combinations were formulated, a ranking and weighting scheme established, and a group of engineers with experience in applicable fields was asked to grade each configuration. Surviving concepts were then selected as detailed below.

#### 3.1 Groundrules and Assumptions

The system configurations to be considered were limited to those utilizing IR image sensing for the purpose of pointing a laser beam for guiding a missile in a beam-rider mode. Tracking could be manual or automatic (electro-optic), but various image processing techniques with regard to finding the desired target point within the scene were not permutated. In other words, the stabilization and pointing techniques were focused on, not the focal plane-image evaluation questions.

For this reason, grading on the IR technique intensive factors of "Aerosols/CM" and "Target Mix" was bypassed for the initial screening. The criteria for the other factors is shown in Table 3-2.

Configurations which included electrical laser beam steering (such as the use of magnetic stripe domains in deflector crystals) were not considered because current state-of-the-art with respect to size, weight and power are felt to be inconsistent with the near-term manportable problem.

#### 3.2 Configurations

The following major configuration elements were considered:

1. Manual tracking
2. Electro/Optic tracking
3. Scene (display) not stabilized
4. Scene (display) stabilized
5. Sensor LOS not stabilized
  - a. No inertial sensing
  - b. With inertial sensing

- 6. Sensor LOS stabilized
  - a. Mirror
  - b. Gimbal
- 7. Projector LOS not stabilized
- 8. Projector LOS stabilized
  - a. Mirror
  - b. Gimbal
- CG. Common gimbal
- CM. Common mirror

The combinational choice branching in which gunner capability would affect performance include only items 1 thru 4, the remainder are implementation choices, in which the design alone would improve or degrade (relatively) the capabilities inherent in what is being asked of the gunner.

All realizable combinations of these elements, excluding those which are illogical, are listed in Table 3-1, using the above element designations. For example, configuration 1-4-6b-8a would provide the gunner with a stabilized scene display(element 4) in which he would be required to place a cross hair reticle on the target (element 1); the sensor line-of-sight (LOS) is mechanically stabilized by mounting it in a gimbal (element 6b), and the laser projector LOS is mechanically stabilised by a rotating mirror (8a). An example of an illogical combination would be 1-3-6b-7, wherein the output of a stabilized sensor drives a scene display which is not stabilized. Combinations wherein complexity must be added to achieve degraded performance were considered illogical.

No combinational distinction was made between the target designation phase and the missile flight phase of operation. Grading implications of the designation phase were considered under the factors "Accuracy", and "Training Ease".

The all manual unaided case was included to help calibrate the scoring process, although the performance of that configuration is known to be less than the acceptable minimum.

### 3.3 Evaluation Method

A pre-screening evaluation matrix was constructed, showing the grading factors and their weightings, and all the configuration combinations from Table 3-1. This form is shown in Fig 3-1. The criteria used for the eight attribute factors is shown in Table 3-2.

TABLE 3-1

POTENTIAL COMBINATIONS

(Designations refer to the elements listed in the text of Section 3.2)

Manual Tracking:

Scene not stabilized

1-3-7  
1-3-8a  
1-3-8b

Scene stabilized

1-4-5a-7  
1-4-5b-7  
1-4-5a-8a  
1-4-5b-8a  
1-4-5a-8b  
1-4-5b-8b

} Sensor LOS not stabilized

1-4-6a-7  
1-4-6b-7  
1-4-6a-8a  
1-4-6a-8b  
1-4-6b-8a  
1-4-6b-8b  
1-4-6a-8a-CM  
1-4-6b-8b-CG

} Sensor LOS stabilized

E/O Tracking:

Scene not stabilized

2-3-5a-8a  
2-3-5a-8b  
2-3-5b-8a  
2-3-5b-8b

Scene stabilized

2-4-5a-8a  
2-4-5a-8b  
2-4-5b-8a  
2-4-5b-8b

} Sensor LOS not stabilized

2-4-6a-8a  
2-4-6a-8b  
2-4-6b-8a  
2-4-6b-8b  
2-4-6a-8a-CM  
2-4-6b-8b-CG

} Sensor LOS stabilized

ALTERNATIVE  
STABILIZATION/  
TRACKING  
APPROACHES

Grading Factors	Accuracy		Weight		Risk		Unit Production Cost		Crossing Target Accuracy		Reliability Maintainability		Training Ease		Development Costs		Weighted Score	
	20	10	20	10	10	10	10	10	10	10	10	5	5	5	5	5	5	5
1-3-7																		
1-3-8a																		
1-3-8b																		
1-4-5a-7																		
.																		
.																		
.																		
.																		
.																		

Grades: ☐ 5 Exceeds Reqmts, Lowest, Best ☐ 4 Meets Reqmts, Good ☐ 3 Fair Perf Medium ☐ 2 Limited Perf, High, Poor ☐ 1 Fails Reqmts, Highest, Worst

Figure 3-1. Concept Pre-Screening Evaluation Form

Table 3-2

Concept Initial Screening Criteria

<u>Consideration Factors</u>		<u>Categories/Remarks</u>
1. System Accuracy (2Km)		Ranking Basis (1 $\sigma$ ,m): Exceeds $\leq$ 0.2, Meets 0.2-0.4, Limited 0.4-1.0, Fails $>1.0$
2. System Weight		Ranking Basis (lbs): Low $\leq$ 2, Medium to 3, High $>3$
3. Risk		SOA Measure (Years): Near $\leq$ 1, Medium 2, Far $>3$
4. Relative Unit Production Cost		(% of Reference Point) Low $\leq$ 100, Medium to 120, High $>120$
5. Crossing Target Accuracy		Min. Range Maintaining Accuracy (m): Best 20-40, Moderate 40-65, Worst $>65$
6. Reliability/Maintainability		Ranking Basis: Best 1-3, Moderate 4-6, Worst 7-10
7. Relative Training Ease		Ranking Basis: Best 5,4, Moderate 3, Worst 2, 1
8. Relative Development Costs		(% of Reference Point) Low $\leq$ 100, Medium to 120, High $>120$

Grading Levels

5	Exceeds requirements, lowest (weight, risk, cost), best
4	Meets requirements, good
3	Fair performance, medium
2	Limited performance, high (weight, risk, cost), poor
1	Fails requirements, highest, worst

Five highly regarded MDAC engineers, each with at least ten years experience in a field directly applicable to this problem, were asked to make their best engineering judgments about the candidate configurations, utilizing the format of Fig. 3-1.

The areas of expertise of the five participants were:

1. Missile and spacecraft guidance evaluation and error analysis
2. Missile and fire control systems design, analysis
3. Mechanical design of optics and servo mechanisms
4. Analysis, concept synthesis of electro-optical systems
5. Missile and spacecraft guidance and control systems design, analysis

Three of the participants had previous experience in anti-armor systems, two did not.

Following some preliminaries to establish uniformity in the grading approach, each engineer independently graded all factors for each of the thirty one combinational configurations, obtaining a weighted score for each.

### 3.4 Results and Selection

The maximum possible score (all 5's) is 450. Twenty-one configurations received scores of 300 or greater by at least one scorer, 10 of which received a score of 300 or greater by 3 or more scorers. These 10 included configuration 1-3-7, the manual unaided case, which was dropped for unacceptable guidance performance, and the other nine retained for further scrutiny. These are shown in Table 3-3. The average score column is simply the average of the 5 scores, with no modifications or weighting for the relative expertise applied to the various scoring factors.

The nine configurations retained all utilize automatic electro-optic target tracking, and provide a scene display to the gunner which is stabilized (isolated) from the angular case motion which he induces. These are performance enhancement features, and performance (guidance accuracy) was heavily weighted.



TABLE 3-3  
Highest Unmodified Scores, Pre-Screening

Configuration Designation	Configuration Description E/O Tracking, Scene (Display) Stabilized	Unmodified Average Score
2-4-6b-8b-CG	Sensor LOS stabilized, and projector beam steered by common gimbal mount	360
2-4-6a-8a-CM	Sensor LOS stabilized, and projector beam steered by common steering mirror	324
2-4-6b-8b	Sensor LOS stabilized by gimbal mount, projector beam steered by separate gimbal mount	319
2-4-6b-8a	Sensor LOS stabilized by gimbal mounting, projector beam steered by mirror	315
2-4-6a-8a	Sensor LOS stabilized by steering mirror, projector beam steered by separate mirror	310
2-4-5a-8b	Sensor LOS not stabilized, no inertial sensor, projector beam steered by gimbal mounting	309
2-4-5a-8a	Sensor LOS not stabilized, no inertial sensor, projector beam mirror steered	295
2-4-5b-8b	Sensor LOS not stabilized, inertial sensing, projector gimballed	292
2-4-5b-8a	Sensor LOS not stabilized, inertial sensing, projector beam steered by mirror	286

The surviving group of nine configurations was then examined against the non-survivors to see if the scoring method appeared to achieve reasonable results, since there is always the possibility that summing weighted scores can be misleading, as was the case with the 1-3-7 combination.

The selections appear reasonable, to the extent illustrated by the following example: If the sensor LOS and projector beam are steered independently, with a mirror for one, and a gimbal mount for the other, then gimbaling the heavier projector, and steering the larger sensor mirror (2-4-6a-8b) should be less attractive than gimbaling the lighter FLIR and pivoting the smaller projector mirror (2-4-6b-8a, which "made the cut").

A potentially better method of utilizing judgment based on experience would be to weight the score of each factor by a measure of the scorer's area of expertise and achieve a "modified" score on a per factor basis, then apply the same factor importance weights as before to obtain a score for each configuration. This method was applied to the nine surviving configurations; the result is displayed in Fig. 3-2.

Four of the remaining nine constructs were selected for the more detailed evaluation, these are indicated with a letter in the right margin in Fig. 3-2. A, B, and C are the three highest scoring in the category of a stabilized sensor LOS. They were also the highest three in unmodified scoring. A fixed sensor LOS has the potential for lighter weight, and with a gyro, might achieve adequate performance. The mirror steered projector version (D) was chosen, in order to have a look at the potentially small steering mirror for that case, not covered among A, B, or C.

It is appropriate at this point to provide a more elaborate description of the four selected configurations, as envisioned at the end of the initial screening activity, after which they will be referred to by the letter designations A, B, C, or D.

ALTERNATIVE STABILIZATION/ TRACKING APPROACHES  ⇓			Grading Factors										Weighted Score						
			Accuracy		Weight	10	Risk	10	Unit Production Cost	10	10	Accuracy Target		Reliability Maintainability	5	5	Training Ease	5	Development Costs
			20	20	10	10	10	10	10	10	10	10		10	5	5	5	5	
LOS Steering:			← Weighting																
Config Designation 2.4.	Sensor	Projector																	
	Gimbal	Mirror	5	1	3	1	5	2	5	3	270								
8b-8a	Gimbal	Gimbal	5	1	4	2	5	2	5	3	290								
8b-8b	Common Gimbal		5	3	4	3	2	4	5	4	335								
8b-8b-CG																			
6a-8a	Mirror	Mirror	5	1	3	2	5	2	5	2	275								
6a-8a-CM	Common Mirror		5	3	2	2	2	3	5	2	285								
5a-8a	Fixed	Mirror	4	4	1	3	1	4	5	1	280								
5a-8b	Fixed	Gimbal	4	4	1	3	1	4	5	1	280								
5b-8a	Fixed (+ Gyro)	Mirror	4	4	1	2	4	3	5	1	280								
5b-8b	Fixed (+ Gyro)	Gimbal	4	4	1	2	4	3	5	1	280								

Grades: [5] Exceeds Reqmts, Lowest, Best [4] Meets Reqmts, Good [3] Fair Perf Medium [2] Limited Perf, High, Poor [1] Fails Reqmts, Highest, Worst

Figure 3-2. Concept Pre-Screening Evaluation Summary (Modified Scoring)

#### Configuration A

The display to the gunner is stabilized from his angular motion. This is achieved by mounting the sensor, a miniturized FLIR, on a 2-axis gimbal, with active control. The target line of sight (LOS) to the aim point is initially established by the gunner, and during missile flight by the sensor image processor. The control system maintains the target within the field of view (FOV) of the sensor. The laser beam is directed along the aimpoint LOS by mounting the projector on a separate gimbal, the job of the control system being to point it where the image processor determines the aimpoint to be, plus any biases useful for reducing miss distance, such as compensation for missile autopilot error hangoff due to the laser beam rotation to follow crossing targets. By separately moving the projector, the tracker and display are not disturbed by the biases or control dynamics of that part of the system.

#### Configuration B

This is the same as configuration A except that the laser beam projector is mounted rigidly to the same 2-axis gimbaled platform as the sensor, and boresight aligned to the sensor. Biasing the laser beam angle for guidance lead is not possible without degrading sensor performance and, possibly, display meaning.

#### Configuration C

The displayed scene again is stabilized from gunner motion and the target is auto-tracked by the image processor, however the FLIR and projector are fixed to the case, and the sensor LOS and projector beam are steered together by a single, common steering mirror. The configuration B restrictions on guidance beam lead apply here.

#### Configuration D

In this case the sensor is fixed, it's LOS being steered only by case (gunner) motion, while the projector beam is pointed by a steering mirror. Case motion is sensed by a gyro, the displayed scene is stabilized by electronic means, and the target auto-tracked after manual designation.

#### 4.0 Evaluation of Candidates

Each of the four remaining candidates was evaluated in some detail, to see what the important design parameters and risks would be. Some common groundrules used in the evaluation are given, followed by the results of the analysis for each candidate.

#### 4.1 Groundrules and Assumptions

A one-man portable, shoulder held weapon is assumed. The gunner jitter model for controls analysis is 4 milliradians at 2 hertz. There are to be a minimum of gunner tasks during battlefield operations.

Maximum range to the target is 2 km, minimum guided range is 60 m. The assumed missile performance is as shown in Figure 4.1-1, and is the same as the MDAC proposed IMAAWS weapon. Targets are to be the same as stated in that proposal (Appendix, Ref. 30).

Many of the configuration trades involve the provision for pointing the laser beam ahead of the line-of-sight in a crossing target situation, in order to reduce missile beam centering error. The maximum amount of beam lead required is  $\pm 2^\circ$ , as derived from Figure 4.1-2. The required accuracy of pointing the laser beam, with respect to the sensor aimpoint LOS, in order to not introduce more than 0.08 meters of additional miss distance, is shown in Figure 4.1-3.

The laser beam will be at  $10.6 \mu\text{m}$  wavelength, and the sensor will be a miniaturized serial scan FLIR, operating in the  $8\text{-}12 \mu\text{m}$  spectral band.

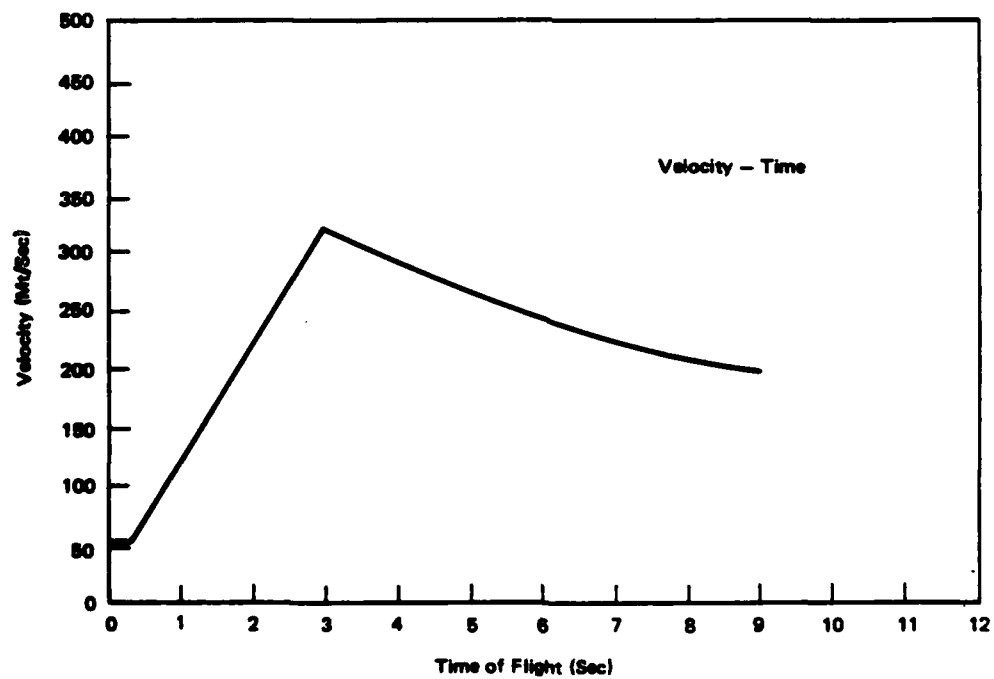
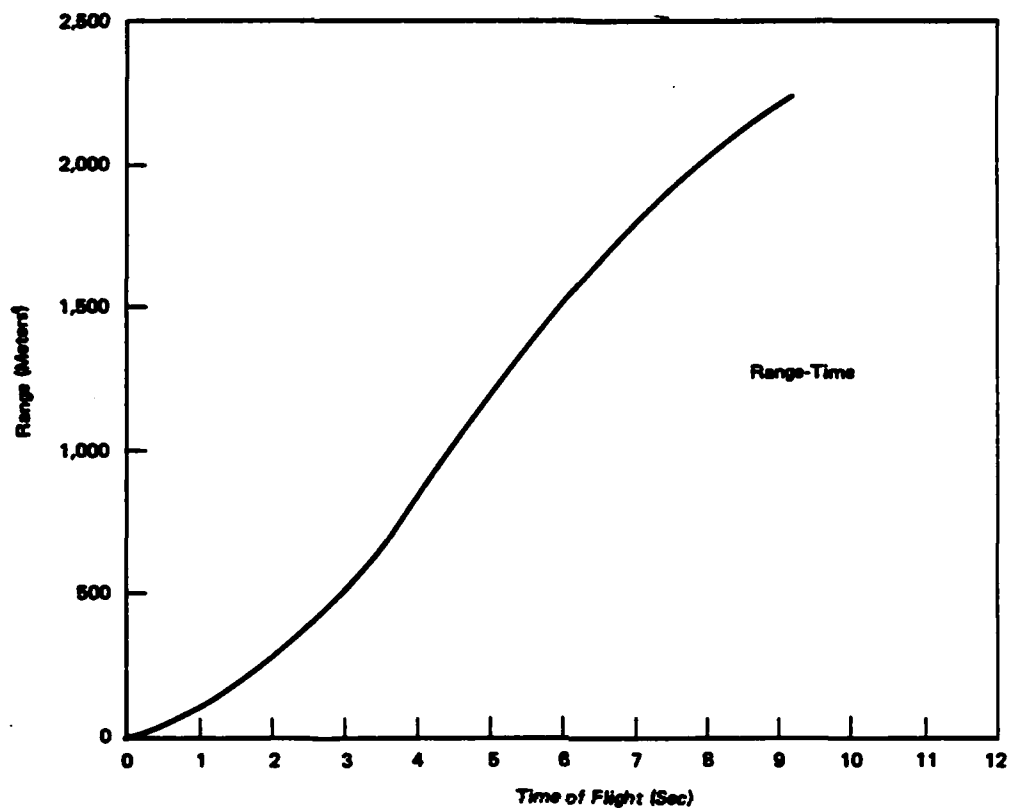


Figure 4.1-1. Missile Performance Assumptions

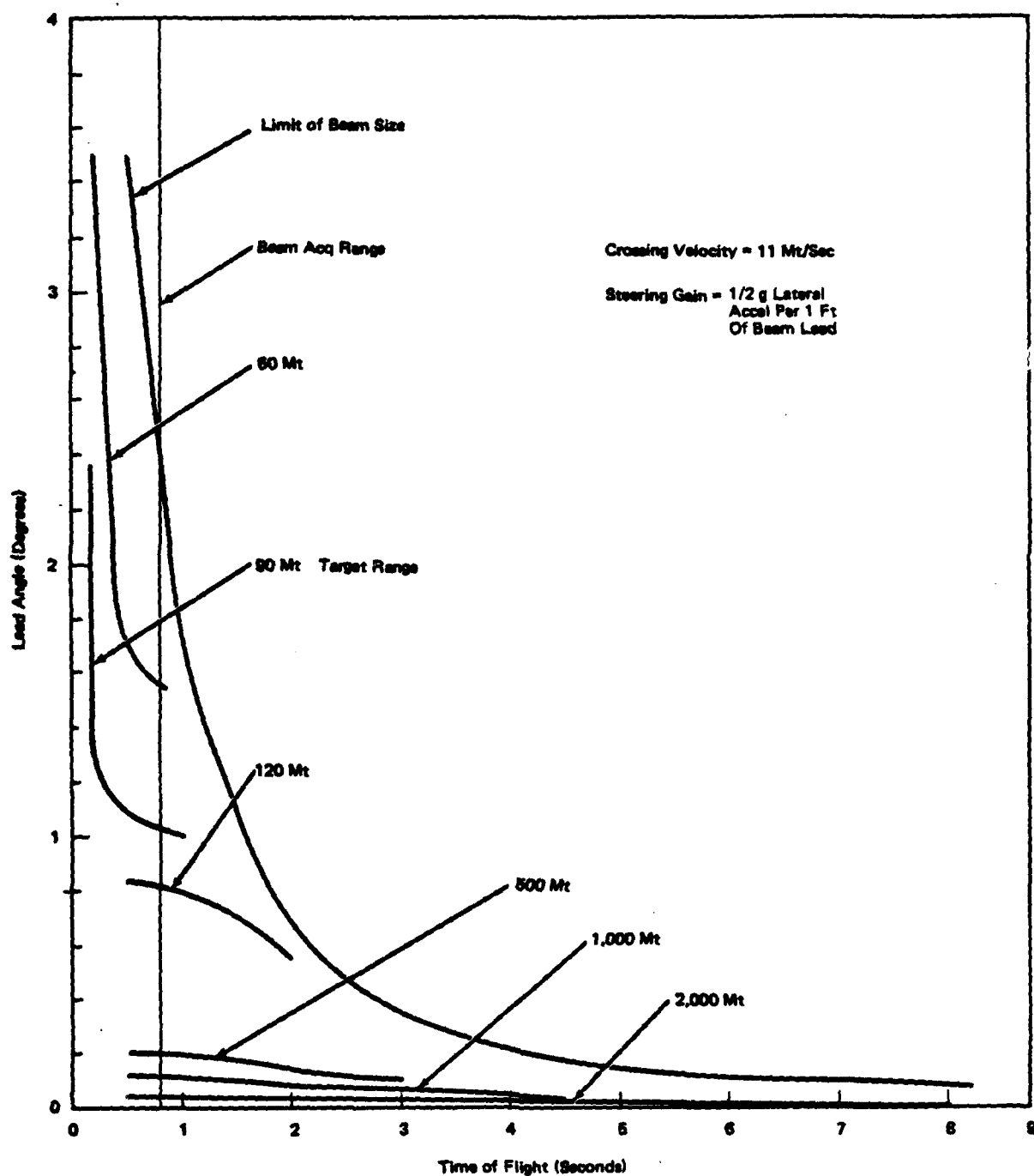


Figure 4.1-2. Crossing Target Lead Angle Requirements

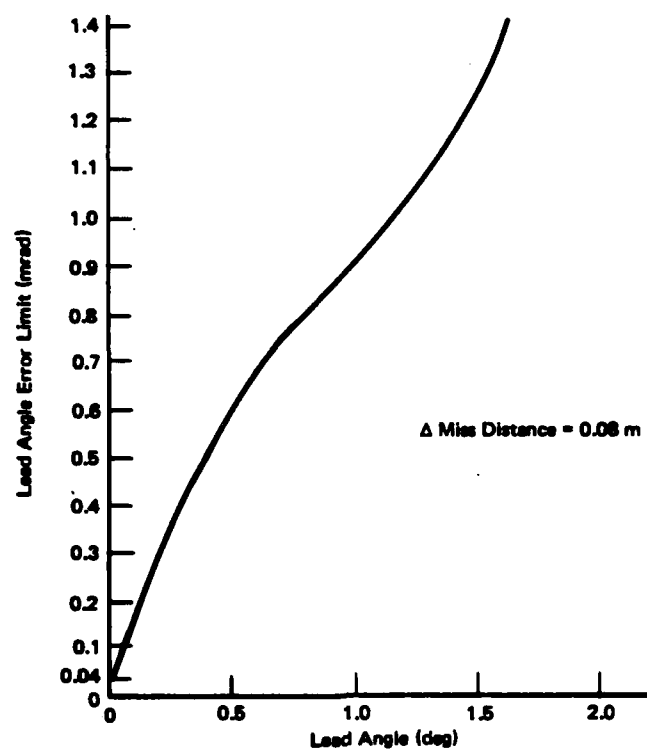


Figure 4.1-3. Beam Lead Accuracy Requirement

The trade studies leading to these baselines are reported in MDC G8512P, Vol. II. (Ref. 30)

The overall accuracy goal of the pointer-tracker system is 100 micro radians, one sigma, with a useful upper limit of 200 micro-radians.



## 4.2 Evaluation Criteria

Following is a discussion of each of the evaluation factors to be used. The relative weights for the evaluation matrix are given in Section 5.1.

### A. Accuracy

An accuracy analysis of each candidate configuration was performed, using a combination of simulation results and analytical techniques. Error sources are identified and their effect on ultimate laser beam pointing error determined.

### B. Weight

To obtain an accurate weight estimate, an optical layout was made for each configuration showing significant parameters such as aperture sizes, mirror sizes, beam excursion, and spacing of all major optical and electro-optical components. The tracker drive components' size and weight for each configuration is attained by analysis of the control requirements and identification of available components satisfying these requirements. A summary of component weights is then tabulated.

### C. Risk

Risk arises in three areas; technical, schedule and cost. There is a strong interrelationship between the three areas and is, to some degree, subjective. Technical risk is related to (1) the degree to which the desired performance or design technology have been demonstrated (present status) and (2) its criticality to the achievement of operational success. Schedule risk is directly related to technical risk because as the degree of technical uncertainty grows, it is more likely that development problems will arise causing a schedule impact. Cost risk is a function of the

technical risk as it impacts the schedule and the uncertainties in cost estimation. The relative grading on risk was based primarily on the degree of technical difficulty perceived in achieving a design that would be rugged and reliable.

#### D. Relative Unit Production Costs

A relative unit production cost was determined for each alternative, based on past experience with similar hardware. The number of optical and active control elements was used as a primary indicator of unit cost.

#### E. Crossing Target Accuracy

The relative grading for crossing target accuracy was based on the ability to steer the laser beam independently of the sensor aimpoint LOS, to obtain a guidance bias to compensate for missile autopilot error "hang-off" when the LOS is rotating. There are other possible methods of achieving this bias correction, however, and a tradeoff study to determine the best approach is beyond the scope of this study. Some of the potential methods are: (1) modulate the laser beam encoder rotational speed; (2) offset the sensor LOS from the aimpoint, and deal appropriately with the resultant image processing and display problems; (3) integrate the guidance error signal at low frequencies in the missile electronics; and (4) provide a bias signal to the missile control processor at launch, proportional to the initial LOS rate. Because of these considerations, the weighting given to this factor will be lower than if independent LOS steering were the only possible method of achieving guidance lead.

#### F. Adverse Environmental Effects

Aerosols and countermeasures (e.g., smokes) were approached in terms of

the target signal attenuation which they impose and the background (scattered solar and self-emitted) noise which they provide. Each of these phenomena impacts the system by reducing the target signal-to-background contrast ratio. The impact of aerosols and countermeasures on system performance was determined via modeling the system minimum resolvable temperature which is dependent upon the modulation transfer function and signal-to-noise ratio.

#### G. Reliability and Maintainability (R&M)

R&M evaluations are developed considering the complexity and types of hardware used to implement each of the four candidate concepts. Tabulation of piece parts and classification by failure rate were the primary factors in establishing an R&M grading.

#### H. Target Mix Accommodation

The primary targets of concern are modern main battle tanks. However, the manportable guidance systems considered here are also applicable to attacking helicopters, bunkers and other fortifications. As a result, this study has emphasized response to the tank threat and considers response to other threats whose imposed requirements are not in conflict. Surveys were undertaken to acquire target signature information for each of the potential targets. Analysis is then conducted to estimate the tracking capability of tank-oriented error sensing and correcting techniques with respect to the other targets of concern.

### I. Training

Each of the alternatives for gunner error sensing and error correction was analyzed to identify and define the gunner tasks required for target acquisition and tracking. These tasks include manual operations such as control activation, perceptual discriminations (e.g., visual, auditory, and somatic), interpretation and calculation (e.g., tank or APC recognition, range estimation, target location at point of impact), and decisions. Each task identified is evaluated as difficult to train on a 10-point scale, with a rating of "1" defining a task which requires essentially no training and "10" defining tasks which are not trainable.

### J. Relative Development Cost

An estimate was made of the relative cost to fully develop each of the candidate configurations. Design complexity and technical risk were used as the main influences in assigning grades for this factor.

### 4.3 Analysis

In order to establish quantitative tradeoff data in the areas of accuracy performance and weight, the most influential selection factors, a sensor analysis and a control system analysis were performed for each of the four remaining candidate configurations. These analyses also aided in developing grades for cost, reliability and training factors.

Much of the analysis was, by the necessity of the schedule, derivational and parametric in nature, however a tracking/stabilization simulation, previously developed for beamrider guidance system analysis, was invaluable in quantifying performance parameters and in gaining insight into system behavior.

Following is a brief description of the methods and results of those analyses.

#### 4.3.1 Candidate A (Separately Gimballed Projector and Sensor)

##### 4.3.1.1 Concept Description

Assuming the ability to make use of all information available, the most general system concept would make use of independently gimballed instruments. This would allow for the most general target mix requirements, and allow for a more stressing crossing target engagement. Specifically, the ability to lead the signal to the missile, in both azimuth and elevation, would reduce errors caused by both horizontal and vertical target motion at significant rates. Independent instrument pointing is highly desirable at the minimum ranges of interest (see Figure 4.1-2.).

Several candidate arrangements have been evaluated. Each offers a different trade between complexity, weight, and effectiveness against crossing targets. These candidates are, 1) completely separate gimbal systems for both instruments, 2) a common elevation gimbal with separate azimuth gimbals mounted within, 3) two-axis gimballed projector mounted on the sensor platform, and 4) a single azimuth gimballed projector mounted on the sensor platform. Each

of these arrangements require some means of maintaining alignment between the sensor and projector. The error due to the initial bore-site aligning is to be no more than  $70 \mu$  radians. It is also assumed that the dynamic error between the instruments must not exceed  $40 \mu$  rad.

Totally separate gimbal systems offer the greatest flexibility, however, the severe alignment requirements make this option seem very unattractive. There is no practical way to torque the projector gimbals precisely enough to follow the sensor and respond to rapidly changing beam lead requirements within a  $40 \mu$  radian limit. Weight and complexity for this system are also unfavorable.

Option (2) offers the same flexibility in azimuth as option (1), however, it also has the same alignment limitation. Further, a single large elevation gimbal may not be lighter and could result in packaging problems. Option (3) offers the freedom of option (1) with somewhat less alignment difficulties, since the projector gimbals can be accurately aligned to the sensor platform. The projector gimbals are only required for beam lead, and as such, require less travel, but quick response and high precision. It is possible that the accuracy requirements can be met by this system; however, option (4) offers the same advantages with only the loss of separately gimballed elevations. Since an armored vehicle is not likely to have a significant vertical velocity component, this loss is acceptable, in view of the reduced complexity and weight that it offers. It is anticipated that the alignment requirements can be met by using a linear potentiometer having .0001 inch resolution on a 3.3 inch lever arm. The resulting  $30 \mu$  radian error, RSSed with  $30 \mu$  radians for random errors caused by the system, yields approximately  $40 \mu$  radians accuracy. The implementation of beam lead will require line-of-sight rate data. This data can be derived from the optical tracker data, gyro data, or a combination of both.

Figure 4.3.1.1-1 presents a functional block diagram for this concept, based on option (4) as described above.

#### 4.3.1.2 Sensor Analysis

Some thermal IR imaging sensors employ serial scan detectors with time delay integration to compensate for high bandwidth requirement and

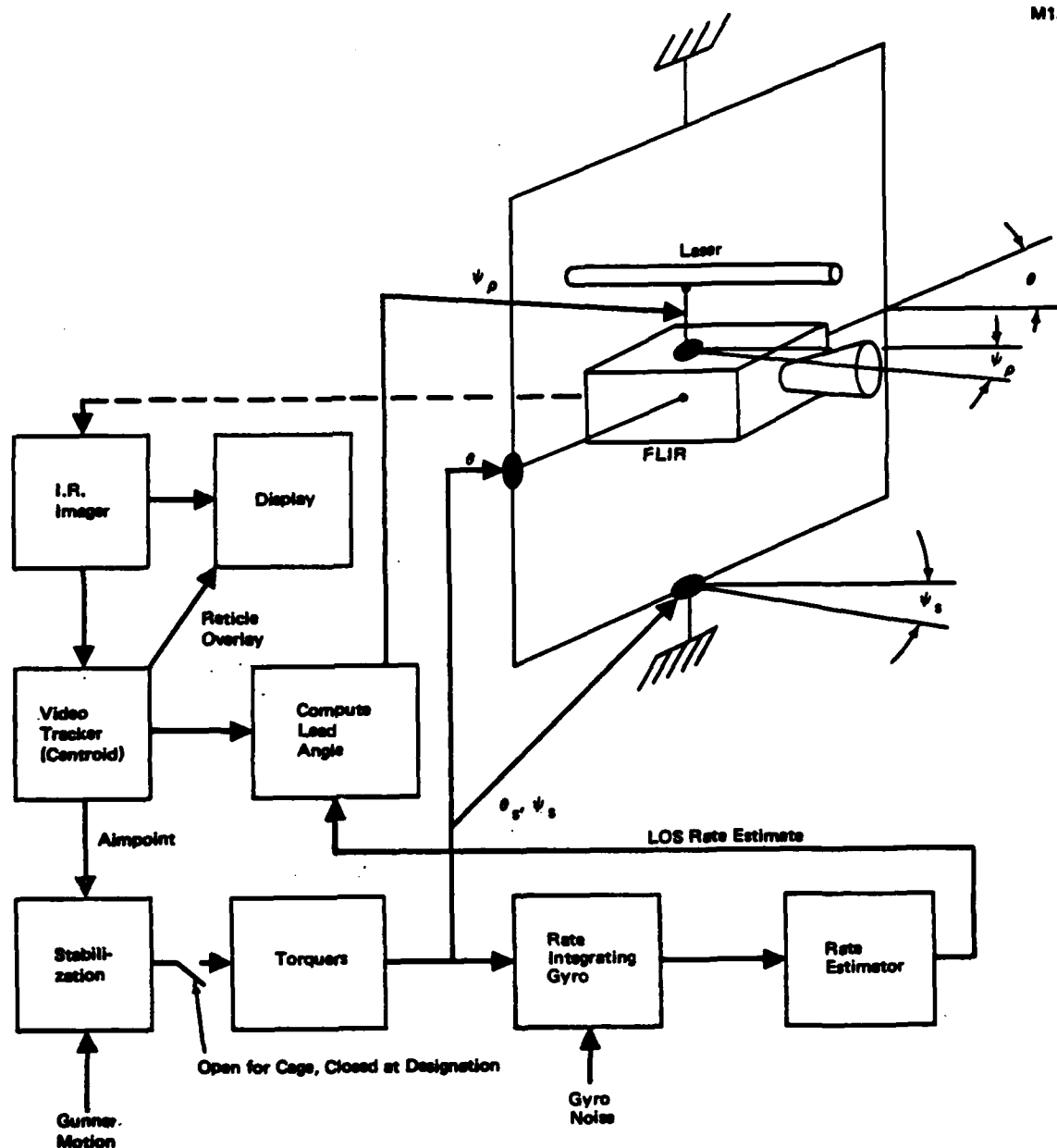


Figure 4.3.1.1-1. Separate Gimbal Concept, Functional Description

resultant low sensitivity. Other types, including the scanning linear array (and mosaic detectors) can be made more sensitive but require more costly detectors in the focal plane and more sophisticated signal processing. Each of the types mentioned can give near equal performance as far as pointing and tracking capability. However, in case of hazy and dusty conditions the linear scan sensor can out perform the serial scan imaging system in that

it can produce a higher output tracking signal to noise ratio which may, in a marginal condition, give it an advantage.

In this study the merits of the different tracking schemes is compared. We will assume that each tracking scheme has an identical IR imaging sensor.

In Candidate A the imager sensor produces electronic signals corresponding to IR intensity for every pixel element in the scanned scene. This data is stored in the image converter which converts the data to signals that modulate a TV raster so that it can be displayed. Video tracker electronics also process the stored data to determine the target centroid from target edge contrast data. The video tracker generates tracking gates corresponding to target position with respect to the axis center. Error signals derived from the tracking gate signals are used to drive the gimbals to a zero error position or, in other words, position the target centroid (aim point) at the aligned zero position corresponding to the video display center. The laser gimbal is slaved to the image sensor gimbal, plus guidance lead bias. At shorter ranges it also becomes possible to place the laser beam at a spot on the target different from the centroid and corresponding to a more vulnerable kill spot. This can be accomplished with a separate gimballed system such as Candidate A by utilizing a bias error signal to torque the laser projector gimbal to the desired position with respect to the target centroid. This bias signal would be range dependent, which adds complexity to the image processing, since range, or something equivalent would have to be deduced from image characteristics.

The sensor caused pointing errors would be composed of errors due to centroid tracking errors, image blur due to turbulence, and alignment errors. These will be discussed separately below.

#### Centroid Tracking Errors

Potential tracking errors of the target image centroid will depend on the image resolution. The centroid can usually be tracked to an accuracy of approximately one-half resolution element. The sensor recommended for this study would have an angular resolution in azimuth of  $270 \mu$  rad and



180  $\mu$  rad in elevation or an average of 220  $\mu$  rad. The potential centroid tracking error would therefore be:

$$\epsilon_{\text{TRACK}} = \frac{\Delta\theta_{\text{resol}}}{2} = \frac{220 \mu \text{ rad}}{2} = 110 \mu \text{ rad}$$

#### Tracking Errors Due to Image Blur Caused by Atmospheric Turbulence

The amount of image blur due to atmospheric turbulence can be shown to be:

$$\langle \Delta\theta^2 \rangle^{1/2} = \frac{1}{R} \left[ \int_0^R \frac{1.26 \times 10^{-2}}{\lambda} D_0^2 C_N^2 \log_e \left( \frac{1.4 R \lambda}{D_0^2 \ell_0} \right) \frac{z^2}{L_0} dz \right]^{1/2} \quad (1)$$

where

$$\lambda = \text{wavelength} \sim 11.0 \times 10^{-6} \text{ M}$$

$$D_0 = \text{optics diameter} \sim .08 \text{ M}$$

$$\begin{aligned} \ell_0 &= \text{inner scale of turbulence} \sim 10^{-3} (h)^{1/3} \text{ meter} \\ &= 1.7 \times 10^{-3} \text{ for height } (h) \sim 3 \text{ M above earth} \end{aligned}$$

$$\begin{aligned} L_0 &= \text{outer scale of turbulence} \sim 2\sqrt{h} \\ &\sim 3.5 \text{ for } h = 3 \text{ meters} \end{aligned}$$

$$R = \text{path length} \sim 2 \text{ KM}$$

$$\begin{aligned} C_N^2 &= \text{turbulence structure constant which depends on} \\ &\quad \text{altitude } h \text{ and time of day} \\ &= 5 \times 10^{-14} \text{ day} \quad (h = 3 \text{ M}) \\ &= 3 \times 10^{-14} \text{ night} \end{aligned}$$

from equation (1)

$$\langle \Delta\theta^2 \rangle^{1/2} = \frac{1}{R} \left[ \frac{1.26 \times 10^{-2} D_0^2 C_N^2}{\lambda} \log_e \left( \frac{1.4 R \lambda}{D_0^2 \ell_0} \right) \times \frac{R^3}{3 L_0} \right]^{1/2} \quad (2)$$

Figure 4.3.1-2 shows typical values of  $C_N^2$  for altitude  $h$  (M) and time of day.

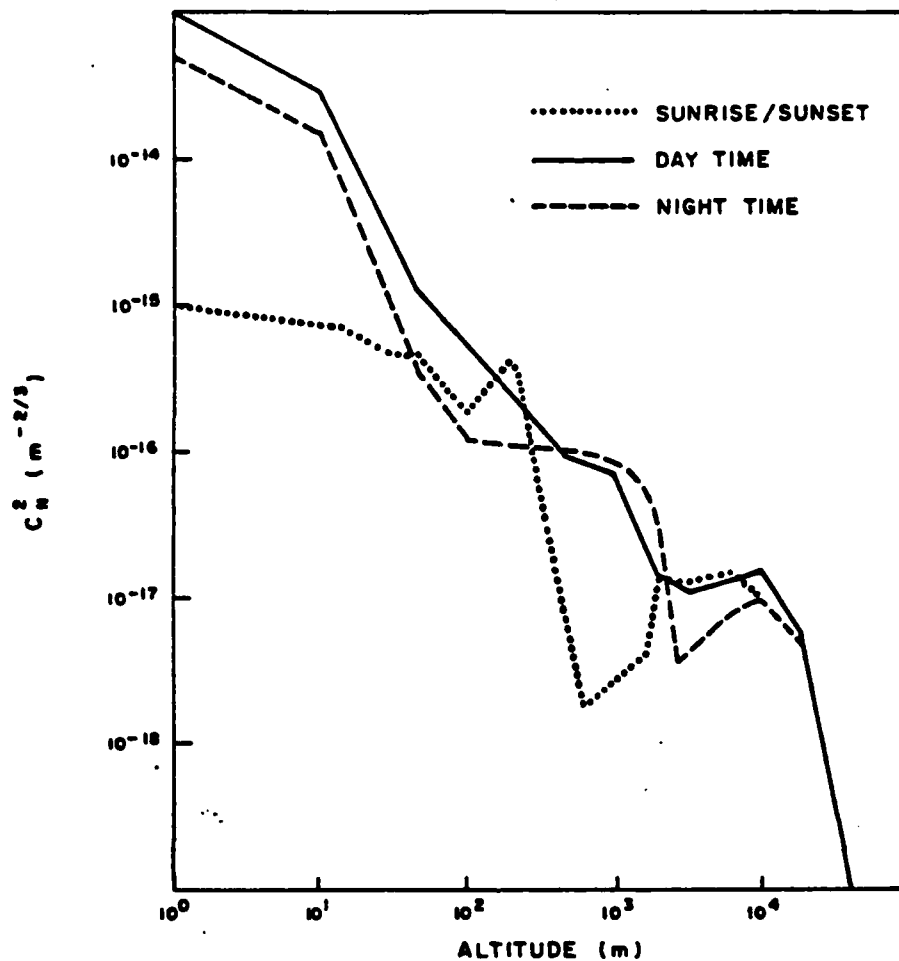


Figure 4.3.1-2.  $C_N^2$  as a Function of Altitude and Time of Day

Inserting the parameters in equation (2) we obtain, for image blur due to turbulence,

$$\begin{aligned} \langle \Delta \theta^2 \rangle^{1/2} &\sim 68 \mu \text{ rad} \quad (\text{day}) \\ &\sim 52 \mu \text{ rad} \quad (\text{night}) \end{aligned}$$

The centroid tracking errors due to turbulence would be approximately half this image blur or

$$\begin{aligned} \epsilon_{\text{Turb}} &\sim 34 \mu \text{ rad} \quad (\text{day}) \\ &\sim 26 \mu \text{ rad} \quad (\text{night}) \end{aligned}$$

### Alignment Pointing Error

Mechanical alignment errors of 70  $\mu$  radians between the two gimbals and telescopes are considered obtainable. An electrical alignment error of 40  $\mu$  radians is estimated for the null uncertainty of the gimbal angle sensor. The total RMS alignment error is

$$\begin{aligned}\epsilon_{\text{alignment}} &= \sqrt{\Delta\theta^2_{\text{MECHANICAL}} + \Delta\theta^2_{\text{ELECTRICAL}}} = \sqrt{(70)^2 + (40)^2} \\ &= 81 \mu \text{ rad.}\end{aligned}$$

The total pointing error for Concept A could be

$$\begin{aligned}\epsilon_{\text{tot}} &= \sqrt{\epsilon^2_{\text{TRACK}} + \epsilon^2_{\text{TURB}} + \epsilon^2_{\text{ALIGN}}} \\ &= \sqrt{(110)^2 + (34)^2 + (81)^2} \approx 141 \mu \text{ rad} \\ &\quad \text{(DAY TIME)}\end{aligned}$$

These errors would be gaussian in distribution.

### Sensor Transfer Function

To do a servo analysis of the dynamic performance of the pointing system requires a transfer function of the sensor system along with sensor tracking and alignment errors.

In most sensors whether serial scan, linear array scan, or staring, the scene is loaded into a frame memory. This is shown in Figure 4.3.1-3.

By the time that the scan data is loaded, it contains information that on the average occurred one half cycle earlier. An additional period of time is required to process the data to determine the location of the target centroid. The period of time required to do this processing is highly dependent upon sophistication of the image processing algorithms but it must be less than one cycle time. Image correlation techniques

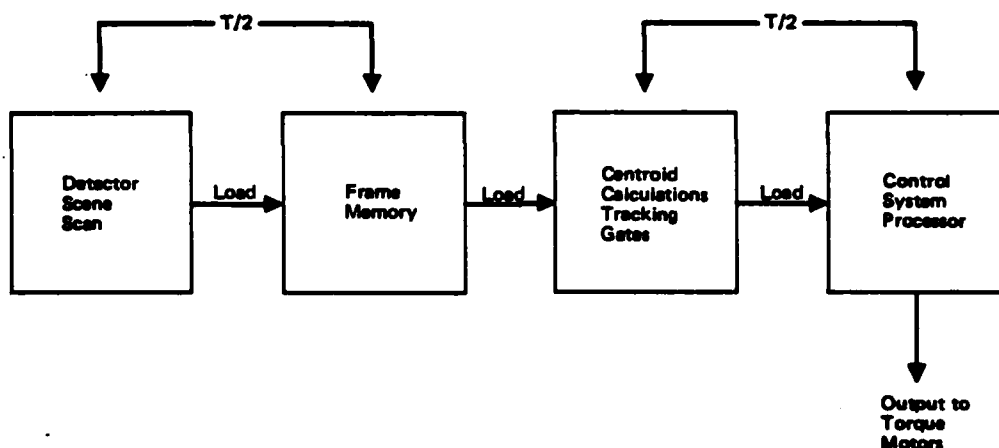


Figure 4.3.1-3. Time Partitioning of Sensor and Tracking Electronics

tend to use a large portion of the cycle time for processing whereas centroid and edge tracking techniques can be done in shorter times. A one half cycle processing time was used for this study since centroid tracking techniques are used. This value is also consistent with the DBA tracker which will be used in Phase II. The total transport delay for both the image gathering and image processing is one full cycle time or 1/60 second and the sensor transfer function is  $e^{-TS}$ .

#### 4.3.1.3 Control Analysis

As explained in the concept description, the most encouraging separate gimbal system would involve a projector gimballed in azimuth only, mounted on the stable platform holding the image sensor. As a result, the control system designs for the common azimuth and elevation gimbals is identical to that found in Section 4.3.2, and will not be repeated here.

The projector azimuth gimbal control system will benefit from the stabilization supplied by the platform gimbals and therefore will only need to respond to the low frequency beam lead command. As a result, a bandwidth of approximately 1 to 2 hz should be sufficient, and the resulting torque required will be less than that required by the platform gimbals. Allowing for a bandwidth of 2 hz and assuming a gimbal inertia of 1.8 oz-in-sec<sup>2</sup>, the resulting maximum torque required would be 1.08 oz-in.

Figure 4.3.1.3-1 presents a functional description of the control loop and a simplified block diagram.

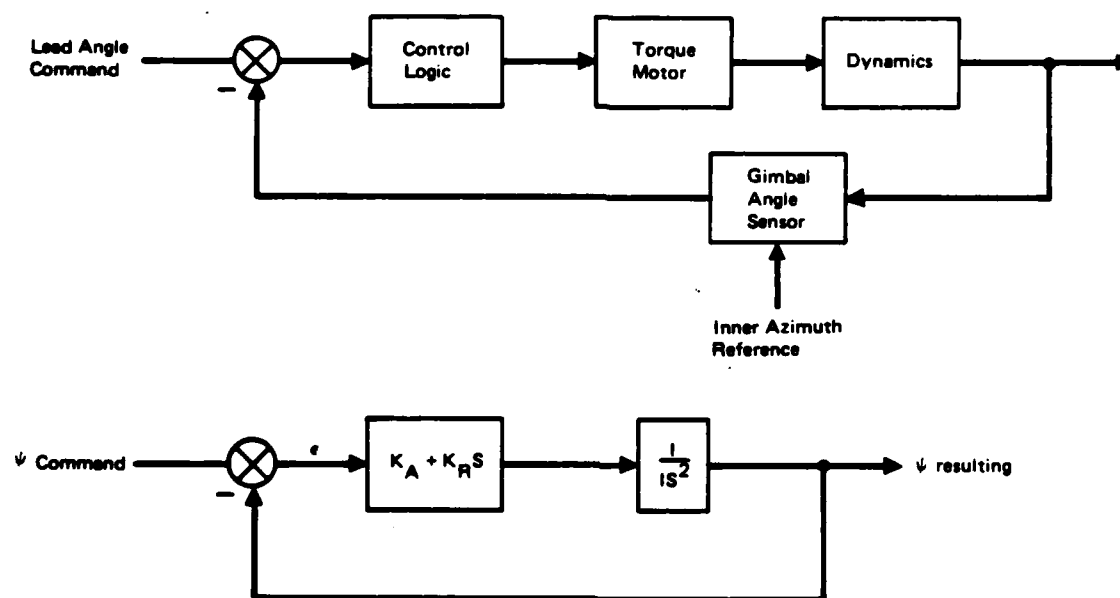


Figure 4.3.1.3-1. Projector Gimbal Control

## 4.3.2 Candidate B (Common Gimbal)

### 4.3.2.1 Concept Description

The common gimbal concept is the next logical simplification of the system discussed for Candidate A. That is, both the projector and sensor are mounted on a single platform which is gimballed in azimuth and elevation (Fig 4.3.2.1-1). The platform will achieve attitude reference sensing from a single two axis gyro. Each gimbal will have a travel of  $\pm 5$  degrees. Beam lead, to eliminate hang-off error caused by crossing targets, is not directly achievable by separately pointing the laser beam. Essentially, this represents the MDAC proposed IMAAWS concept as described in reference 30.

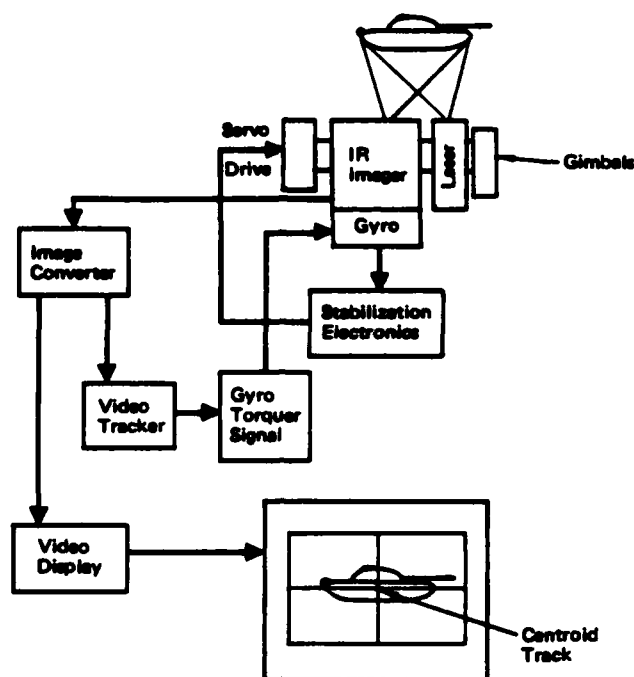


Figure 4.3.2.1-1. Concept "B" Block Diagram

This concept provides a stabilized projector beam and a stabilized scene. The scene will be stabilized throughout the tracking process and may also be stabilized during the designation process if it is found that unaided gunner designation results in unsatisfactory performance.

Once designation has been accomplished, the centroid tracker logic will compute an aimpoint and cause a reticle to appear in the display. Aimpoint information will be used to compute torquer commands while the reticle information will provide visual feedback to the operator to aid him in keeping the stable platform within the gimbal limits.

This configuration of sensors can provide an estimate of target LOS rate for use by one of the alternate guidance lead schemes mentioned in section 4.2.

#### 4.3.2.2 Sensor Analysis

This Sensor concept is shown in Figure 4.3.2.1-1. In Candidate B, the laser projector and IR imager sensor are mounted on the inner gimbal and rigidly static aligned to within 70  $\mu$  radians. Errors due to resolution and turbulence are the same as those discussed for candidate A (4.3.1.2).

The total pointing error will be a combination of centroid tracking errors due to resolution capability; image blur due to turbulence; and misalignment errors. The expected values are:

Resolution Centroid Errors	110 $\mu$ Rad
Turbulence Induced Centroid Errors	34 $\mu$ Rad (max)
Misalignment Pointing Errors	70 $\mu$ Rad
<hr/>	
Total Pointing Error RMS	135 $\mu$ Rad

These error values would be gaussian in distribution with the above total error being the 1  $\sigma$  value.

#### Sensor Transfer Function

The delay time and transfer function would be the same for Candidate B as for Candidate A which was

$$F(S) = e^{-TS}$$

Where T is the frame time  $\sim 1/60$  sec.

#### 4.3.2.3 Control Analysis

Analysis of the common gimbal concept was performed to determine torque requirements, power requirements, and accuracy. Torque and power requirements relate directly to weight. The major design trade on which the final selection will be made is weight versus accuracy. System accuracy has been estimated using a combination of analysis and digital simulation.

A simplified single axis block diagram of the common gimbal concept is shown in Figure 4.3.2.3-1. Because of the limited angular freedom ( $\pm 5^\circ$ ) the two axes can be treated independently with no significant error. The system shown in this figure has been configured so that the stabilization function is separated from the tracking function. This allows independent design of both functions so that the different requirements can be addressed separately to achieve the best overall performance.

The gimbals provide a natural isolation from high frequency gunner jitter. The second order stabilization loop has been designed to remove the gunner jitter which enters the system via friction torque and magnetic drag. Torquer motor back EMF is virtually eliminated by using a current drive instead of a voltage drive. It has been found that a bandwidth around 7-10 hz provides good response. Since stabilization and tracking functions are separated, the tracking filter can be designed to handle the low frequency target motion. A bandwidth near 1 hz has been found to provide good response to target motion while filtering the high frequency tracker noise.

The feed forward loop serves to increase the type of the control system to allow the system to track a moving target with no "hang-off error." It also provides line-of-sight rate for the missile guidance needs.

#### Torque Requirements

The torque requirements were determined as a function of both system bandwidth and gimbal inertia. Maximum torque requirements occur during the target acquisition transient. Maximum target line-of-sight rate and initial gunner tracking error prior to designation are the causes of the acquisition transient. Figure 4.3.2.3-2 presents torque requirements as a function of bandwidth for the common gimbal case. Torque has been normalized for gimbal inertia. Section 4.3.3.3 presents a detailed derivation of the equations used to obtain this data and, for convenience, will only be summarized here. Maximum torque required to handle the



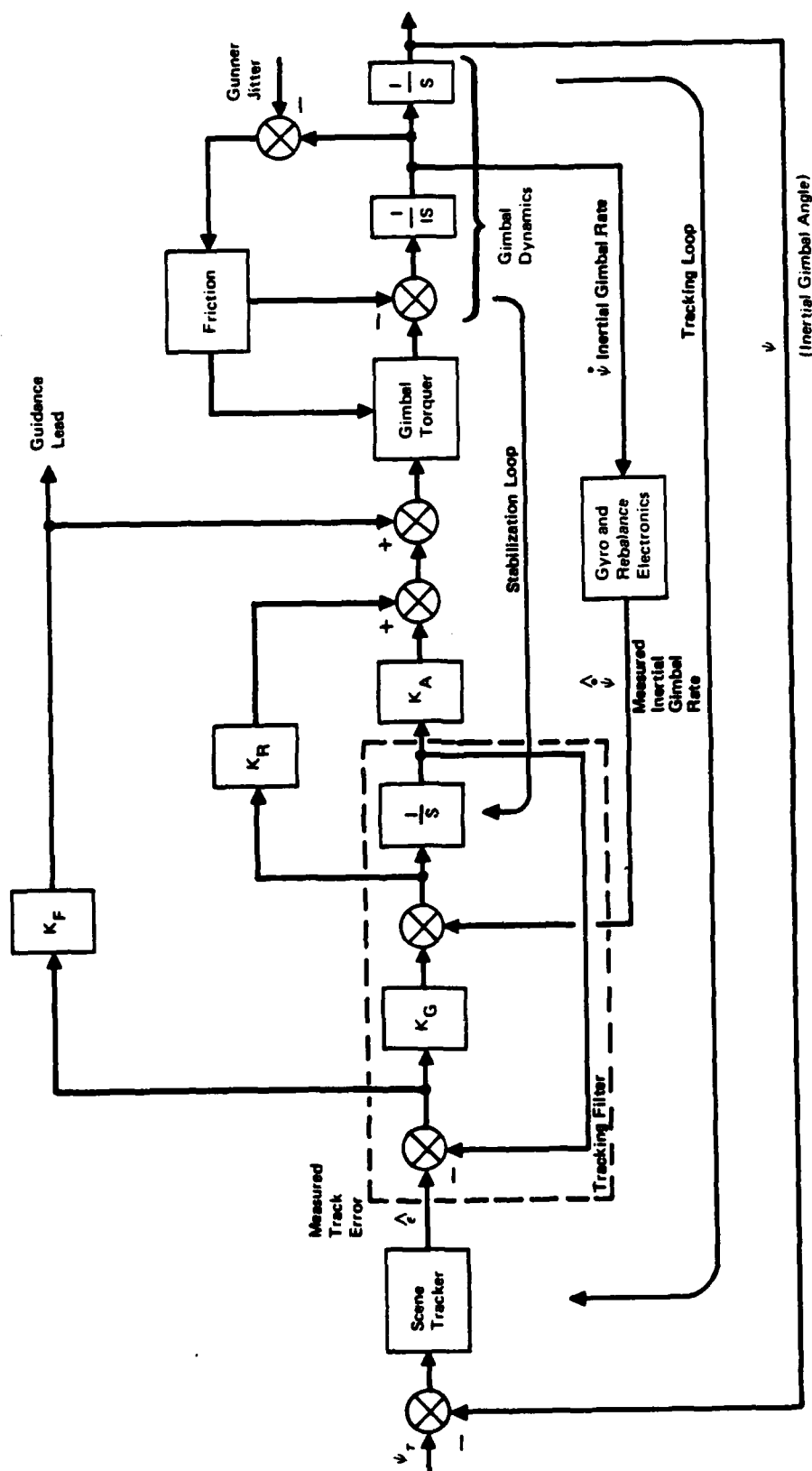


Figure 4.3.2.3-1. Gimbaled Tracking and Stabilization System

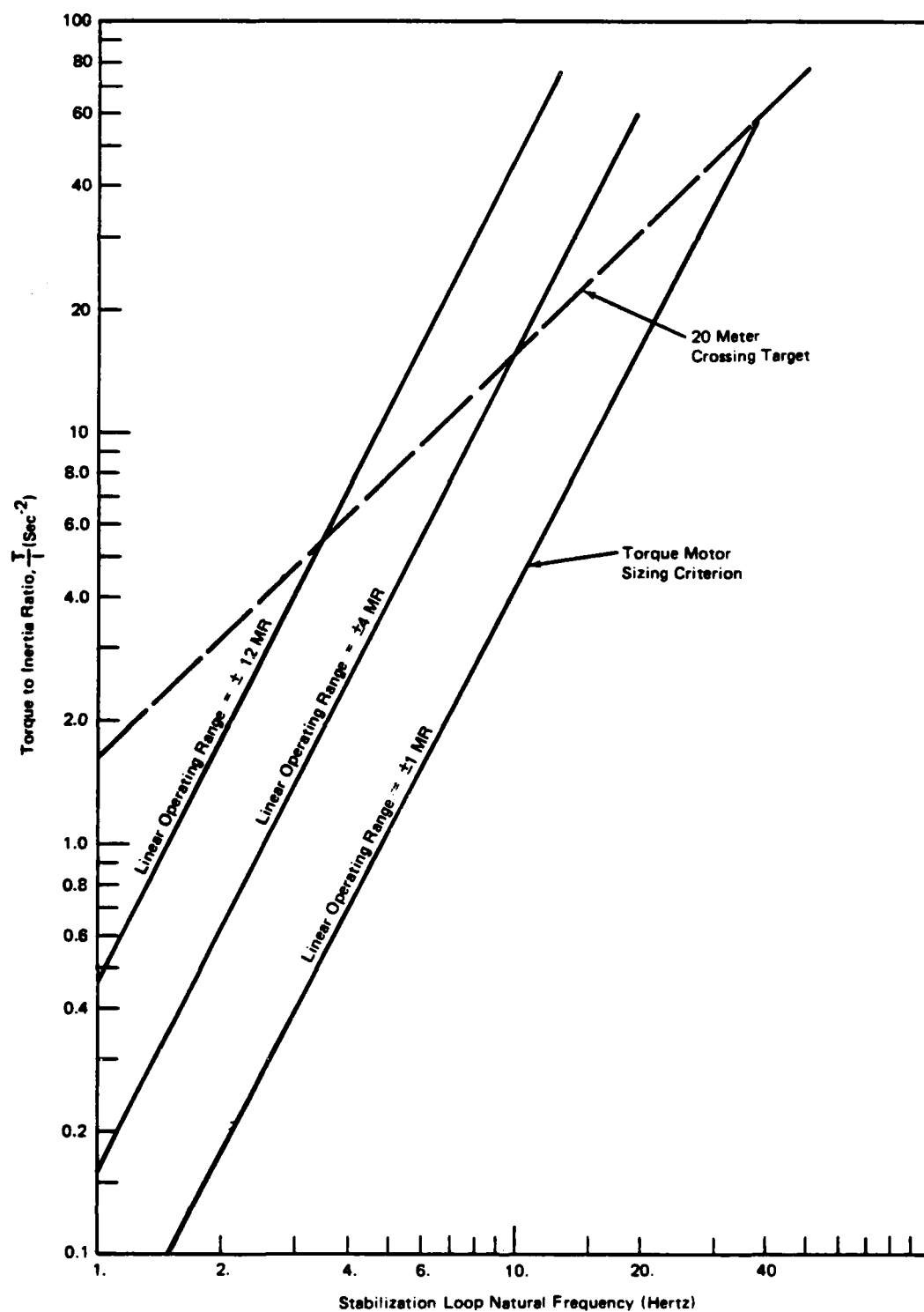


Figure 4.3.2.3-2. Torque Motor Sizing Criteria

acquisition transient due to a crossing target having a velocity of 11 m/sec is

$$\frac{\tau}{I} (\max) = 2.5 \frac{W_N}{R}$$

where R is the range to the target in meters, I is the inertia, and  $W_N$  is the natural frequency of the stabilization loop. The torque required to prevent saturation due to gunner pointing error at designation is

$$\frac{\tau}{I} = W_n^2 E_G$$

where the value  $E_G$  (gunner pointing error at initiation) is used to size the torque motor and define the operating range for the system.

Torque requirements for gunner acquisition errors indicate that any final design will probably provide an acquisition mode to aid in reducing this error prior to the designation initiation.

The MDAC IRAD project hardware for this configuration was used as a basis to estimate a gimbal inertia of 2.4 oz-in-sec<sup>2</sup> in each axis for this configuration. This corresponds to a maximum torque requirement of approximately 19 oz-in. Figures 4.3.2.3-3 and -4 present simulation results for this configuration.

#### Power Requirements

It can be shown (Section 4.3.3) that power required is proportional to torque squared. Figure 4.3.3.3-4 presents data for both the common gimbal and common mirror concepts. As can be seen, power required for the gimbal concept will be well below an equivalent mirrored system. It is questionable whether the mirror inertia can be reduced to a point that would make that concept competitive with the gimbal concept, on a power consumption basis.

#### Accuracy

Imaging sensor errors and base motion disturbances are the dominant error sources impacting the control design. Imaging sensor errors show up as both a

FIGURE 4.3.2.3-3  
COMMON GIMBAL SIMULATION

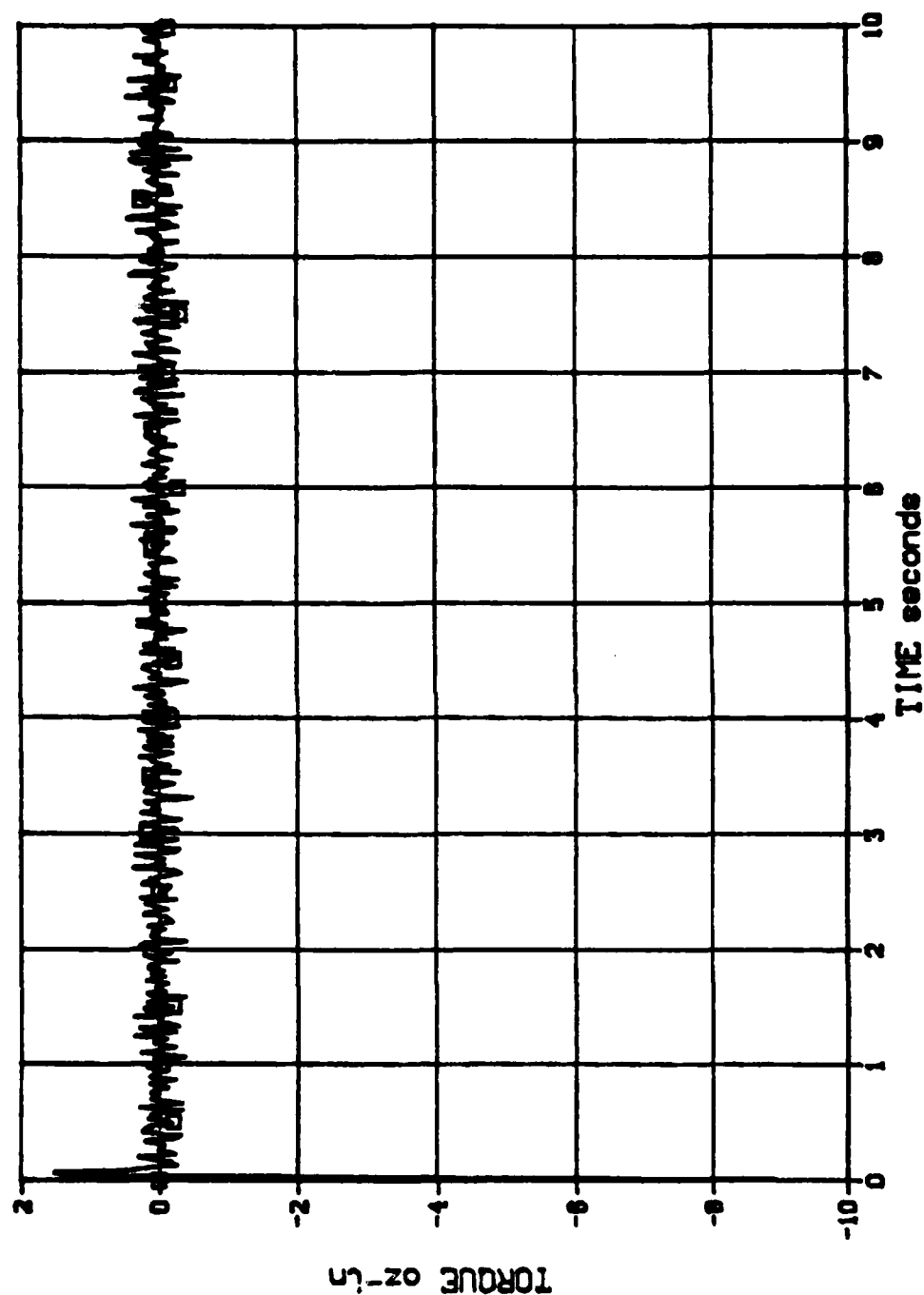
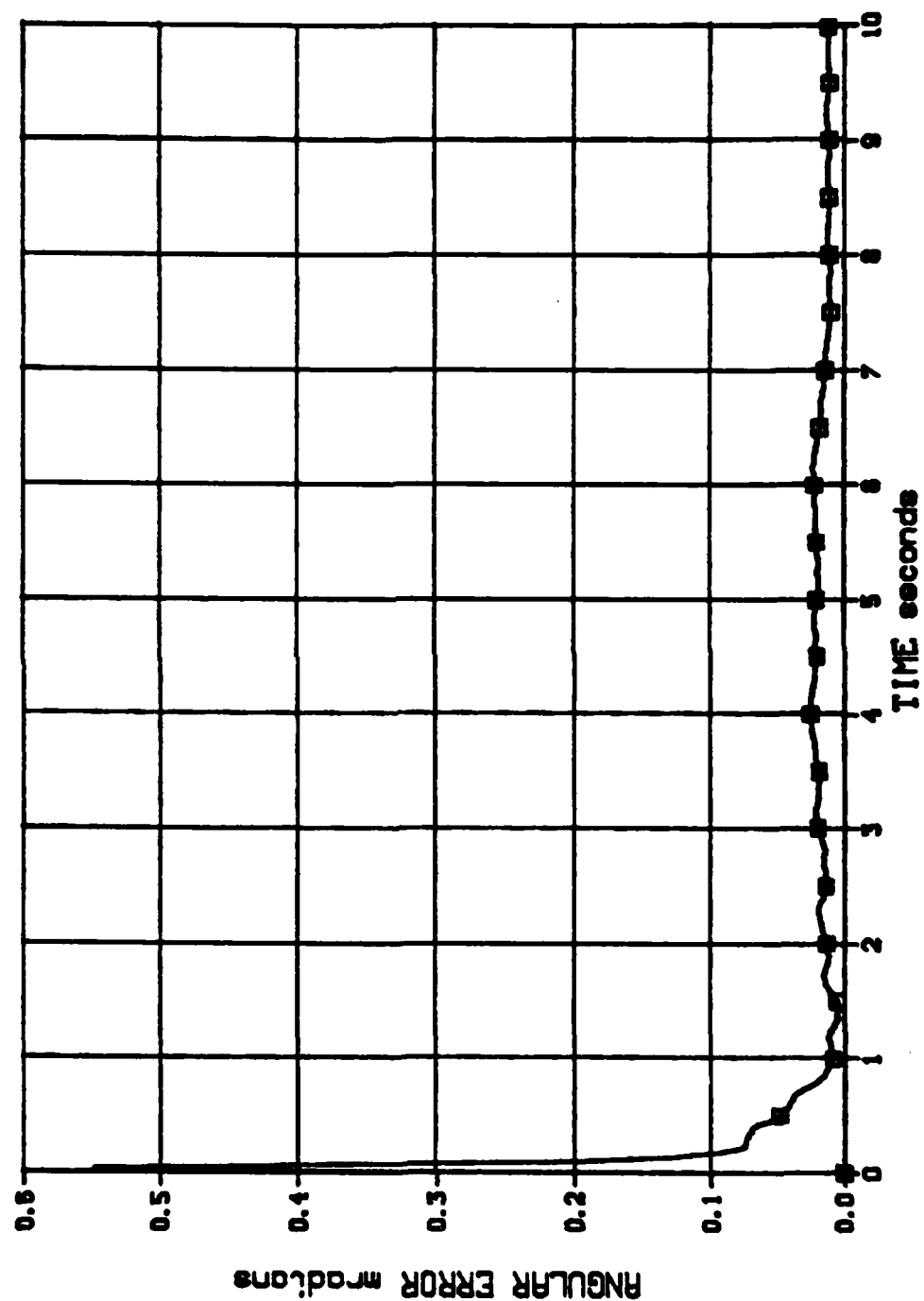


FIGURE 4.3.2.3-4  
COMMON GIMBAL SIMULATION



bias and a random error. The basis error is caused by the steady state error in the ability to define the aimpoint. This error remains the same for all candidate systems and does not show up as an evaluation factor.

The tracking error resulting from the random error source (sensor noise) increases with the control system natural frequency. The dynamic error which results from base motion decreases with increasing control system frequency.

The performance of this system has been optimized by selecting the stabilization system natural frequency that minimized the total tracking error from these two error sources. Tracking errors due to gyro drift, gyro noise, and gimbal angle sensor noise were also investigated and found to be at least an order of magnitude lower than the image sensor noise.

#### 4.3.3 Candidate C (Common Mirror)

##### 4.3.3.1 Concept Description

This concept uses a common steering mirror to simultaneously stabilize both the sensor and laser line-of-sight as shown in Figure 4.3.3.1-1. The laser and imaging sensor are mechanically aligned so that nulling the sensor aimpoint error also causes the laser line-of-sight to intersect the aimpoint. Beam lead required to reduce the guidance error for crossing targets must be implemented by modulating the laser beam, or one of the other schemes mentioned in Section 4. Gyros and gimbal angle sensors are used to isolate the line-of-sight from base motion caused by gunner jitter.

This configuration has an optical gain of 2 to 1 in line-of-sight motion about the gimbal axis parallel to the mirror surface. This property has the undesirable effect of coupling base motion directly into the line-of-sight. More control system effort is required to stabilize this axis than the other gimbal axis which has a one to one line-of-sight rotation with mechanical rotation. In the one to one axis, the line of sight is naturally isolated from base motion through the inertia of the mirror. Base motion only effects the line-of-sight through indirect effects such as friction

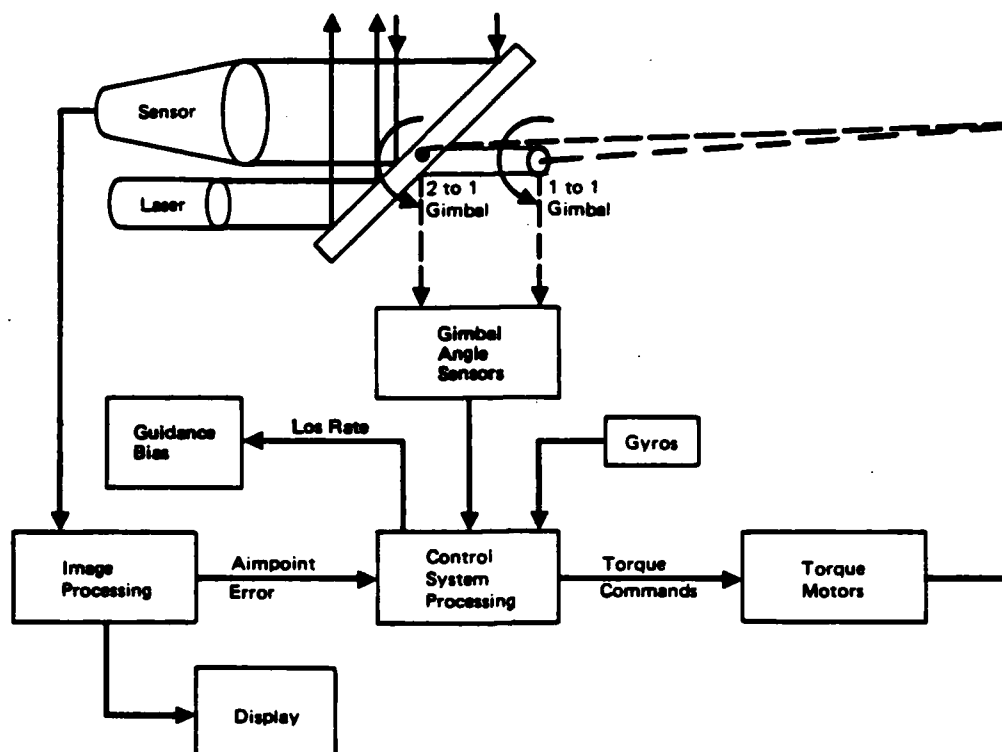


Figure 4.3.3.1-1. Functional Diagram Common Mirror Concept

and electrical wire torques. In a well designed system, these indirect effects can be an order of magnitude less than the direct coupling in the 2 to 1 axis.

Several alternate common mirror concepts were considered in an effort to:

- reduce system weight by using shared optics, and
- provide base motion isolation in two axes.

These alternatives generally resulted in more complex and higher risk systems and were therefore not considered as the baseline common mirror concept. The alternate concepts are discussed below.

### Common Mirror Alternatives

#### Concept C1

Several approaches were considered for stabilizing the optical line-of-sight of the thermal sight and the laser beam with a common, servoed

optical system. Illustrated in Figure 4.3.3.1-2 is the minimum complexity approach, but the size of the servoed element is largest.

For separate FLIR and laser optical paths, the turning flat is elliptical and measures about 15 cm x 23 cm x 5 cm. This accommodates  $\pm 6^\circ$  motion, 120 mrad laser beam divergence, and 80% useful optical area. If the optical paths are shared, using dichroics or other techniques discussed below, the mirror dimensions can be reduced by about 30 percent to 11 cm x 16 cm x 3 cm for a weight reduction of roughly 70 percent. In either case, the weight can be estimated at about 35 percent of an equivalent solid aluminum mass; this assumes that a lightweighted (honeycombed, cored, etc.) substrate of aluminum, graphite/epoxy, or other suitable material is used. The larger mirror mass is approximately 1.3 kg and the small is 0.4 kg, a significant difference.

An actuation concept which has been used in other systems is shown in Figure 4.3.3.1-2b. Linear electromagnetic or hydraulic actuators are used to move the short distances required to achieve  $\pm 6$  degrees of motion about a pivot. The actuation is oriented to achieve one-to-one line-of-sight stabilization in elevation (by aligning downstream leg of FLIR input path parallel to E1-axis) and two-to-one compensated control in azimuth.

It should be noted that the rotations of the line-of-sight in elevation will be accompanied by an equal image and laser beam rotation about the line-of-sight.

#### Concept C2

Another concept considered, shown in Figure 4.3.3.1-3, is considerably more complex but features the advantage of providing LOS stability by one-to-one inertial stabilization of two relatively small folding mirrors, each gimballed in one axis. An afocal telescope with a magnification of 2 is used to compensate for the two-to-one ratio of LOS



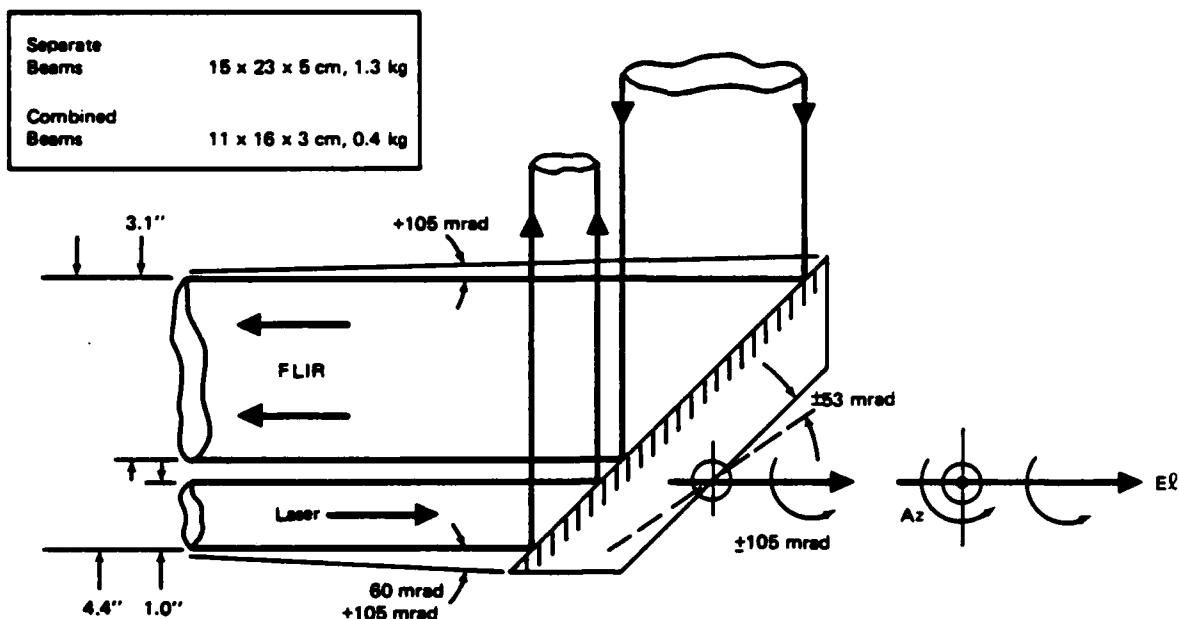


Figure 4.3.3.1-2a. C1 Common Mirror Stabilization

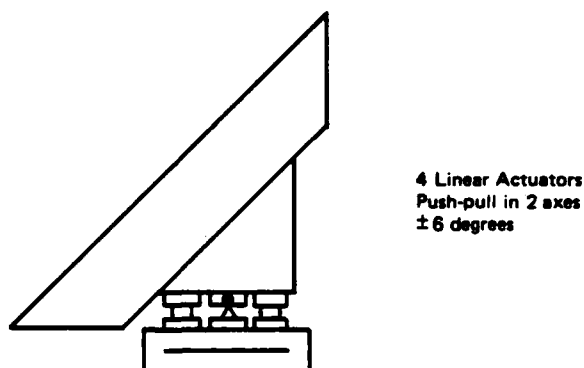


Figure 4.3.3.1-2b. Linear Actuation for C1 Mirror

Figure 4.3.3.1-3. Single Mirror Stabilization of FLIR and Laser

motion. All optics, the FLIR, and the laser are rigidly tied together. Only mirrors M1 and M3 are gimbaled to allow inertial stabilization. M1 compensates for motion about one axis (e.g., elevation) and M3 compensates for motion about the orthogonal axis (e.g., azimuth). The extra fold through M2 is required to allow true inertial stabilization of M3 about the azimuth axis with a gimbal axis parallel to the mirror reflecting surface (i.e., the one-to-one stabilization of the Az mirror results in an effective two-for-one Az LOS motion to compensate for the X2 telescope).



Note that the FLIR sensor optics  $f/\# \sim 1.2$  must be met or exceeded by the telescope objective. The FLIR optics are then replaced by a factor of two shorter focal length objective with  $f/\# > 1.2$ . The laser divergence values must be increased a factor of two to compensate for the X2 demagnification which will occur as the beam passes through the telescope.

Furthermore, the telescope objective and secondary must be increased in size to accommodate the diverging laser beam. Assuming that the laser starts out at 1.25 cm diameter with 240 mrad divergence, 15 cm from the telescope secondary, we find the following:

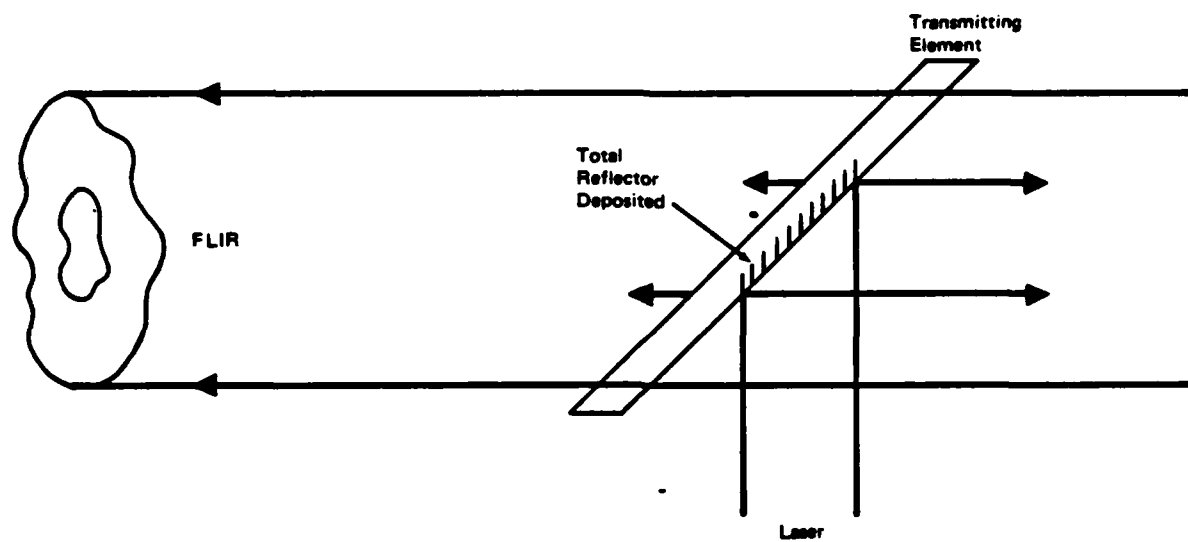
<u>Leaving</u>	<u>Beam Diameter</u>	<u>Divergence</u>
Laser	1.25 cm	240 mrad
Secondary L <sub>2</sub>	4.85 cm	1120 mrad
Primary L <sub>1</sub>	10.8 cm	120 mrad

Thus the technique requires about 25 percent larger aperture size and a minimum of three sizable mirrors to accomplish the job. The alternative approach C1 requires only a single large mirror and appears considerably simpler to implement.

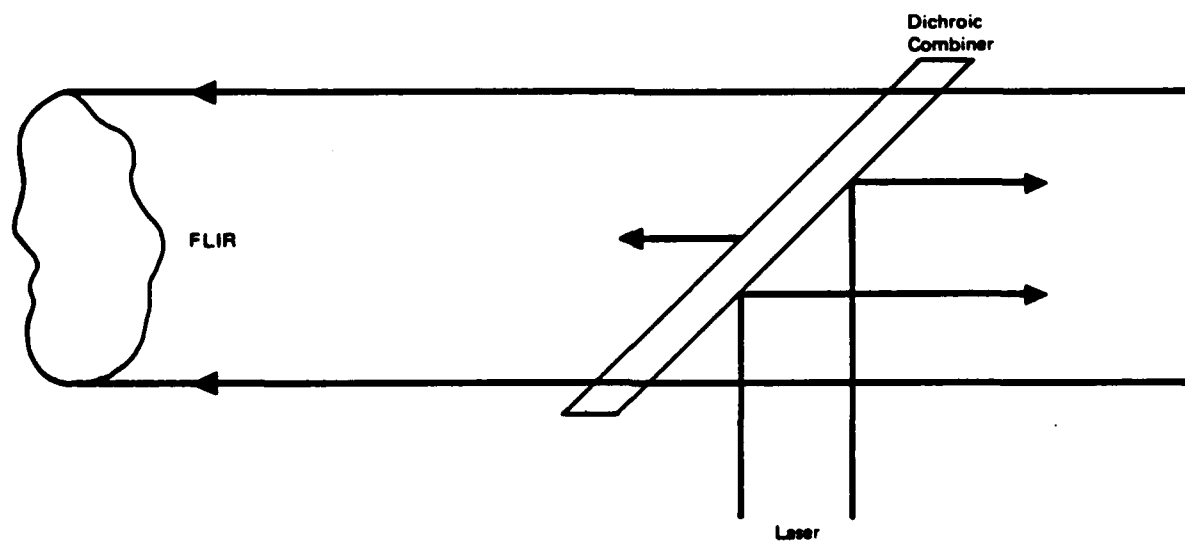
Other stabilization concepts were considered such as the coelostat and variable prism compensation approaches (Appendix, Reference 6) but both suffered from even greater size and complexity problems than approach C2 above.

#### Concept C3 - Shared Beam-paths

A number of approaches to reducing the optical size requirements by combining transmit and receive paths into common areas of the optical elements - i.e., aperture sharing - are available for use in this application. Two of the simplest are shown in Figure 4.3.3.1-4. The first is a spatial sharing approach which simply introduces a folding mirror into the receive path - obscuring part of the sensor aperture. The second uses a dichroic which reflects the 10.6  $\mu\text{m}$  laser beam and a narrow band of wavelengths around that value, but passes the rest of the 8-to-12  $\mu\text{m}$  IR wavelength band.



a. Aperture Sharing - Spatial



b. Aperture Sharing - Spectral

Figure 4.3.3.1-4. Example Aperture Sharing Techniques

In each case where aperture sharing is used, some risk is introduced into sensor performance due to the inevitable coupling of detectable amounts of scattered laser radiation into the focal plane. This is not an insurmountable technical issue, however, and can be solved through appropriate development efforts.

#### Concept C4 - Belt and Pulley System

MDAC has developed and patented (No. 3, 518, 016) an image stabilization system which uses belt and pulley to stabilize the image in the 2 to 1 mirror axis. The Belt and Pulley system uses a 2 to 1 drive ratio to force the 2 to 1 axis of the steering mirror to rotate at one half the angle of the base. This is accomplished by stabilizing the inner gimbal using a gyro and torque motor. The inner gimbal is coupled to the mirror through a 2 to 1 pulley/belt drive. When the base is moved, the torque required to move the mirror reacts against the stabilized inner gimbal. This reaction, which tends to disturb the inner gimbal, is opposed by the inertia of the inner gimbal. The higher the inertia of the inner gimbal, the lower the stabilization errors due to these reaction torques. In the limit, as the inertia of the inner gimbal becomes very large in comparison to the mirror inertia, this system tends to provide a natural isolation from base motion comparable to that of a gimballed system.

#### 4.3.3.2 Sensor Analysis

The sensor and beam steering configuration is shown in Figure 4.3.3.1-1. The total pointing error will consist of

- Centroid tracking errors
- Turbulence created image blur and
- Misalignment errors

The centroid tracking error due to resolution would be the same as concepts A and B which was  $110 \mu$  rad. The centroid tracking error caused by image blur due to turbulence would, however, be different since the stabilized

mirror has an angular multiplication of two. This would in effect multiply the image blur due to turbulence by a factor of two giving a maximum tracking error due to turbulence of

$$\epsilon_{\text{Turb}} = 68 \mu \text{ rad (day)}$$

Alignment errors of 70 micro-radians are the same as Concept B.

The total error would be the RMS value of the component errors or

$$\begin{aligned}\epsilon_{\text{Tot}} &= \sqrt{\epsilon_{\text{Track}}^2 + \epsilon_{\text{Turb}}^2 + \epsilon_{\text{Align}}^2} \\ &= \sqrt{(110)^2 + (68)^2 + (70)^2} \\ &\approx 147 \mu \text{ rad}\end{aligned}$$

#### 4.3.3.3 Control Analysis

The tracking and stabilization system shown in Figure 4.3.3.3-1 has been configured so that the stabilization and tracking functions are uncoupled. This allows both functions to be treated independently so that two different sets of requirements can be addressed separately to achieve the best overall performance. Both imaging data and gyro information are utilized to take advantage of the characteristics of each sensor. The gyros are used to sense the high frequency gunner motion and "stabilize" the optical line-of-sight to the target line of sight. The target line-of-sight is continuously updated by the low frequency, drift free imaging sensor data to "track" the target line-of-sight. The use of both sensors also allows the target line-of-sight rate required for missile guidance to be extracted from the combination of gunner and target motion.

The gyros are operated in a rebalance mode to obtain the optimum performance which is achieved when the gyros operate at or near null. In this configuration, the output from the rebalance electronics is a signal proportional to the inertial rate of the base assembly. Addition of the gimbal rate information to the gyro signal provides an estimate of the line-of-sight rate.

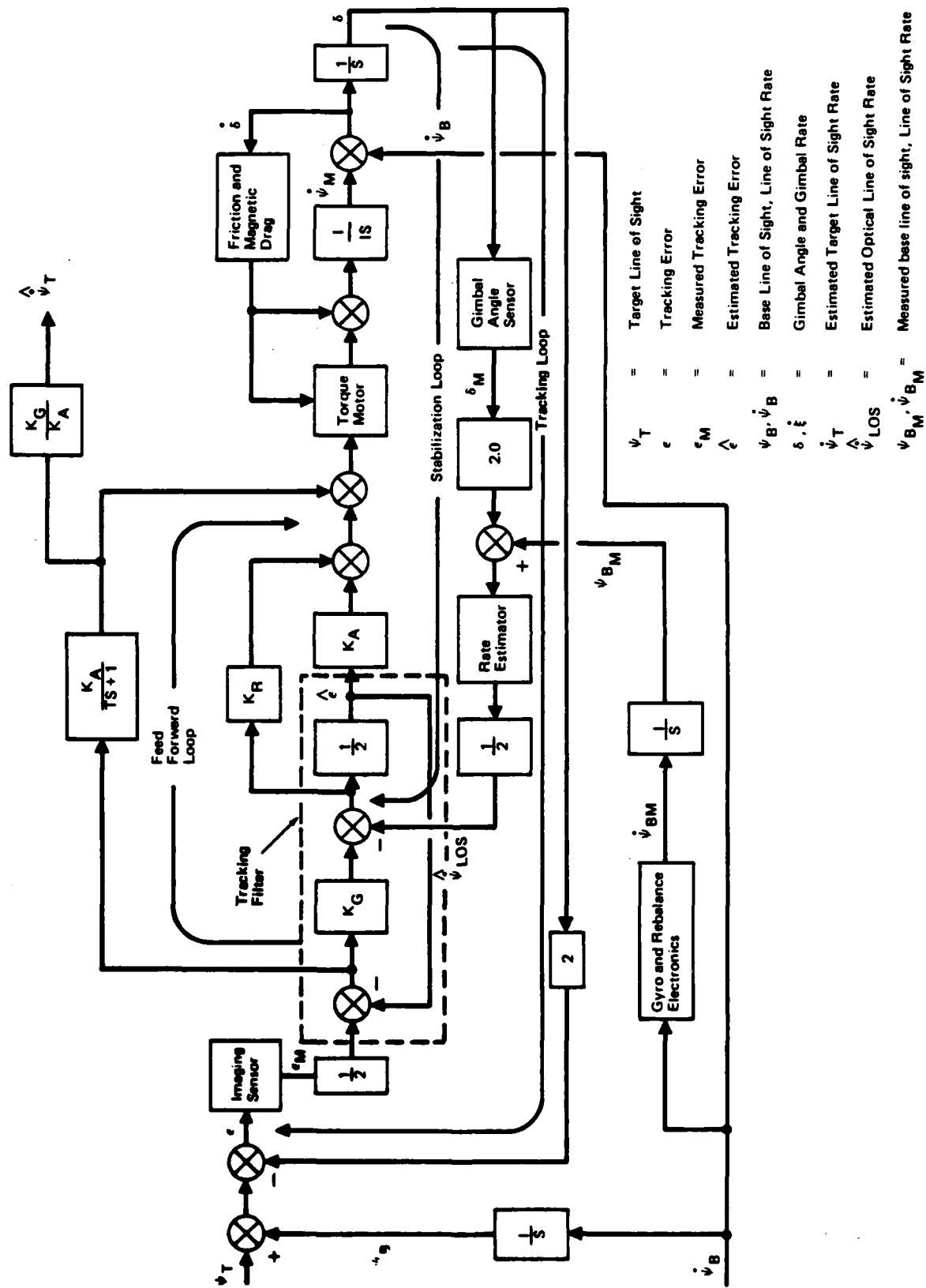


Figure 4.3.3-1a. Common Mirror Concept

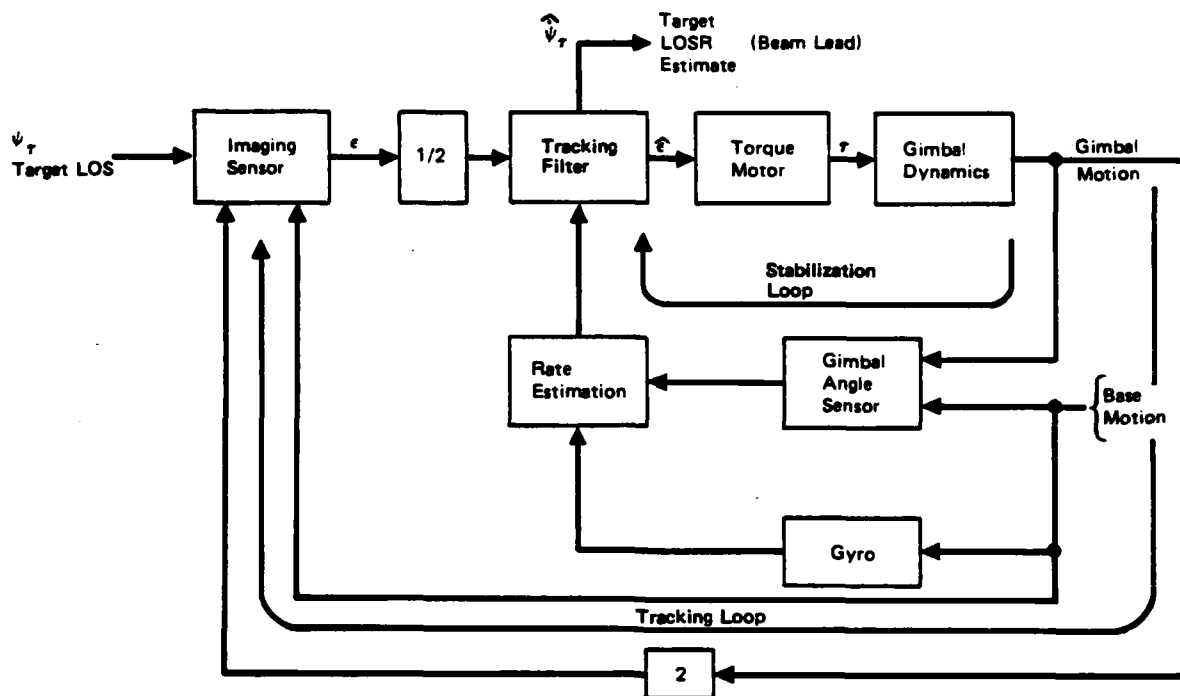


Figure 4.3.3-1b. Common Mirror Concept

The line-of-sight rate estimate is input to the tracking filter consisting of an integrator which is slaved to the imaging sensor output. In this configuration, the system acts as a second order stabilization loop in response to gunner motion since the transfer function of the integrator output to base motion input is ideally unity. Because the gyro and gimbal angle sensors are relatively high frequency devices compared to the scene tracker, the stabilization loop frequency can be made high enough to respond to gunner motion and provide optimum performance. The stabilization loop provides a stable base from which the target can be tracked using the imaging sensor information. The line-of-sight reference is continuously updated through the tracking filter, which is used to attenuate imaging sensor noise. The scene tracker bandwidth, although not high enough to provide stabilization, is more than adequate to provide line-of-sight information of the low frequency target.

The feed forward loop serves two purposes:

- By increasing the type of the control system, it allows the system to track a moving target with no "hang off error."
- It provides line-of-sight rate for the missile guidance system.



Analysis of the common mirror concept was performed to determine: Torque requirements; power requirements; and accuracy for the final evaluation. Torque and power requirements ultimately appear in the concept selection as weight, and it is this factor that directly influences the final selection. In addition to using analytical techniques to estimate system accuracy, a digital simulation was used to provide a more in-depth indication of system performance to substantiate the analytical results.

### Torque Requirements

A simplified single axis block diagram of the common mirror system is shown in Figure 4.3.3-2. The block diagram represents the axis in which there is a two to one optical gain in the steering mirror configuration. It is this axis that is discussed in this section since the one to one axis has the same characteristics as the gimbal system discussed in Section 4.3.2.3 and all discussions in that section apply to the one to one axis of the common mirror configuration. Because of the limited angular freedom ( $\pm 6$  degrees) the two axes can be treated independently with no significant error.

The torque requirements were determined as a function of both system bandwidth and gimbal inertia. The maximum torque requirements occur during the target acquisition transient which is a function of two parameters:

1. The maximum line-of-sight rate of a crossing target and
2. the maximum gunner tracking error that exists when auto-track is initiated.

The maximum torque required to acquire and track a crossing target is computed from the following transfer function:

$$\frac{T(s)}{\psi_T(s)} = \frac{0.5s^2 [(K_A + K_G K_R)s + K_A K_G]}{(s + K_G) (s^2 + \frac{KR}{I}s + \frac{KA}{I})}$$

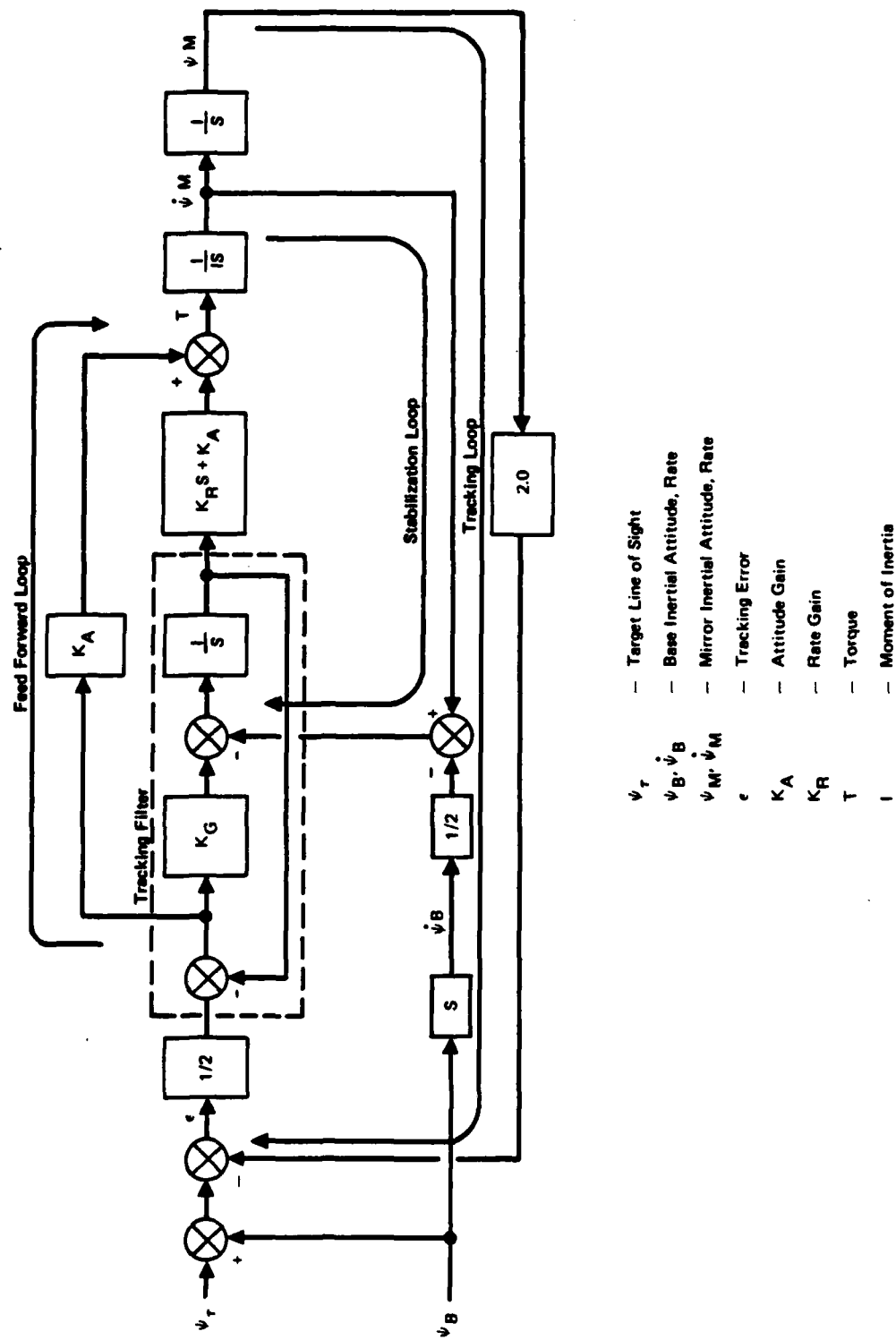


Figure 4.3.3-2. Simplified Block Diagram

OR

$$\frac{T(S)}{\Psi_T(S)} = \frac{0.5 (K_A + K_G K_R) S^2 (S + \frac{K_A K_G}{K_A + K_G K_R})}{(S + K_G) (S^2 + \frac{K_R}{I} S + \frac{K_A}{I})}$$

let

$$\frac{K_A}{I} = W_N^2 \quad (W_N = \text{The natural frequency of the stabilization loop})$$

and

$$\frac{K_R}{I} = 2\zeta W_N \quad (\zeta = \text{damping ratio})$$

then

$$\frac{T(S)}{\Psi_T(S)} = \frac{0.5 I S^2 (W_N^2 + 2\zeta W_N K_G) (S + \frac{W_N^2 K_G}{W_N^2 + 2\zeta W_N K_G})}{(S + K_G) (S^2 + 2\zeta W_N S + W_N^2)}$$

To achieve the desired pointing accuracy for this system it will be true that

$$W_N^2 \gg 2\zeta W_N K_G$$

Therefore the torque to target line-of-sight transfer function can be approximated as:

$$\frac{T(S)}{\Psi(S)} \approx \frac{0.5 I W_N^2 S^2}{S^2 + 2\zeta W_N S + W_N^2}$$

A crossing target can be represented as a ramp line-of-sight input to the control system,

$$\Psi(S) = \frac{A}{S^2}$$

and the torque to inertia ratio becomes,

$$\frac{T(S)}{I} \approx \frac{0.5 A W_N^2}{S^2 + 2\zeta W_N S + W_N^2}$$

The time response for this transfer function is:

$$\frac{T}{I} = \frac{0.5A W_N}{\sqrt{1-\zeta^2}} e^{-\zeta W_N t} \sin [(W_N \sqrt{1-\zeta^2}) t]$$

The maximum amplitude occurs when

$$\zeta W_N t = \frac{\pi}{4} \text{ or } t = \frac{\pi}{4\zeta W_N}$$

For  $\zeta = 0.707$ ,

$$\frac{T}{I} (\text{MAX}) = 0.228A W_N.$$

The target line-of-sight rate  $A = \frac{V}{R} \frac{(\text{Velocity})}{(\text{Range})}$ .

For a target crossing at 11 meters per second

$$\frac{T}{I} (\text{MAX}) = \frac{2.5 W_N}{R} \quad (R \text{ in meters})$$

Or

$$\frac{T}{I} (\text{MAX}) = \frac{15.7 F_N}{R} \quad (F_N = \frac{W_N}{2\pi})$$

This ratio is shown as a function of  $F_N^2$  the stabilization loop natural frequency, in Figure 4.3.3.3-3 for a target crossing at a range of 20 meters. The torque to inertia requirements for the common gimbal system is also shown. The common mirror system requires half the torque of the common gimbal because of the 2 to 1 optical steering mirror. This is one advantage of steering mirror concepts.

The torque required to prevent saturation when automatic tracking is initiated is

$$T = K_A E_G \quad ; \quad E_G = \text{Gunner pointing error at initiation}$$

Or 
$$\frac{T}{I} = W_N^2 E_G$$

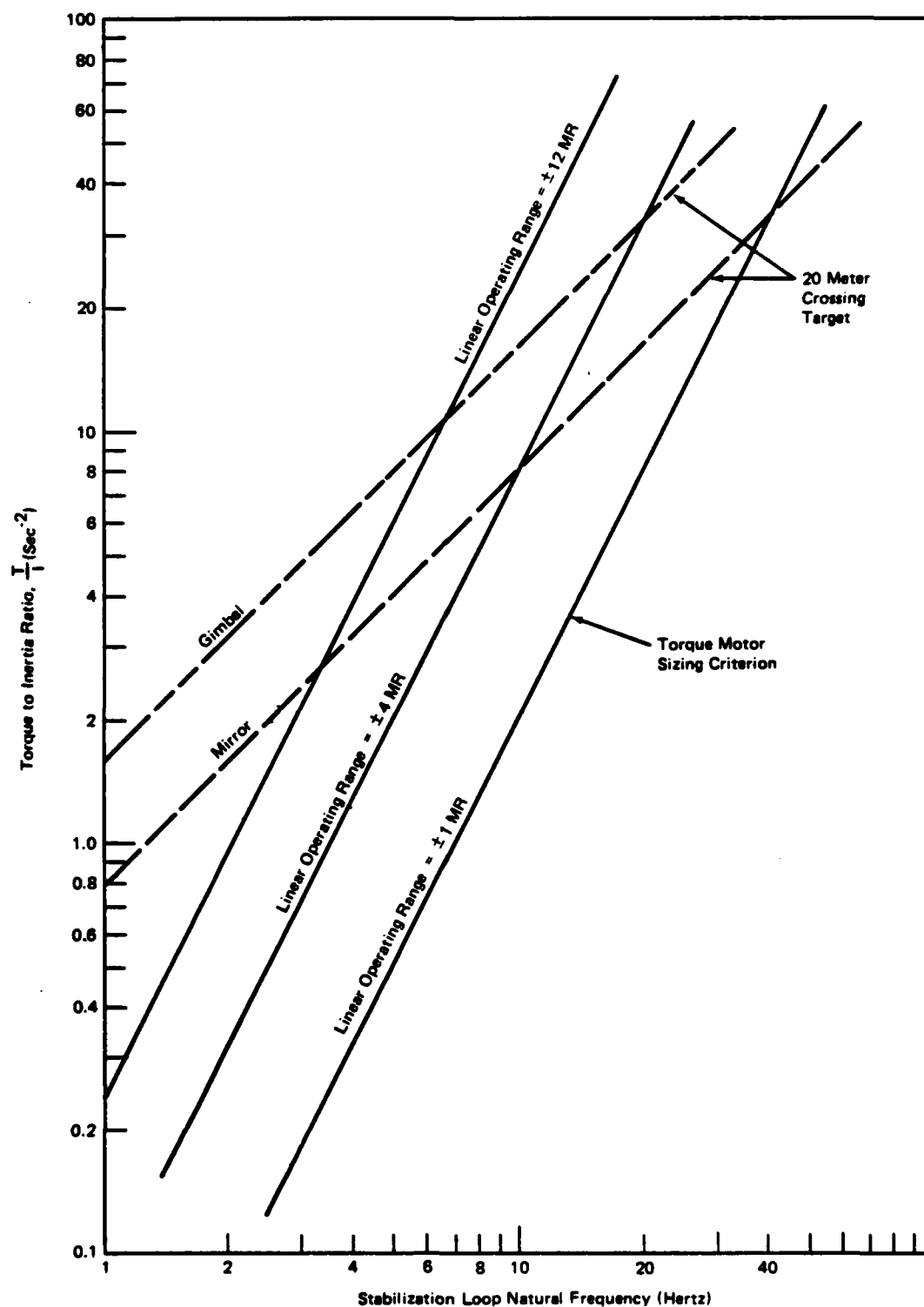


Figure 4.3.3.3-3. Torque Motor Sizing Criteria

The value of  $E_G$  used to size the torque motor defines the linear operating range for the system. The torque to inertia requirements for a linear operating range of 1, 4 and 12 milliradians are shown in Figure 4.3.3.3-3. The 12 milliradian case represents a three sigma pointing error for the gunner error model used in this study. A control system natural frequency in the range of 20 to 30 Hertz is required to achieve the best performance for the system. In this frequency range a 12 milliradian linear operating capability requires torque motor sizes which are impractical for a man portable system. Since it is undesirable to operate with the system largely over-saturated, a practical solution is to provide an acquisition mode in which the system operates at a lower than optimum natural frequency until the error is reduced to a predetermined level at which time the system will automatically switch to the track mode where it will operate at the higher optimum frequency. Once the system is operating in the track mode, the tracking errors will be small.

A linear operating range of  $\pm 1$  milliradian provides for 10 sigma tracking error transients which should be more than adequate. With this value of torque available, an acquisition frequency that is 25% of the tracking frequency will provide more than the desired 12 milliradian linear acquisition range and will provide adequate capability to acquire the short range crossing target. The torque to inertia ratio providing a 1 milliradian linear operating range during the track mode was used to evaluate the common mirror design concept.

The moments of inertia for the common mirror system were estimated as:

0.64 oz-in-sec <sup>2</sup>	for the 2 to 1 axis
0.61 oz-in-sec <sup>2</sup>	for the 1 to 1 axis

Using a stabilization natural frequency of 30 hertz (see section under accuracy), results in the following torque motor requirements:

10 oz-in	for the 2 to 1 axis
20 oz-in	for the 1 to 1 axis

### Power Requirements

Steering mirror concepts require continuous torquing of the steering mirror to compensate for base motion even in the absence of friction torques. For every degree of base motion, the mirror must move 0.5 degree to maintain the line-of-sight in a fixed inertial attitude. The power required can be estimated by determining the torque required in steady state tracking to continuously compensate for gunner motion. The torque to base motion (Figure 4.3.3.3-1) transfer function is

$$\frac{T(S)}{\Psi_B(S)} = \frac{0.5S^2 (K_R S + K_A)}{S^2 + \frac{KR}{I} S + \frac{K_A}{I}}$$

Or

$$\frac{T(S)}{\Psi_B(S)} = \frac{0.5S^2 I (2\zeta W_N S + W_N^2)}{S^2 + 2\zeta W_N S + W_N^2}$$

For a sinusoidal base motion input

$$\Psi_B(S) = \frac{A\lambda}{S^2 + \lambda^2}$$

And

$$\frac{T(S)}{I} = \frac{0.5A\lambda S (2\zeta W_N S + W_N^2)}{(S^2 + \lambda^2) (S^2 + 2\zeta W_N S + W_N^2)}$$

Or

$$\frac{T(S)}{I} = \frac{A\lambda\zeta W_N S (S + \frac{W_N}{2})}{(S^2 + \lambda^2) (S^2 + 2\zeta W_N S + W_N^2)}$$

The steady state value of the transfer function is a sinusoid whose frequency is  $\lambda$  and whose amplitude is:

$$\left| \frac{T}{I} \right|_{\text{peak}} = A\zeta W_N \left[ \frac{\left( \frac{W_N \lambda^2}{2\zeta} \right)^2 + \lambda^6}{(2\zeta W_N \lambda)^2 + (W_N^2 - \lambda^2)^2} \right]^{1/2}$$

Power is proportional to torque squared. Using the gunner jitter model for this study

$$A = 0.004 \sqrt{2} \text{ Radians}$$

$$\lambda = 4\pi \text{ Radians}$$

The square of the torque to inertia ratio as a function of control system natural frequency is shown in Figure 4.3.3.3-4. The same parameter is shown for the common gimbal system for comparison. The power requirements for the common mirror system will be significantly higher than the gimbal system unless the inertia of the steering mirror is significantly less than the gimbal inertia.

### 3. Accuracy

Two sources of error predominate in defining system accuracy: imaging sensor errors and base motion disturbances. Imaging sensor errors are of two types, bias and random. The bias error is caused by the steady state error in the ability to define a desired aimpoint. This error is the same for all four candidate systems and therefore has no influence on the final selection.

The tracking error resulting from the random error source (sensor noise) increases with the control system natural frequency. The dynamic error which results from base motion decreases with increasing control system natural frequency. To a first order approximation, the performance of the system is optimized by selecting the control system natural frequency that minimizes the total tracking error from these two sources.

The transfer function of dynamic error due to base motion (Figure 4.3.3.3-2) is:

$$\frac{\epsilon(s)}{\psi_B(s)} = \frac{s^2}{s^2 + 2\zeta\omega_N s + \omega_N^2}$$



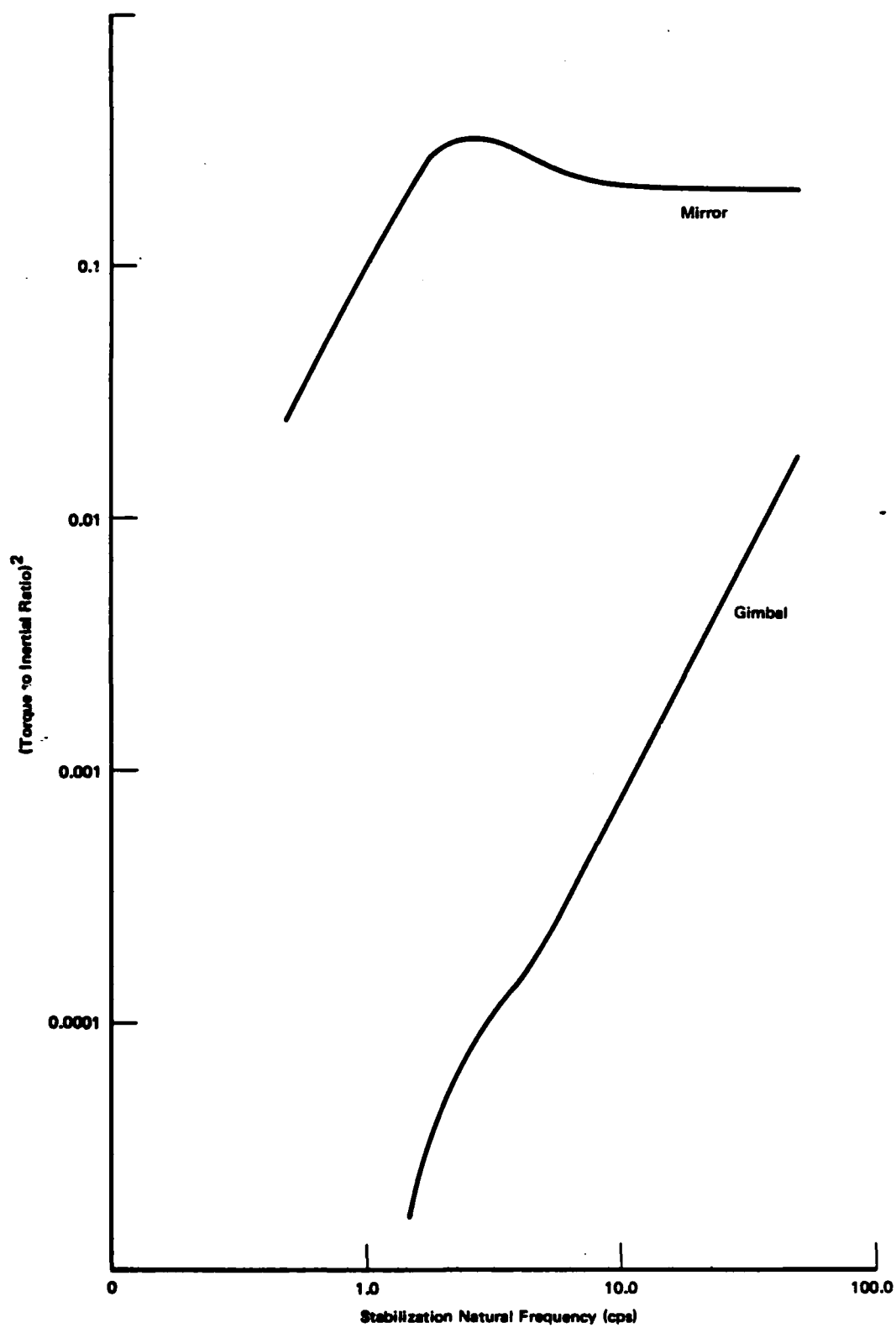


Figure 4.3.3.3-4. Power Requirements

(The error due to friction has been neglected here since it is a second order effect in the two to one optical axis. Friction is the prime error source in the one to one axis and in the gimbal systems).

Using a 4 milliradian sinusoidal base motion

$$\psi_B(s) = \frac{4\lambda}{s^2 + \lambda^2} \quad \lambda = 4 \pi \text{ Rad/Sec}$$

And

$$\epsilon(s) = \frac{4\lambda s^2}{(s^2 + \lambda^2)(s^2 + 2\zeta W_N s + W_N^2)}$$

The steady state value of this transfer function is a sinusoid of frequency  $\lambda$  whose RMS value is

$$\epsilon_{\text{RMS}} = 4.0 \left[ \frac{\lambda^4}{(2\zeta W_N \lambda)^2 + (W_N^2 - \lambda^2)^2} \right]^{1/2} \quad (\text{milliradians})$$

A plot of this dynamic error as a function of the stabilization loop natural frequency ( $f_N = W_N/2\pi$ ) is shown in Figure 4.3.3.3-5.

The error due to sensor noise was analyzed using covariance analysis techniques programmed on a digital computer. The block diagram in Figure 4.3.3.3-6 was used to determine the RMS error due to sensor noise. This block diagram includes the effect of sampling at 60 times per second and a first order filter in the feed forward loop. This filter does not affect the steady state dynamic error discussed previously but does reduce the tracking error caused by sensor noise. The bandwidth of this filter and the tracking loop filter are selected on the basis of target dynamics, transient performance and stability considerations. From our experience on the IMAAWS IRAD program, a 1 hertz bandwidth in both filters provided good transient performance and stability margin. It is also high enough to encompass the anticipated low frequency dynamics of the target which should be much less than 1 hertz. Figure 4.3.3.3-5 shows the resultant RMS error due to sensor noise as a function of the

## Analytical Results

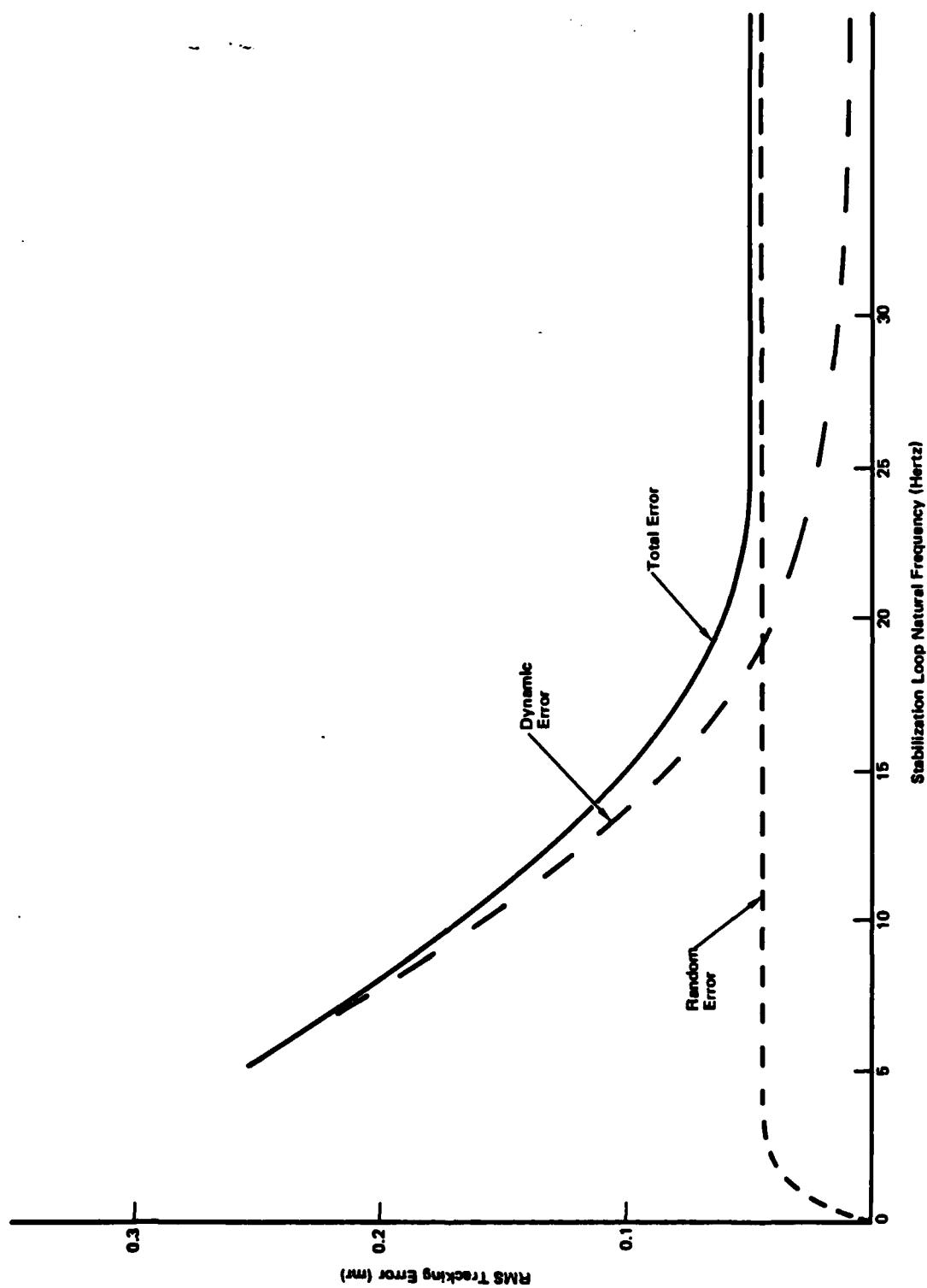
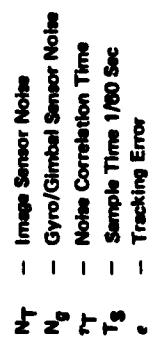


Figure 4.3.3.3-5. Accuracy



#### Figure 4.3.3.3.6. Covariance Analysis Model

stabilization loop natural frequency. The resultant total RMS error is also shown in the figure. The optimum stabilization loop frequency is around 30 hertz.

Tracking error due to gyro drift, gyro noise and gimbal angle sensor noise were also investigated. Tracking errors due to these sources were at least an order of magnitude less than the error from the image sensor noise and therefore had an insignificant affect on the overall accuracy.

A simulation of the steering mirror concept was made so that the effects of nonlinearities such as transport lags of the imaging sensors and magnetic drag in the DC torquers could be included in the accuracy estimate. Bearing friction was found to be negligible in comparison to the torque motor magnetic drag which was the predominant coupling effect. A first order Dahl model was used to simulate the magnetic drag.

The peak torque used in the Dahl model was 1% of the peak torque motor output. This was the value estimated by Aeroflex Laboratories Incorporated, manufacturers of brushless D.C. torquers used in this type of system. The slope of the Dahl model was chosen so that 90% of the peak torque was reached after 20 degrees of travel, a figure also supplied by Aeroflex.

The imaging sensor was modeled with a 1 sample ( $\frac{1}{60}$  sec) transport delay; a sample to sample RMS error of 130 micro-radians; and a first order sample and hold. The sample to sample RMS error of 130 micro-radians includes the effect of image resolution and turbulence discussed in Section 4.3.3.2. Alignment errors are treated in Section 4.3.5.1, Accuracy. Gyro drift, gyro noise and gimbal angle sensor noise were also included.

A comparison of the stabilization loop optimization for the analytical and simulation results are shown in Figure 4.3.3.3-7. The results of the simulation agree fairly well with the analytical results. A time history of the tracking error is shown in Figure 4.3.3.3-8. The transient performance is well behaved as shown in the plot of the tracking error transient for a crossing target (Figure 4.3.3.3-9).

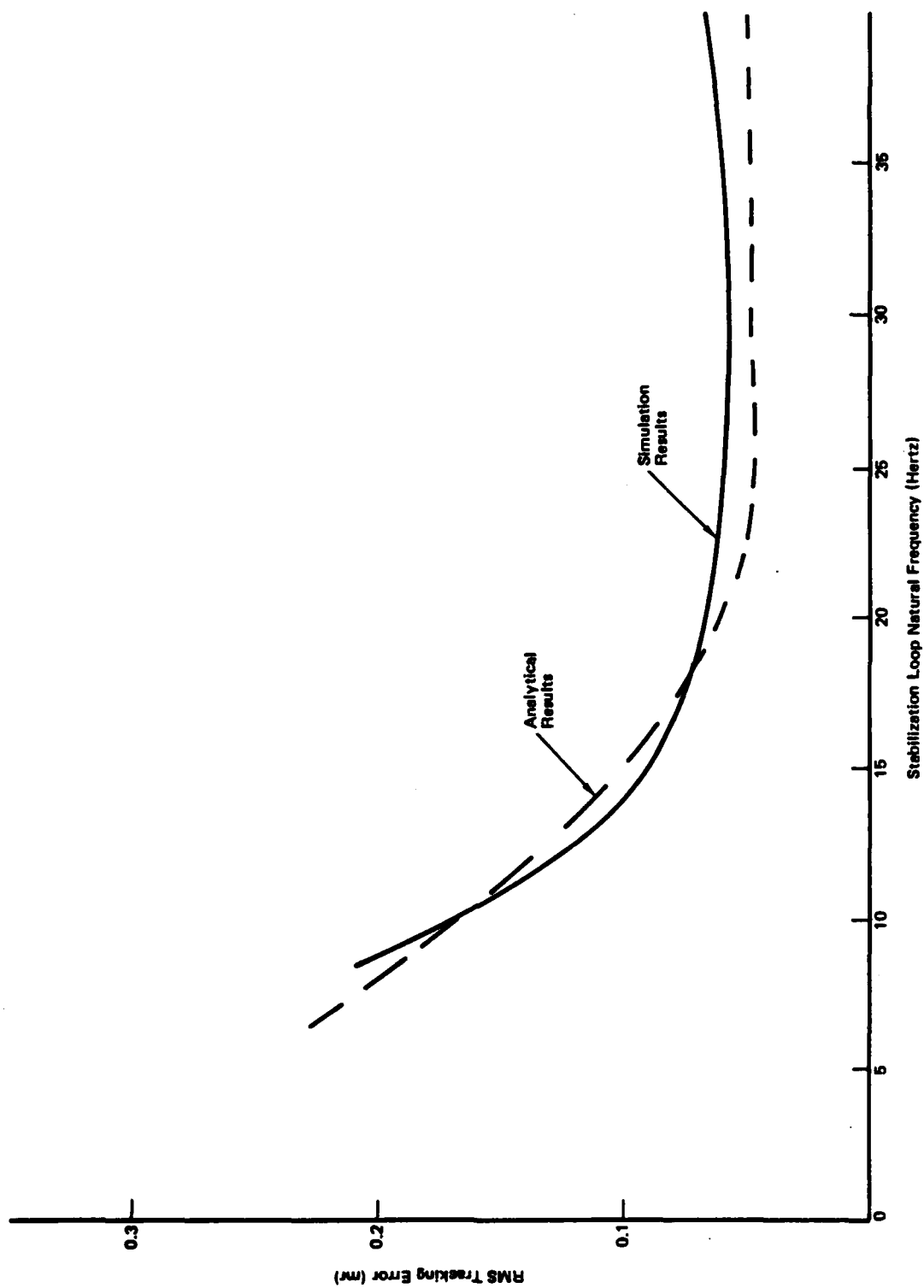


Figure 4.3.3.2-7. Comparison of Analytical &amp; Simulation Results

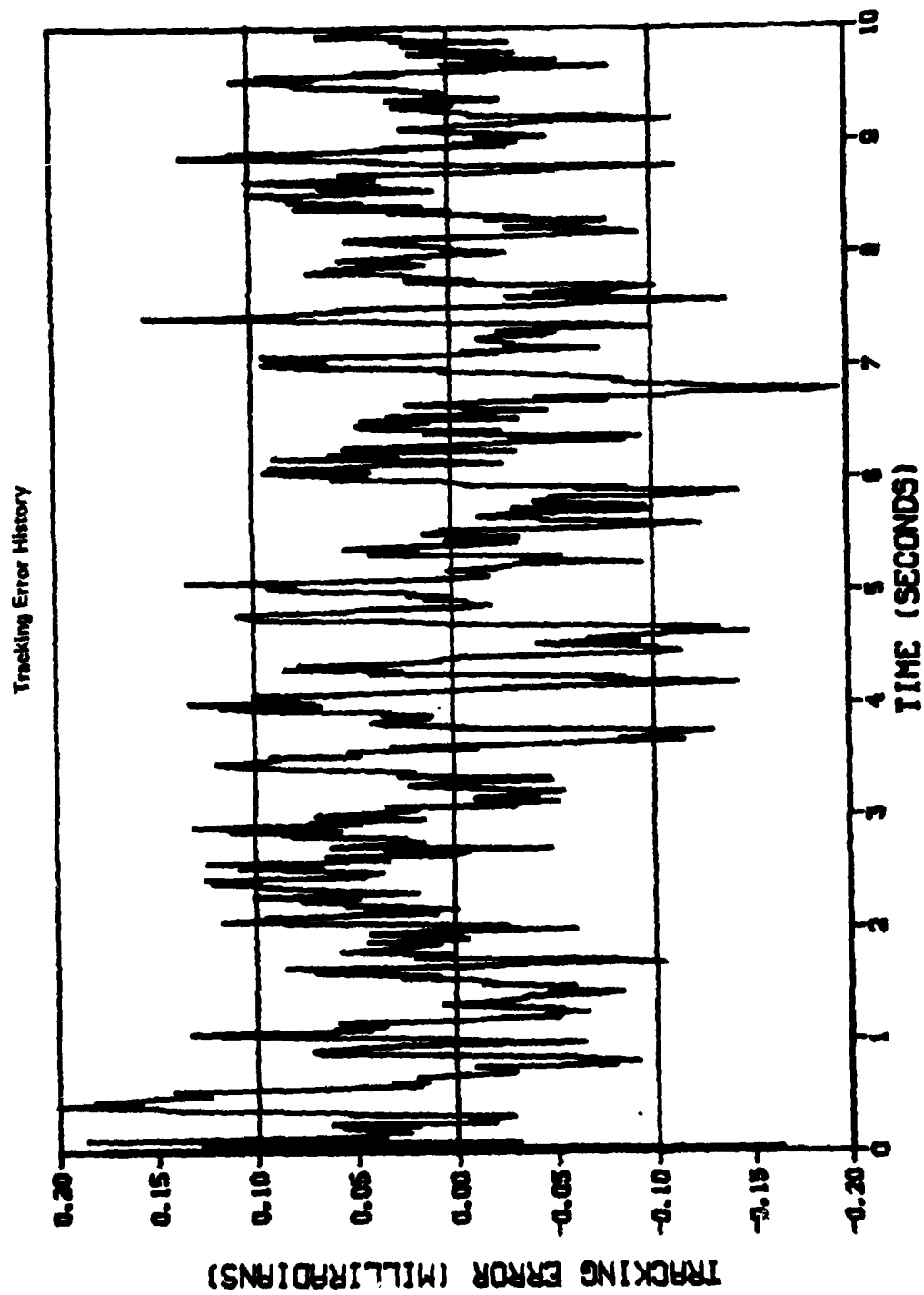


Figure 4.3.3.3-8. Tracking Error History

**TRANSIENT RESPONSE**

**(MOVING TARGET-11 M/SEC AT 20 METERS RANGE)**

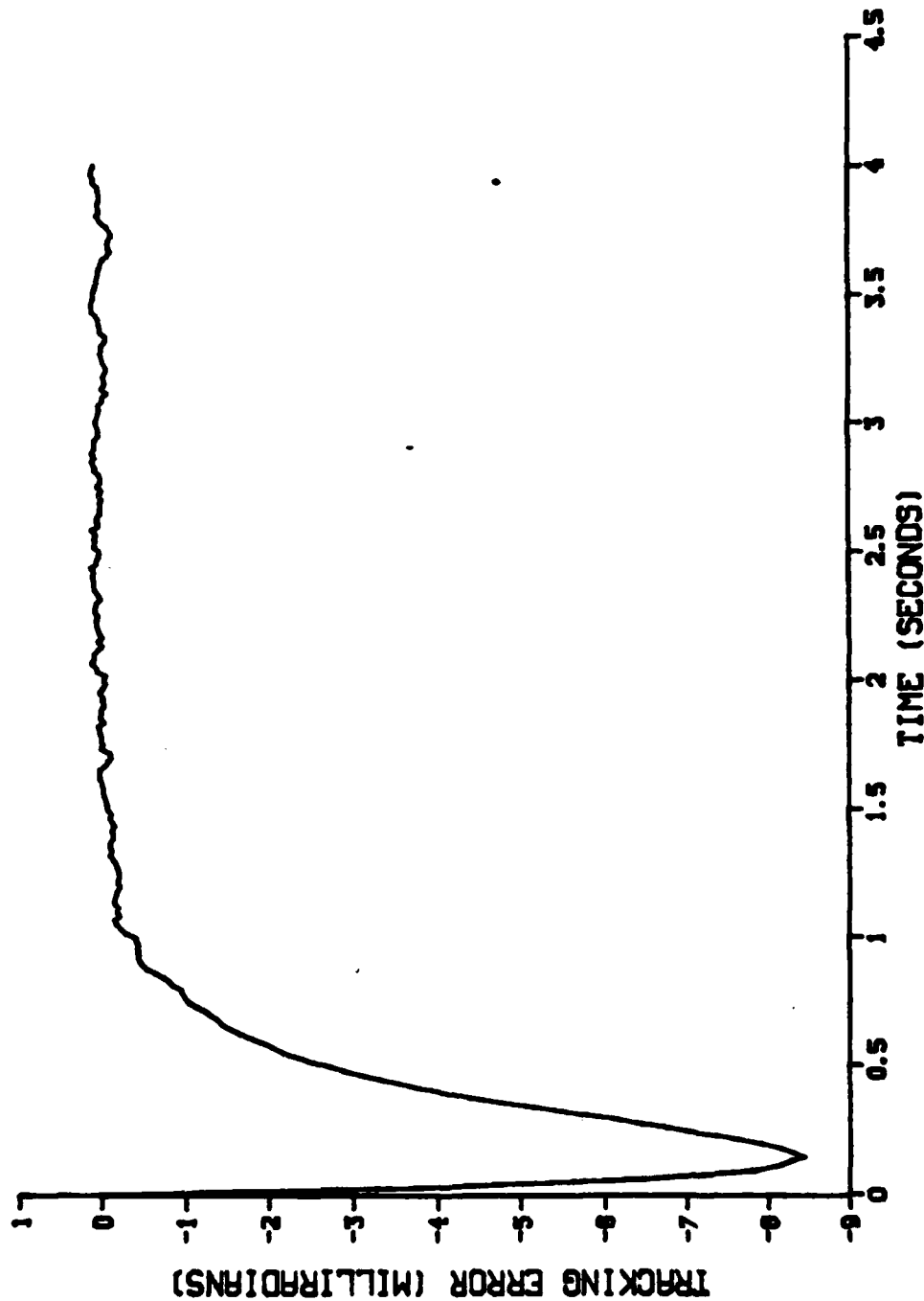


Figure 4.3.3-9. Crossing Target Transient Response



#### 4.3.4 Candidate D (Sensor Fixed)

##### 4.3.4.1 Concept Description

A functional block diagram of Candidate D is shown in Figure 4.3.4.1-1. With this candidate, the sensor is fixed (not stabilized) and is aimed by the operator, and the laser beam is pointed by a stabilized mirror. This mirror is made to track the target position by completing the loop from the video tracker to the gimbal torquers. It is not necessary that the target image be in the center of the sensor FOV for the gimbal to point the laser to the target aimpoint position. Through electronic feedback from the control system processing to the image display, the target position can always be made to be displayed at the display screen center.

In Candidate D, since the tracker is not stabilized, the sensor will require an enlarged scan field by nearly a factor of two. The baseline FLIR (Candidates A, B & C) utilizes a sensor scan field of  $2^\circ$  elev X  $4^\circ$  az. Doubling this field would require a  $4^\circ$  X  $8^\circ$  scan to achieve adequate angular coverage for the unstabilized imager. Increasing the scan field would degrade the

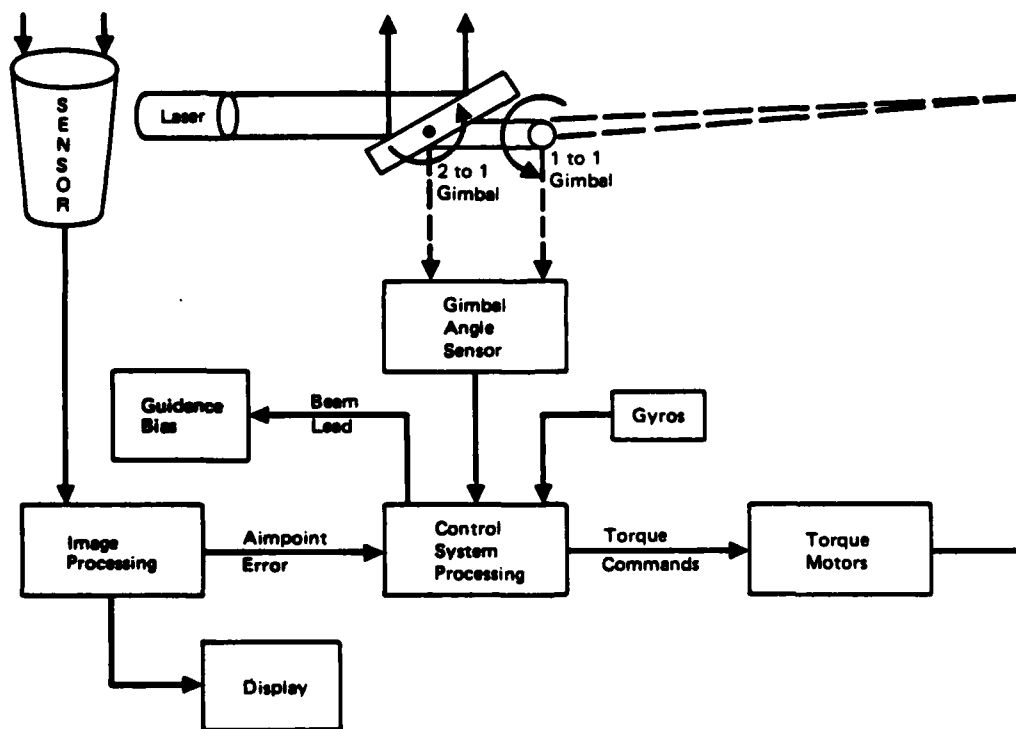


Figure 4.3.4.1-1. Functional Diagram, Fixed Sensor/Steering Mirror Concept

sensor performance somewhat. The detector dwell time on the target would be reduced by a factor of 4. This will necessitate an increase in video bandwidth, resulting in system sensitivity and signal to noise reduction, by a factor of 2. To compensate for this loss it will be necessary to increase the sensor aperture by a factor of  $\sqrt{2}$ .

Decreasing the focal plane dwell time by a factor of 4 will require scanning the sensor at a rate 4 times faster. This would probably result in significantly higher development costs for the sensor and data processing, compared to A, B or C. This could have a significant effect on the sensor production cost. The sensor would likely cost at least 20% more than for the other candidate configurations.

Additional sensor weight could amount to a 4 oz. (112 gm) increase due to the larger aperture lens, plus some small weight increase in the scanner/focal plane area.

Many techniques for beam stabilization and steering are available for use with the smaller laser beam. Two approaches are shown in figure 4.3.4.1-2.

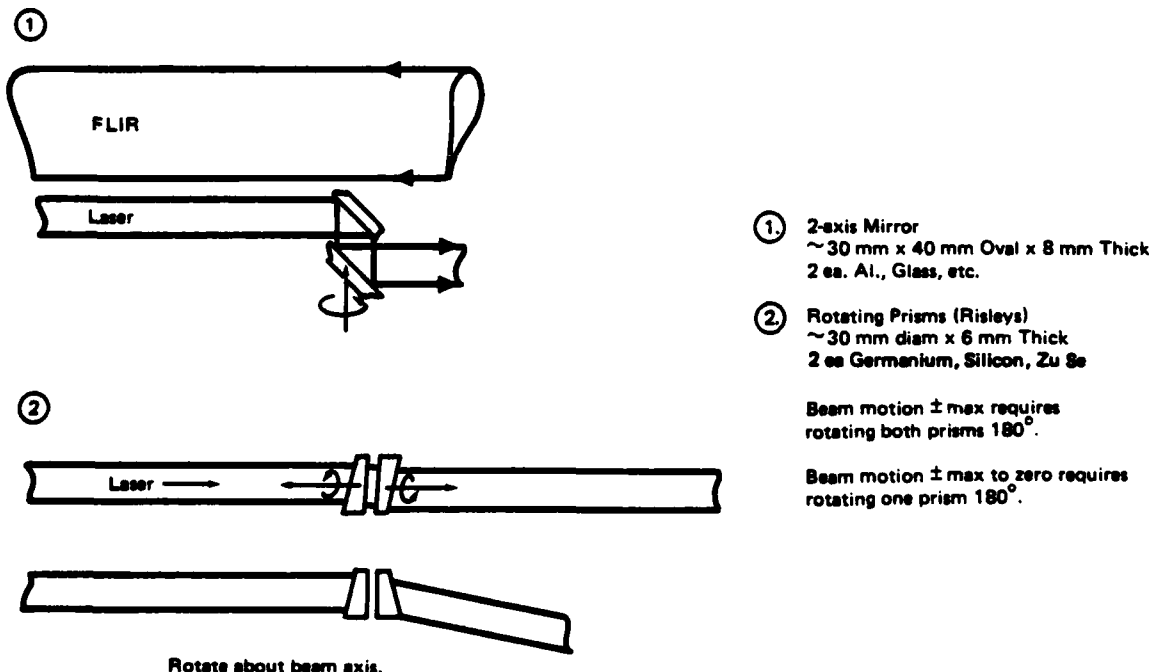


Figure 4.3.4.1-2. Laser Stabilized With Mirror (Candidate "D")

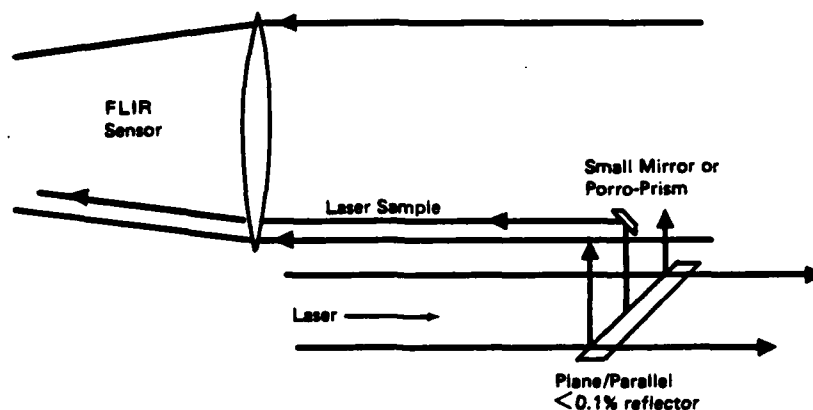
The first is simply the analog of one of the approaches for Candidate C, described in section 4.3.3.1, and requires a minimum of one diagonal mirror with dimensions of about 4.8cm x 7.7cm x 1.5cm and a mass of approximately 40 grams.

The second approach is less straight forward and is based upon the variable effective wedge angle which can be achieved by rotating two prisms relative to one another. The required transformation for beam steering in two axes is not complicated, but may turn out to be excessive in cross coupling. The optical elements are of low inertia due to the rotation through the symmetry axis of the circular cross section prism.

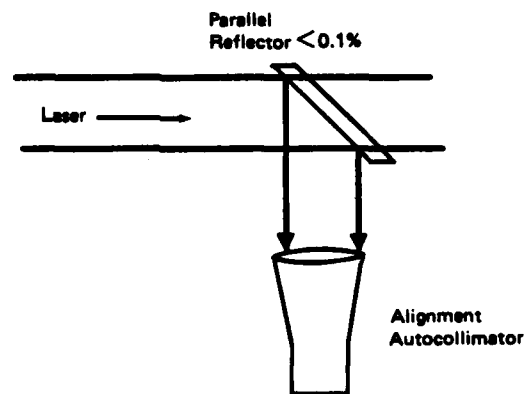
For this reason, the use of an optical feedback technique was considered. Two general approaches are shown in figure 4.3.4.1-3. In the first approach the FLIR is used as the alignment monitor and the accuracy of the beam position measurement is limited only by the mechanical stability of the folding optics and by the resolution of the FLIR.

The second approach uses an additional alignment measuring instrument to measure beam position and will give an accurate azimuth and elevation error signal using a cheap, simple instrument. It's only drawback, which is probably minor, is the additional mechanical alignment error between the IR sensor axis and the alignment autocollimator. This error is no larger than that associated with the additional folding mirror required in the first approach discussed above. No modification of the IR sensor is required, as would be the case with the first approach.

Pointing accuracy for this candidate is effected directly by the accuracy with which the laser beam direction, with respect to the sensor boresight, can be measured for pointing control. It is difficult to design a light but rugged mechanical angle pickoff having micro radian accuracy over a 3 or 4 degree angular range.



a. Auto-Sampling



b. Alignment Sensing Instrumentation

Figure 4.3.4.1-3. Laser Beam Alignment Monitoring (Concept D)

#### 4.3.4.2 Sensor Analysis

Because the IR sensor would not be stabilized in Candidate D, some blurring of the scene would occur with image motion. It is felt that the scene jitter due to the operator could cause an error in image position determination of up to 3 resolution elements. This would cause centroid tracking precision to be degraded by almost a factor of three compared with a stabilized tracking sensor such as Candidate B. This would result in an approximate centroid track error of

$$\epsilon_{\text{TRACK}} = 330 \text{ } \mu\text{rad.}$$

The pointing error due to turbulence would be the same as for Candidate B already discussed which was

$$\epsilon_{\text{Turb}} = 34 \text{ } \mu\text{rad.}$$

The alignment error is assumed to be a total of 81  $\mu$ radian which would be approximately equivalent to that calculated for Candidate A as discussed in Section 4.3.1.2 or

$$\epsilon_{\text{ALIGNMENT}} = 81 \text{ } \mu\text{rad.}$$

The total tracking error would be the RMS combination of the above individual errors or

$$\begin{aligned} \text{TOTAL} &= \sqrt{\epsilon^2_{\text{TRACK}} + \epsilon^2_{\text{TURB}} + \epsilon^2_{\text{ALIGN}}} \\ &= \sqrt{(330)^2 + (34)^2 + (81)^2} \\ &\sim 341 \text{ } \mu\text{rad } (1\sigma). \end{aligned}$$

The transfer function of Candidate D would be the same as for all other candidates which was

$$F(s) = e^{-TS}$$

#### 4.3.4.3 Control Analysis

From a control analysis viewpoint this concept is functionally identical to the common mirror concept (Configuration C) discussed in Section 4.3.3.3. The analyses used to define the normalized torque to inertia and power to inertia ratios in Section 4.3.3.3 are applicable to this concept. The actual torquer size and power requirements for this concept are lower due to the smaller moment of inertia of the steering mirror. The moments of inertia for this system were estimated as:

$$\begin{array}{ll} 2.3 \times 10^{-3} \text{ oz-in-sec}^2 & \text{in the 2 to 1 axis} \\ 2.1 \times 10^{-3} \text{ oz-in-sec}^2 & \text{in the 1 to 1 axis} \end{array}$$

Using a 30 hertz natural frequency for the stabilization loop results in a maximum torque requirement of

0.04 oz-in	in the 2 to 1 axis
0.08 oz-in	in the 1 to 1 axis

These values are smaller than off the shelf hardware. A value of 0.5 oz-in was used in both axis as a torque motor size because of its availability and therefore low cost.

The Fixed Sensor will be less accurate in determining the target line-of-sight due to the smearing of the image caused by gunner jitter. The image sensor noise used for this concept is 0.341 milliradians as discussed in Section 4.3.4.2. This is a factor of 2.7 times higher than the common mirror concept.

The same techniques to estimate system accuracy, discussed in Section 4.3.3.3, were used for the Fixed Sensor concept. The analytical and simulation results are shown in Figure 4.3.4.3-1. As anticipated, the tracking performance of this system is considerably worse than the common mirror system due to the high increase in image sensor noise.

The pointing accuracy of this concept is also degraded in comparison to the common mirror concept. In addition to the boresight alignment error between the sensor and the laser, the uncertainty in measuring the gimbal angle between the sensor and the steering mirror is an additional source of error in this concept. The effect of this error on the total pointing accuracy is discussed in Section 4.3.5.1.

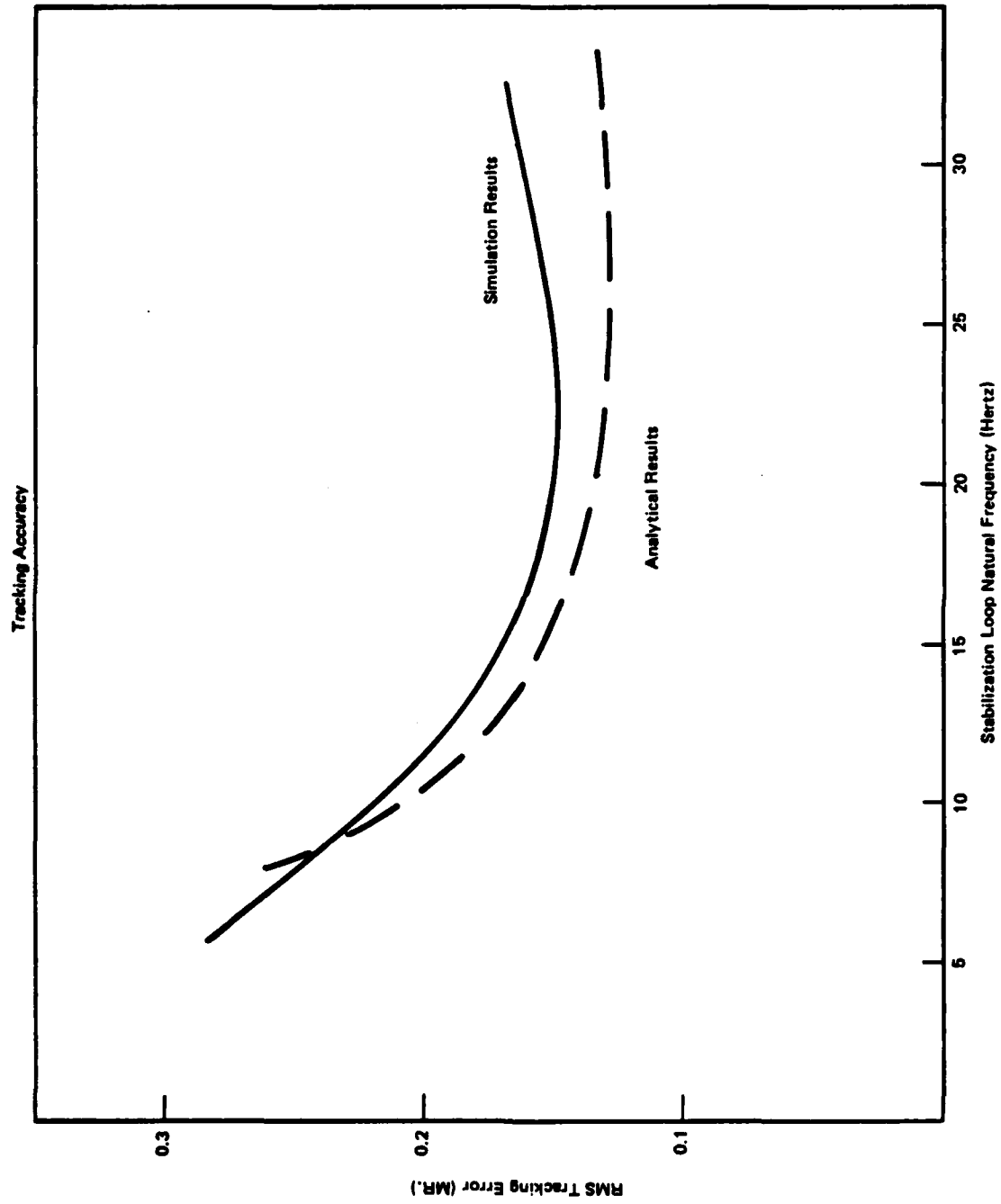


Figure 4.3.4.3-1. Tracking Accuracy

### 4.3.5 Evaluation Factors

#### 4.3.5.1 Accuracy

The pointing and tracking accuracies for the four candidates are summarized in Table 4.3.5.1-1. Tracking errors are errors in controlling or defining the IR sensor line of sight to the target. Pointing errors are errors in pointing the laser line of sight along the tracking line of sight defined by the sensor. The ultimate measure of performance is the statistical sum of these two errors which defines the total tracking and pointing error.

Table 4.3.5.1-1. Accuracy

		One-Sigma Pointing/Tracking Error (μrad)			
Error Source	Error Magnitude (1σ)	Dual Gimbal (Candidate A)	Common Gimbal (Candidate B)	Common Mirror (Candidate C)	Fixed Sensor (Candidate D)
<b>A) Tracking Errors</b>					
Gunner Jitter	± 4 MR at 2 Hz	4	4	45	45
IR Sensor					
• Track	110 μrad	43	43	43	43
• Turbulence	34 μrad	13	13	26	13
• Smear	311 μrad	N/A	N/A	N/A	128
Gyro					
• Noise	9.5 (°/Hr) <sup>2</sup> /CPS	2	2	2	2
• Drift/Align	20 Deg/Hr	2	2	2	2
• Threshold	0.01 Deg/Sec	10	10	10	10
RSS Tracking Error		46	46	68	143
<b>B) Pointing Errors</b>					
IR Sensor/Laser Null Alignment	70 μrad	70	70	70	70
Gimbal Angle Sensor					
• Null Uncertainty	40 μrad	40	N/A	2	40
• Linearity	0.025%	NEG	N/A	2	100
RSS Pointing Error		81	70	71	128
RSS Tracking and Pointing Error		93	84	98	192

The first three candidates stabilize the IR sensor line of sight and have comparable performance. The common gimbal system has the highest accuracy because of its inherent isolation from gunner jitter and the elimination of the need for gimbal angle sensors and their associated errors.

The common mirror and dual gimbal systems have approximately the same performance. The dual gimbal system has a much higher sensitivity to gimbal angle sensor errors and therefore represents a higher risk in achieving the desired 100 micro-radian accuracy. The common mirror system



is much less sensitive to this error and can achieve the desired pointing accuracy even with an order of magnitude increase in the gimbal angle sensor errors, and therefore is a lower risk approach.

Candidate D does not stabilize the IR sensor and the accuracy of this concept is the poorest of the four candidates. There are two basic reasons for its poor performance: degradation of the image sensor accuracy due to image smear; and the need to accurately measure the large relative angles between the image sensor and the laser.

The accuracy in pointing the laser beam is directly dependent upon the accuracy with which the relative angle between the image sensor boresight and the laser boresight can be measured. In order for candidate D to meet the minimum acceptable performance requirement, a high precision gimbal angle sensor is required which represents a high development risk.

The pointing and tracking accuracy for crossing targets is essentially the same as for stationary targets. The principal consideration in evaluating the candidates for crossing target performance is the ability to provide beam lead to improve guidance accuracy. Candidates A and D can mechanically provide beam lead since the sensor and laser line of sight are not mechanically constrained.

The beam lead required varies inversely with the target range and therefore pointing angle errors which are proportional to the lead angle (eg. gimbal sensor linearity) tend to be self compensating in terms of miss distance. At long ranges the principal lead angle error is caused by the null uncertainty in the gimbal angle sensor. At 2000 meters a null uncertainty of 40 micro-radians causes a miss of 0.08 meters. Without any lead the miss is 0.14 meters so that at the longer ranges the advantage of beam lead is questionable.

At short ranges beam lead can significantly improve performance. At 100 meters the miss distance without beam lead or other compensation is 1.75 meters. This error can be significantly reduced with a relatively inaccurate gimbal sensor. Figure 4.3.5.1-1 shows the allowable angle measurement error as a function of lead angle that contributes a 0.08 meter miss at all ranges. This accuracy can be met with a gimbal angles sensor linearity of 6 percent, an easy requirement to meet with a low cost off the shelf sensor.

The common mirror and common gimbal concepts do not have the capability of providing beam lead directly, and would have to utilize other methods of compensation. For the purpose of the study, an accuracy estimate of 0.3 meters for the 100 meter crossing target was used. The selection of this value is based upon the autopilot and guidance analyses performed for the IMAAWS proposal. In these analyses, an initial bias term generated

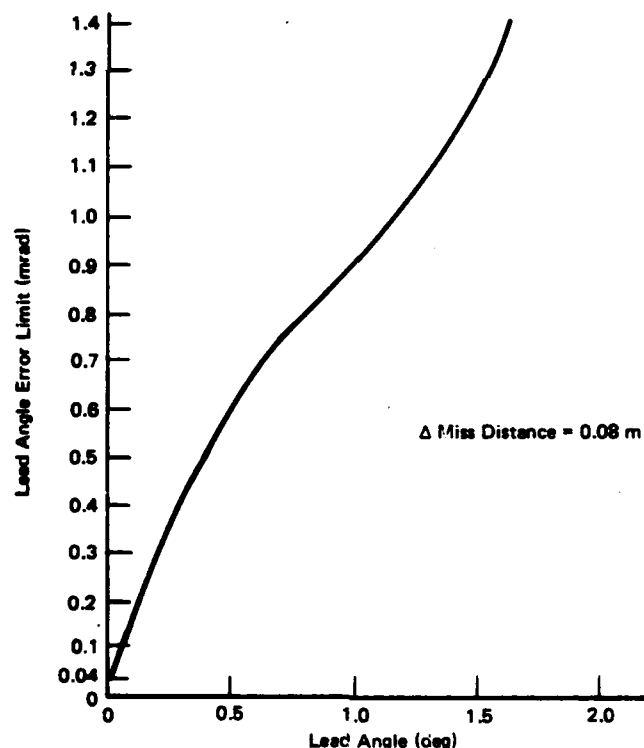


Figure 4.3.5.1-1. Beam Lead Accuracy Requirement

in the acquisition and guidance unit was used to compensate for crossing targets. A number of other methods may also be used to provide the required compensation as discussed in Section 4.2. Any of these compensation techniques should be able to meet the 0.3 meter goal required to achieve high kill probability for a man portable weapon system.

#### 4.3.5.2 Weight and Cost

Weight and cost estimates for each of the four candidates are presented in Tables 4.3.5.2-1 thru -4. The weights shown are for all parts and structure associated with the pointing and stabilization system, as additions beyond an imaginary configuration where the baseline FLIR and laser projector are rigidly mounted to a guidance unit frame. The weight of the guidance unit outer case for such a baseline was estimated at 823 grams, so that required growth in case size for each stabilization configuration could be charged to it. The "structure" element represents that structure, within the case, required to support the various pointer-tracker elements.

Unit costs for the pointer-tracker elements were estimated, again as deltas, based on production quantities in the thousands. There is felt to be a great deal of uncertainty in the \$2100. delta cost estimate for the wide angle FLIR in Configuration D.

#### 4.3.5.3 Targets and Environments

All of the discussion in this section applies equally to all four of the candidate configurations.

##### Environmental Factors

The signal to noise ratio of a thermal sensor is directly proportional to the contrast temperature differential of the target and background or

$$VSNR = k \frac{\Delta T}{NET} e^{-\gamma R}$$

Table 4.3.5.2-1 Weight and Cost Summary

## CONFIGURATION A - SEPARATE GIMBALS

ELEMENT		QUANTITY	UNIT WT. (GRAMS)	UNIT COST (\$)
CONTROLS	GYROS	1	110	1500
	TORQUE MOTORS			
	2 AXIS GIMBAL (18 oz-in)	2	113	85
	1 AXIS GIMBAL (1 oz-in)	1	68	55
	PIVOT BEARINGS	5	-	6
	POWER AMPS			
	2 AXIS GIMBAL	2	175	70
	1 AXIS GIMBAL	1	31	40
	POSITION PICKOFFS			
	m RAD	2	11	55
	$\mu$ RAD	1	100	300
	DAC'S, ADC'S	3,3	-	-
	WIRING		50	20
	IR SENSOR*			
OPTICS	SENSOR OPTICS*			
	PROJECTOR OPTICS*			
	PACKAGING:			
	CASE	1	243	360
	STRUCTURE	1	220	170
TOTALS			1420	2895

\*ADDITIONS BEYOND UNSTABILIZED BASELINE

Table 4.3.5.2- 2 Weight and Cost Summary

## CONFIGURATION B - COMMON GIMBAL

		ELEMENT	QUANTITY	UNIT WT. (GRAMS)	UNIT COST (\$)
CONTROLS		GYROS	1	110	1500
		TORQUE MOTORS			
		18 oz-in	2	113	85
		PIVOT BEARINGS	4	-	6
		POWER AMPS	2	158	60
		POSITION PICKOFFS mRAD	2	11	55
		DAC'S, ADC'S	2,2	-	-
		WIRING		45	15
OPTICS		IR SENSOR*			
		SENSOR OPTICS*			
		PROJECTOR OPTICS*			
		PACKAGING:			
		CASE	1	175	280
		STRUCTURE	1	170	135
TOTALS				1064	2354

\*ADDITIONS BEYOND UNSTABILIZED BASELINE

Table 4.3.5.2-3 Weight and Cost Summary

## CONFIGURATION C - COMMON MIRROR

	ELEMENT	QUANTITY	UNIT WT. (GRAMS)	UNIT COST (\$)
CONTROLS	GYROS	1	110	1500
	TORQUE MOTORS			
	20 oz-in	1	114	85
	10 oz-in	1	114	85
	PIVOT BEARINGS	4	-	6
	POWER AMPS	2	159	85
	POSITION PICKOFFS m RAD	2	11	55
	DAC'S, ADC'S	2,6	-	
OPTICS	WIRING		20	10
	IR SENSOR* }	1	1700	390
	SENSOR OPTICS* }			
	PROJECTOR OPTICS*			
	PACKAGING:			
	CASE	1	479	485
	STRUCTURE	1	135	110
	TOTALS		3012	2969

\*ADDITIONS BEYOND UNSTABILIZED BASELINE

Table 4.3.5.2- 4 Weight and Cost Summary

## CONFIGURATION D - FIXED SENSOR, MIRRORED PROJECTOR

	ELEMENT	QUANTITY	UNIT WT. (GRAMS)	UNIT COST (\$)
CONTROLS	GYROS	1	110	1500
	TORQUE MOTORS			
	0.5 oz-in	2	28	45
	PIVOT BEARINGS	4	-	6
	POWER AMPS	2	39	45
	POSITION PICKOFFS			
	μ RAD	2	140	460
	DAC'S, ADC'S	2,6	-	-
OPTICS	WIRING		16	8
	IR SENSOR*	1	31	2100
	SENSOR OPTICS*	1	123	95
	PROJECTOR OPTICS*	1	100	130
	PACKAGING:			
	CASE	1	111	270
	STRUCTURE	1	60	80
TOTALS			965	5307

\*ADDITIONS BEYOND UNSTABILIZED BASELINE

where

$k$  = proportionality constant

$\Delta T$  is the contrast temperature differential

NET is the noise equivalent temperature sensitivity.

The term  $e^{-\gamma R}$  is the atmospheric degradation factor which degrades the temperature differential contrast signal over the range  $R$  (km). The term  $\gamma$  is the extinction coefficient ( $\text{km}^{-1}$ ) of the atmosphere which is dependent on the wavelength band and the atmospheric conditions.

Figure 4.3.5.3-1 shows the maximum permissible extinction coefficient for a thermal imager sensor in the 8 - 12.0  $\mu\text{m}$  band and the extinction coefficient for the laser link.

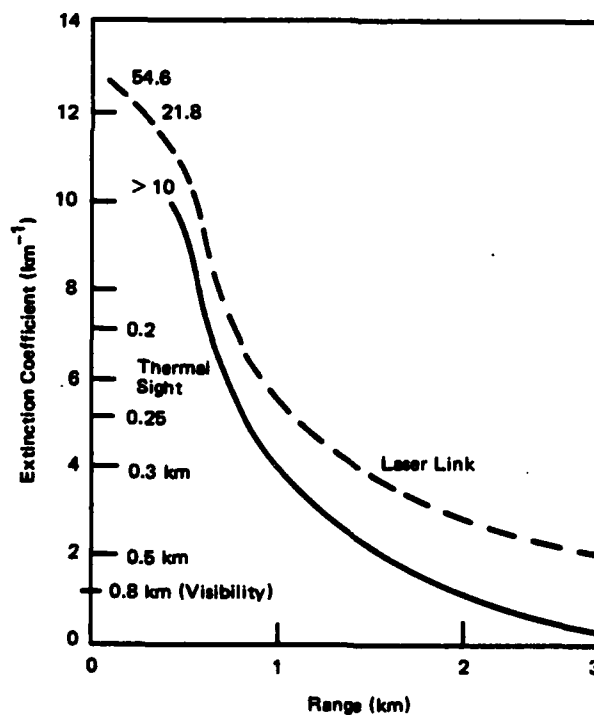


Figure 4.3.5.3-1. Maximum Permissible Extinction Coefficient



It can be seen from Figure 4.3.5.3-1 that a maximum extinction coefficient of approximately 1 is permissible for a 2 Km range. This corresponds to a transmission of 13% at that range. It also corresponds to a 0.8 Km visibility which represents a moderate fog. Table 4.3.5.3-1 shows the visual conditions.

Table 4.3.5.3-1  
Visual Conditions

<u>Visual Condition</u>	<u>Visibility [km]</u>		
Exceptionally clear	70	-	180
Very clear	18	-	70
Clear	9	-	18
Light haze	3.9	-	9
Thin fog	0.9	-	3.9
Moderate fog	0.48	-	0.9
Thick fog	0.18	-	0.48
Dense fog	0.048	-	0.18

The case of countermeasures, where aerosols are used, corresponds to a dense fog where the capability of track would be reduced to almost zero range. However aerosols do not last long as a general rule, and therefore would not seriously degrade system effectiveness.

Other environmental effects, such as turbulence, are discussed in Section 4.3.1.2 (sensor analysis).

#### Target Mix

A thermal sensor operating in the 8 - 12.0  $\mu$  band does not require large target temperature differentials in order to track the target. Temperature differentials of less than 1°C between target and background may be adequate in most cases for target centroid track. The difference between

target emissivity and background makes it possible to track several types of vehicles equally well, including trucks, armored carriers and helicopters.

In the case of bunkers, the emissivity of concrete, metal and openings would be somewhat different than that for soil and trees. This should make it possible for them to be seen as a contrast by the operator; however, it is not clear how well the IR tracker might maintain a good aimpoint.

If effective use of the weapon against this type of target is important, then it may be advisable to provide a manual tracking mode, so that whatever aimpoint target features were used by the gunner during target acquisition could be employed for target track, since the aimpoint selection of the IR autotracker might be very uncertain from target to target.

The target mix score could be stated as follows:

Target	Auto-track capability	
	Yes	No
Tank	X	
Truck	X	
Armored Vehicle	X	
Helicopter	X	
Bunker		X
Emplacement		X

Score: 4/6

#### 4.3.5.4 Development Costs and Risks

Configuration D involves two concepts which would require considerable development effort: the wide angle FLIR and the angle pickoff for the laser steering mirror. To regain the original IR sensitivity, the scanning rate in the sensor is increased, a change which ripples through at least 2 or 3 of the electronics modules (see Section 4.3.4.1). This is pushing the state-of-the-art somewhat since the highly miniturized FLIR needed for a

shoulder held 2 km guidance unit already involves a technical development advance over current operational hardware.

The steering mirror angle sensor for D has very severe accuracy demands placed on it, because, in addition to the moderate demands of beam lead steering, the laser beam must be precisely rotated over a range of about  $\pm 2$  degrees to follow gunner pointing errors. The ability to achieve the steering accuracy allocated in the pointing error analysis (Figure 4.3.5.1-1) at the modest weight allocated (140 gms per unit), and yet achieve ruggedness and high reliability, would seem quite risky. The determination of a specific design solution to this difficult problem would be needed in order to properly estimate this risk. For these reasons, D has by far the highest risk and/or cost to develop.

The angle pickoff requirements for the projector pivot in configuration A are not nearly as severe in terms of linearity; however the ability to repeatably seek null within  $40 \mu$  radians is still a challenge, and for that reason, and because the dynamic interaction between the pivoted projector and the stable platform has not been fully evaluated, A is noticeably riskier than B, which is straightforward in all respects.

Configuration B involves off-the-shelf hardware and straightforward design processes. The only major uncertainty is the effect of platform mass unbalance due to the projector zoom mechanism, which could be solved, if need be, by providing a counterbalance mass to the zoom mechanism.

Configuration C suffers from the developmental problem that it is too heavy, the solution for which would almost certainly involve sharing the optical path between the sensor LOS and laser beam (common aperture). There could be a significant challenge in keeping  $10.6 \mu$ m laser backscatter out of the highly sensitive 8-12 $\mu$ m focal plane. Other developmental aspects of C are fairly low risk.

#### 4.3.5.5 Training

The standard for training ease would be Configuration A (dual gimbal) for the following reasons:

- 1) Display stabilization and scene/reticle characteristics can be optimized for maximum gunner assistance, with no regard to compromises for laser beam pointing requirements.
- 2) Guidance "assistance" from the gunner, for close-in, fast moving targets, which might become a trainable feature of other candidates, would never be needed; the missile maneuver capabilities would be the only limiting factor.
- 3) The inherent isolation between gunner and sensor ensures that his jitter movements have virtually no effect on miss distance, and thus training for "handling" during tracking is obviated.
- 4) Large angular excursions of the guidance unit are allowed during tracking, with no effect on miss distance. These allowable excursions could be even larger than the sensor gimbal limits, without pulling the laser beam away from the aim-point, since the projector can be pivoted an additional 2° or so.
- 5) A stabilized scene can be presented to the gunner during the target "search and acquisition" phase of operation, prior to missile launch and auto-track. This should make the acquisition training an easier, less time consuming task.

Configuration B (common gimbal) enjoys most of the training characteristics of A, with slightly degraded "ease" on items 1), 2) and 4), above. These differences would likely be trivial, particularly if one of the alternate guidance bias schemes discussed in section 4.2 were successfully implemented.

The common steering mirror configuration ("C") suffers from a lack of natural gunner jitter suppression, and thus motion of the guidance unit

during missile flight effects miss distance to some degree. Because of this, the gunner should be trained to suppress high frequency rotations of the unit during auto-track. Other than this, "C" would have the same training characteristics as "B".

Candidate D, with its fixed sensor, suffers the most in pointing accuracy degradation due to gunner motion during track, and to some extent during acquisition. Also, allowable angular excursions of the guidance unit are more restrictive, although this configuration, like candidate A, enjoys the advantages (items 1 and 2) of the independently steered laser beam.

All other factors effecting training, such as mode control, sight selection, and initialization are of a difficulty level equal among the candidates. All were found to be excellent in training ease, with candidate "D" not quite as good as the others.

#### 4.3.5.6 Reliability

A relative measure of reliability was developed by first establishing a parts count for each candidate. The parts count included only elements which were required to implement stabilization and tracking functions. The basic components such as the laser, IR sensor, image processor, display and all other parts which would be present on a non-stabilized device were not included. (See Tables 4.3.5.2-1 through 4)

The parts were then separated into a high failure rate category and a low failure rate category based upon experience with similar type devices. The high failure rate category was comprised of the "working" elements which are prone to failure due to their complexity, temperature cycling or wear. This category included elements such as gyros, torque motors and power amplifiers. The "non working" or relatively passive elements comprised the low failure rate group. These included low power electronic devices such as Analog to Digital Converters and passive mechanical components such as pivot bearings.

The gimbal angle sensors could fall into either category depending upon their requirements. If high precision measurements were required, the sensor was classed in the high failure rate category since the device would be more complex and prone to failure by performance degradation as well as a catastrophic failure. Low accuracy sensors were placed in the low failure rate category since they would be relatively simple devices.

A relative weighting of 3 was used for the high failure rate parts. A raw reliability score was made up of the sum of the low failure rate parts and the weighted high failure rate parts. The raw score is a relative measure of failure rate so that a low score indicates a more reliable candidate. These raw scores are as follows:

Candidate A (Dual Gimbal)	28
Candidate B (Common Gimbal)	21
Candidate C (Common Mirror)	25
Candidate D (Fixed Sensor)	29

The common gimbal system has the best (lowest) score because this system requires the least number of additional parts to make a stabilized system out of a non-stabilized system. The common mirror system requires additional components to resolve base motion and gimbal motion and therefore has a higher score. The dual gimbal system is more complex, and requires more components since it has two separate stabilization systems. The fixed sensor concept has the worst score even though the sensor is not stabilized. This results from the fact that the same number of parts are required to control the laser alone as would be required to stabilize both optical devices as in the common gimbal system. Since the sensor is not stabilized, additional electronics is required to stabilize the display. Increased complexity and parts count has been traded for low weight in this system.

The optical elements used in the gimbaled mirror configurations were not included in the parts count. These were treated as structural elements with zero failure rate. This is probably a somewhat optimistic treatment since these elements can fail due to alignment changes caused by the field environment.

Maintainability was considered to have the same relative ranking as the reliability scores. The justification for this assumption is that the MTTRS would be a direct function of the failure rate. Features that affect maintainability such as modularity, repair complexity and adjustment/alignment requirements are influenced by design details that are beyond the scope of the study. The alignment and adjustment requirements will probably be minimum with the common gimbal system since only mechanical integrity is involved.

## 5.0 Evaluation Summary

### 5.1 Factors and Weightings

The various value factors, upon which the competing candidate configurations were judged, were explained in section 4.2. Figure 5.1-1 gives the relative ranking for those factors, in terms of their importance to making the final selection of a pointer-tracker design approach, and the weightings to be applied to the grades arrived at from the section 4 technical data.

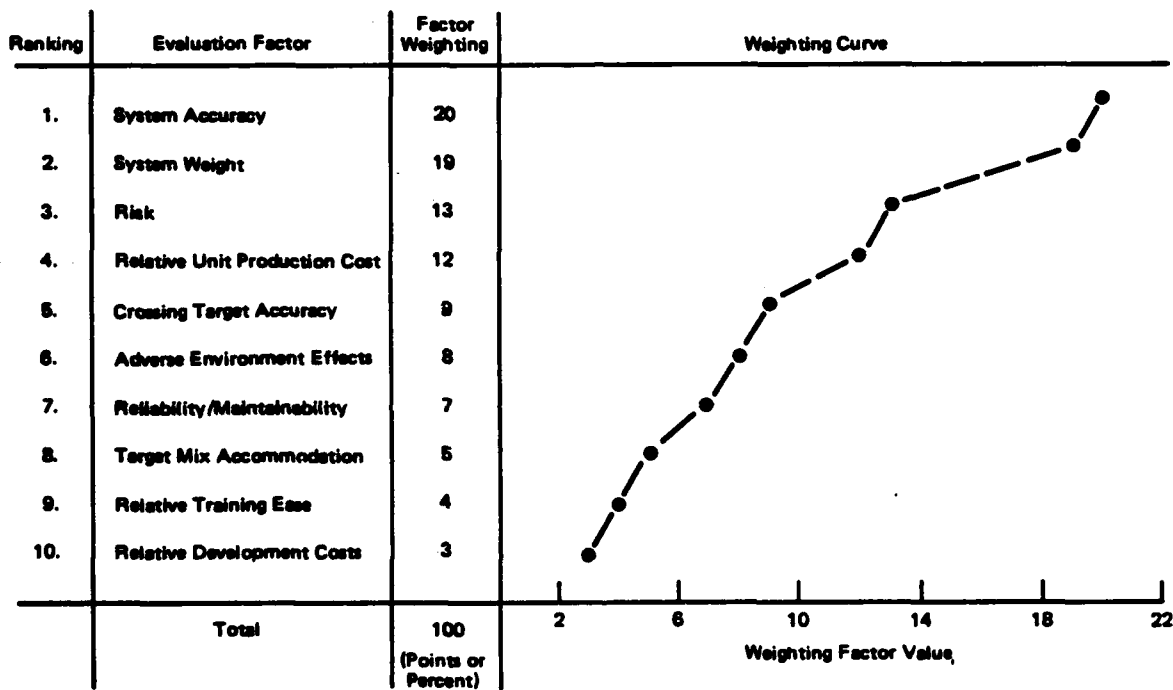


Figure 5.1-1. Concept Final Evaluation Factors and Weighting Measures

### 5.2 Results Matrix

First, the raw grading data developed in section 4 was assembled into a matrix, Fig. 5.2-1, from which relative grades on a scale of 1 to 10 were assigned. Figure 5.2-2 presents the final results in terms of a matrix of grades ranging from the poorest (1) to the best (10), with the sum of the grade-weight products, divided by ten, in the last column. The highest possible score is 100. Grades, in a relative sense among the candidates, are traceable directly to Fig. 5.2-1, however the absolute level of the grades reflects a notion of what might be achievable in early 1980's



Evaluation Factor	Configuration			
	A (Dual Gimbal)	B (Common Gimbal)	C (Common Mirror)	D (Fixed Sensor)
Accuracy (1 $\sigma$ )	93 $\mu$ rad	84 $\mu$ rad	98 $\mu$ rad	192 $\mu$ rad
Weight — kg (lb)	1.42 (3.12)	1.06 (2.33)	3.01 (6.62)	0.97 (2.13)
Risk 10 — High; 1 — Low	4	2	5	9
Prod. Cost — \$ per Unit	2895	2354	2969	5307
X-Tgt Accuracy Miss Contrib — meters	0.1	0.3	0.3	0.1
Environ Effects 10 — Best; 1 — Worst	8	8	8	8
Reliability/Maint (High Prec) / (Low Prec) Number of Parts by Type	4/16 (28)	3/12 (21)	3/16 (25)	5/14 (29) <span style="font-size: small;">3x Number of High Prec Plus Number of Low Prec</span>
Target Mix Number of Targets	4/6	4/6	4/6	4/6
Training Ease 10 — Hard; 1 — Easy	2	3	3	4
Development Cost 5 — High; 1 — Low	2	1	2	5

Figure 5.2-1. Grading Matrix, Raw Data

technology if one were to focus primarily (but not exclusively) on the particular factor in question, and let the others fall as they might. There is quite a bit of subjectivity in that method of absolute level choice, and to see what would result from removing it, grades were assigned wherein the best among the four candidates got a 10 and the worst a 1. The result is that the rank order of the weighted sums did not change, the values were simply more spread out, reflecting the increased emphasis on small differences in performance.

### 5.3 Conclusions

The weighted scoring shows that the poorest grade goes to configuration D, where the sensor (FLIR) is fixed to the guidance unit case, and the laser beam is steered to the aimpoint LOS with a 2 axis steering mirror. This candidate survived the pre-screening on the basis of a weight level perceived to be possibly much lower than the others, with risk and development cost as drawbacks. A closer scrutiny shows that it suffers a great disadvantage in accuracy, being marginal for a 2 km range, and production costs

Alternative  
Stabilization/  
Tracking  
Approaches



Weighting

Evaluation Factors

Accuracy	Weight	Risk	Unit Production Cost	Crossing Target Accuracy	Adverse Environment	Reliability Maintainability	Target Mix	Training Ease	Development Cost	Sum/10
20	19	13	12	9	8	7	6	4	3	
8	5	7	8	9	8	6	7	10	8	73
9	7	8	9	4	8	8	7	9	9	78
8	2	6	8	4	8	7	7	8	7	61
3	8	2	5	9	8	6	7	7	3	56

Grading: 10 - Best; 1 - Worst

Figure 5.2.2. Final Evaluation Results

AD-A136 219

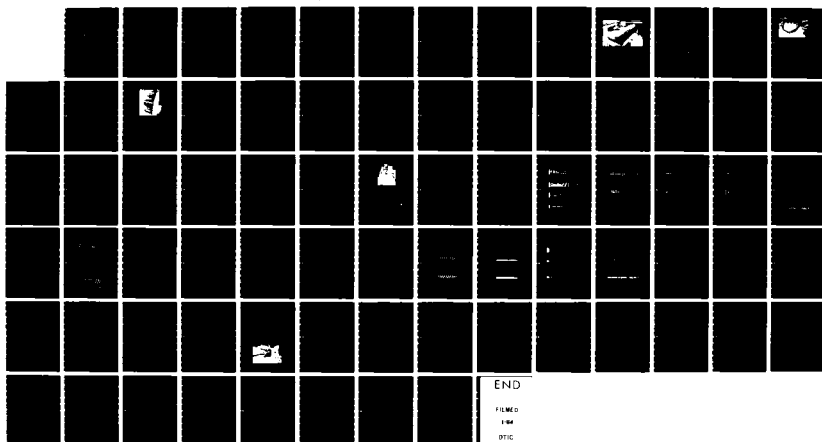
TARGET TRACK AND STABILIZATION FOR MANPORTABLE DIRECT  
FIRE MISSILES(U) MCDONNELL DOUGLAS ASTRONAUTICS CO-HB  
HUNTINGTON BEACH CA F GENTILE ET AL. NOV 81 MDC-69941  
DAAH01-80-C-1618

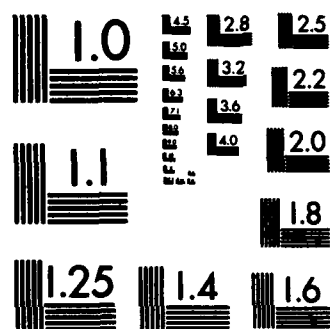
2/2

UNCLASSIFIED

F/G 17/5

NL





MICROCOPY RESOLUTION TEST CHART  
NATIONAL BUREAU OF STANDARDS-1963-A

are perceived to be high due to significantly increased design demands on the FLIR. This concept is probably somewhat ahead of it's time, for if the FLIR could be configured with an even higher focal plane sampling rate than proposed here, it could be made competitive in pointing accuracy. To do this with low weight and volume is probably several years away in FLIR development.

Bringing the maximum range down to one kilometer, and demanding a little more skill from the gunner might improve "D's" prospects, but the considerable design challenge posed by steering the beam mirror very precicely must not be ignored.

Surprisingly, the common steering mirror candidate (configuration C) suffers most from being the heaviest. At the outset, it was generally expected that this arrangement would be at worst no heavier that the common gimbal. That perception was based on the use of a mirror just large enough to handle the FLIR optical path, with the laser path somehow sharing that area. Since the laser beam must turn in common angluar polarity with the FLIR FOV, they would have to share the same mirror surface, and it is felt that the design risks associated with the resulting backscatter problem are too severe. If this problem were solved in some manner which didn't add any weight of its own, then the grading influences would change as follows, compared with the non-shared aperture configuration:

	Aperture Path	
	<u>Shared</u>	<u>Separate</u>
Weight (kg)*	2.35	3.01
Prod. Cost (\$)	3214.	2969.
Risk	6	5
Reliability/Maint (Parts Count)	26	25
Development Cost	3	2

The other factors remain the same. Transforming these to 10-scale grades gives the shared aperature mirror variation a weighted sum grade of 68, compared with 61 for the separate aperature.

\*Optics weight decreases by 0.6 kg, torquer weight decreases by 56 gm.

Another variation of the common mirror concept is one where the gyro is mounted to the inner gimbal, with the mirror 2X axis connected by a 2:1 belt drive to its torquer rotor. This gives it nearly the same pointing accuracy performance as the common gimbal, but increases the weight and complexity such that, even with a shared aperture mirror, its weighted sum grade is only 67.

Figure 5.2-2 shows B, the common gimbal configuration, to be the highest in overall score. A few words about mirrors versus gimbal mounts for pointer-tracker (P-T) systems is in order at this point. P-T systems usually have two angle control jobs to do, in addition to their "electro-optics" or recognition type of tasks. These are (1) to hold a line-of-sight (LOS) fixed when the mounting base moves and the target object does not, and (2) to move the LOS when the target moves but the base does not. From studying designs of P-T systems which have been built and tradeoff studies conducted for proposed systems, it becomes clear that the method chosen is usually influenced heavily by the dynamic characteristics of the two "independent" angle motions, the base and the target. When target LOS rates are high, and base motions slow, mirrors tend to be selected (Refs 2, 3); and when target motion is slow but base motion fast, gimbal mounts prevail (Ref 18,33). Where both base and target motions are fast, one may encounter systems comprised of a gimbal mount supporting a rotating mirror (Ref 6).

Unless the design incorporates compensating mechanisms, inertia of the stable element tends to work against a mirror and to the aid of a gimbal mount in stabilizing against base motions. If the inherent inertia of the sensor and/or transmitting device are large, and target LOS angles change rapidly through fairly large angles, the steering mirror can achieve large weight and power savings over a gimbal mount. The trade turns the other way, however, when steering slowly thru small angles with lots of random base motion. The dynamic environment for the shoulder held LBR guidance unit for this application is characterized by slow moving targets, and rapid base motions over small angles. The inherent simplicity, ruggedness and low production cost of a gimbal mount are hard to ignore when, by its basic nature, it out performs a steering mirror in this application.

Configuration A, which is really a variation of the common gimbal, B, achieves a high score by virtue of it's grade for crossing target accuracy, even though it suffers in weight, cost and risk. This advantage is probably overstated by the grading, because of two considerations: (1) the 0.3 meter miss distance assigned to B, and thus a grade of 4, is virtually the total guidance induced error at the 100m target range used, and is only 0.1m worse than the 2km total error for either A or B; (2) It is likely that, when an optimum design is worked out, one of the other guidance bias methods discussed in section 4.2 will reduce crossing target errors to levels comparable to direct beam lead.

### Section III

#### PHASE II - TEST PROGRAM

##### 1.0 Introduction and Summary

This section describes the testing activities, including a description of the brassboard system, the test equipment, details of the tests that were performed and the results obtained.

The intent of the test program is to evaluate the concept performance and the characteristics of critical components for the tracking/stabilization configuration recommended in the Phase I tradeoff study described in Section II.

The Phase I evaluation concluded that the best configuration for target tracking and guidance beam pointing in a one man portable, direct fire, laser beamrider anti-armor weapon system, consists of a miniaturized FLIR, mounted on a two-axis gimballed platform. A laser beam projector is also mounted on the platform with its axis aligned with the optical axis of the FLIR. Scene imagery from the FLIR containing the target are fed to an image processor/tracker which determines a desired aimpoint in the sensor field-of-view (FOV). A two-axis gyro is mounted on the stable platform, and the signals from the gyro and tracker are acted on by the control logic to produce command signals to the azimuth and elevation torquers to rotate the platform.

At the beginning of the test program, MDAC had, in its electro-optics and circuit study laboratories, most of the major elements of this type of tracker system configuration, as a result of an IRAD study conducted during the first half of CY 1980 and ongoing new business projects. The purpose of that test program included objectives similar to this one.

Using much of the hardware already available, the design and integration of the system was carried out, utilizing a visible band video camera for a



sensor, and a sequence of tests was carried out to determine the performance of the concept.

During and following assembly and integration, key data on the characteristics of the optical tracker, the gyro, the torquers and gimbal angle pickoffs were obtained and evaluated, and the system simulation model updated.

For automatic target tracking and stabilization performance tests, the launcher components were mounted on a 2-axis angular motion table, driven by repeatable sinusoidal motion and random simulated "gunner motion" signals, while the optical tracker viewed a model of a typical target shape. Scene stabilization was qualitatively evaluated via a TV monitor of the sensor video signal, and pointing error determined by a combination of theodolite data and control system internal signals.

For evaluation of the soft cage (acquisition) mode, subjects were asked to hold the mass simulated launcher module, and evaluate responsiveness versus scene stability for various caging loop gains.

The following summarizes the results of these tests:

- o Base motion was attenuated by a factor of at least 150 in the auto track mode. This corresponds to a line-of-sight stabilization of better than 55 microradians with a poor or untrained gunner.
- o The test unit was able to track the equivalent of a 10 meter per second crossing target at 100 meters range to within the accuracy of the performance measuring device ( $120\mu\text{-rad}$ ).
- o In the soft cage mode, base motion was reduced by an order of magnitude for stationary targets.
- o The soft cage mode provided some gunner relief in tracking close-in, high-speed crossing targets. Analysis of the test results indicated that non-linear compensation would be necessary to adapt the degree of responsiveness versus scene stabilization to the gunner's need under various target tracking conditions.

## 2.0 Test Objectives

The broad objectives were:

- A. Optimize the system response for the conflicting desires of responding accurately to desired inputs, on one hand, and ignoring spurious errors on the other.
- B. Measure the tracking/pointing accuracy, and degree of scene stabilization of the optimized system.
- C. Determine the component characteristics most suited to the task, and update the simulation models of those components.
- D. Explore gunner contributions/errors/characteristics in accomplishing the pointing/tracking functions.

There were four categories of test data desired to achieve those objectives:

- 1. The characteristics of selected components, and their relation to the analytical models. This data includes items such as noise levels, bandwidths, hysteresis, nonlinearities, and null shifts, as well as size, weight, and power consumption.
- 2. A measure of the ability of the system to ignore unwanted gunner motion and tracker jitter. This data focuses on laser pointing error.
- 3. A measure of the ability of the system to follow moving targets and reduce "real" tracking errors. This is also laser pointing error data.
- 4. A measure of the ability of the system in the target acquisition, or "soft cage" mode, to follow gunner pointing and yet stabilize the displayed scene. This is likely to be a "handling characteristics" determination.

Objective A was partially achieved. To truly optimize system response, the control logic hardware would have to be much more flexible by use of a microprocessor, for example. The hard-wired linear electronics used in this example were not suited to exploring system optimization to its fullest extent.

All other test objectives were met.

### 3.0 Test Article Description

The test article consists of two major modules, the Launcher Module, which simulates the weapon, and the Electronics Module, which houses the breadboard electrical and electronics functions as well as test controls and monitors. Figure 3.0-1 shows the various functional elements of the system, their module location, and principal interaction paths. The following paragraphs give a description of those system elements.

#### 3.1 Launcher Module

This consists of a simulated IMAAWS-sized missile launch tube, on which is mounted the stabilized sensor unit as well as the eyepiece CRT display. The stabilized sensor unit consists of a two-axis gimbal set, with azimuth (horizontal) and elevation (vertical) pivot bearings, gimbal angle torquers, gimbal angle transducers, vidicon visible band sensor, two-axis gyro and static mass balancing mechanism. The gimbal freedom is  $\pm 5$  degrees in each axis.

Figure 3.1-1 shows a photograph of the launcher module, and the following paragraphs more fully describe the various components.

##### 3.1.1 Sensor

A Sony model AVC-1400, standard TV video camera, was utilized as a sensor. This is a compact, low-cost vidicon device, of standard RS-170 video signal format, with remote power/signal conditioner unit. Figure 3.1.1-1 shows an exploded view of this camera.

Prior to mating with the gimbal set, the outer cover was removed, and the vidicon tube and deflection yoke were rotated 90 degrees so that the inner box chassis could be laid on its side for attachment to the inner gimbal bracket.

The standard AVC-1400 lens was replaced with a Bell & Howell type V 102mm lens of f/4.5.

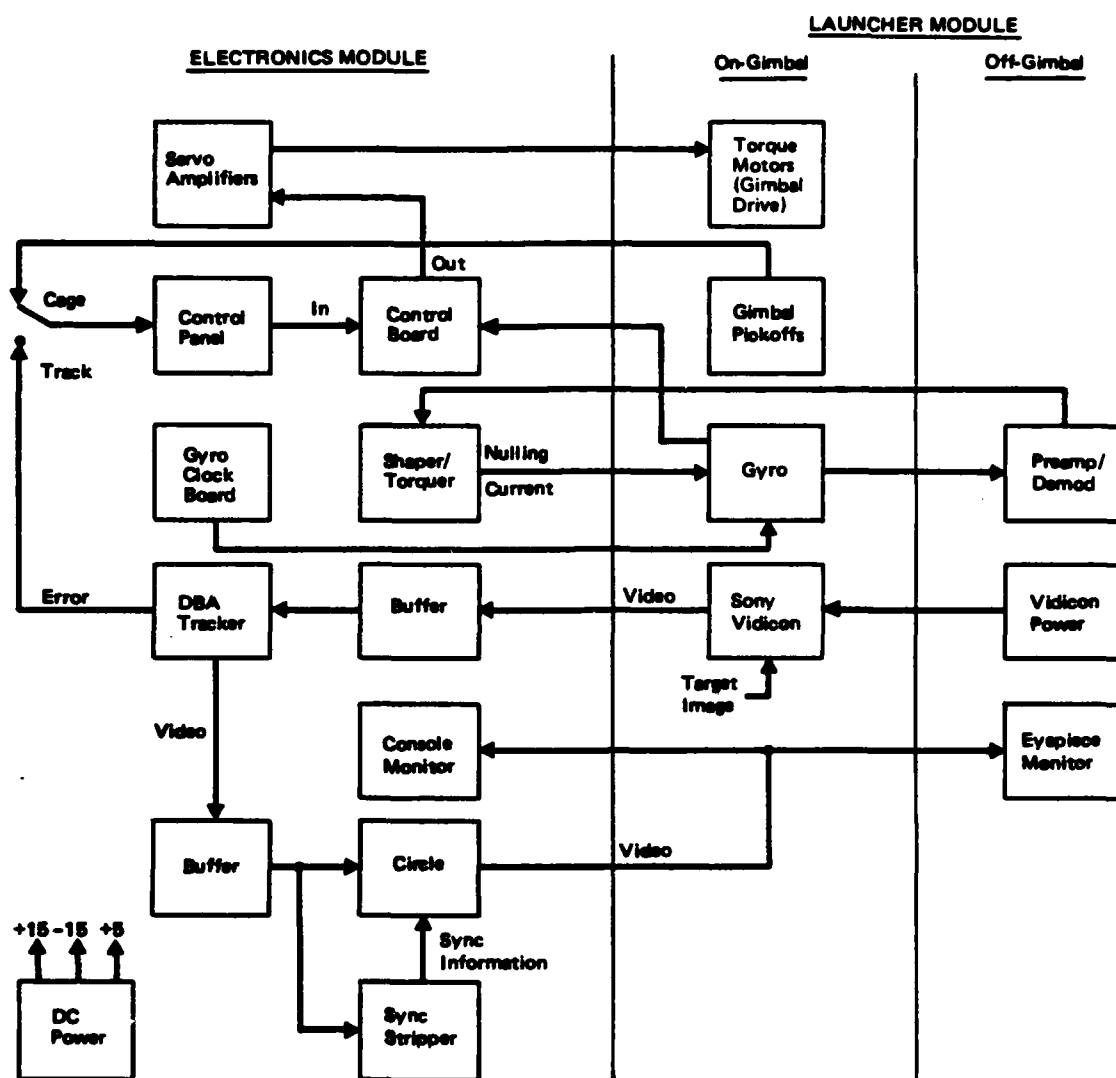
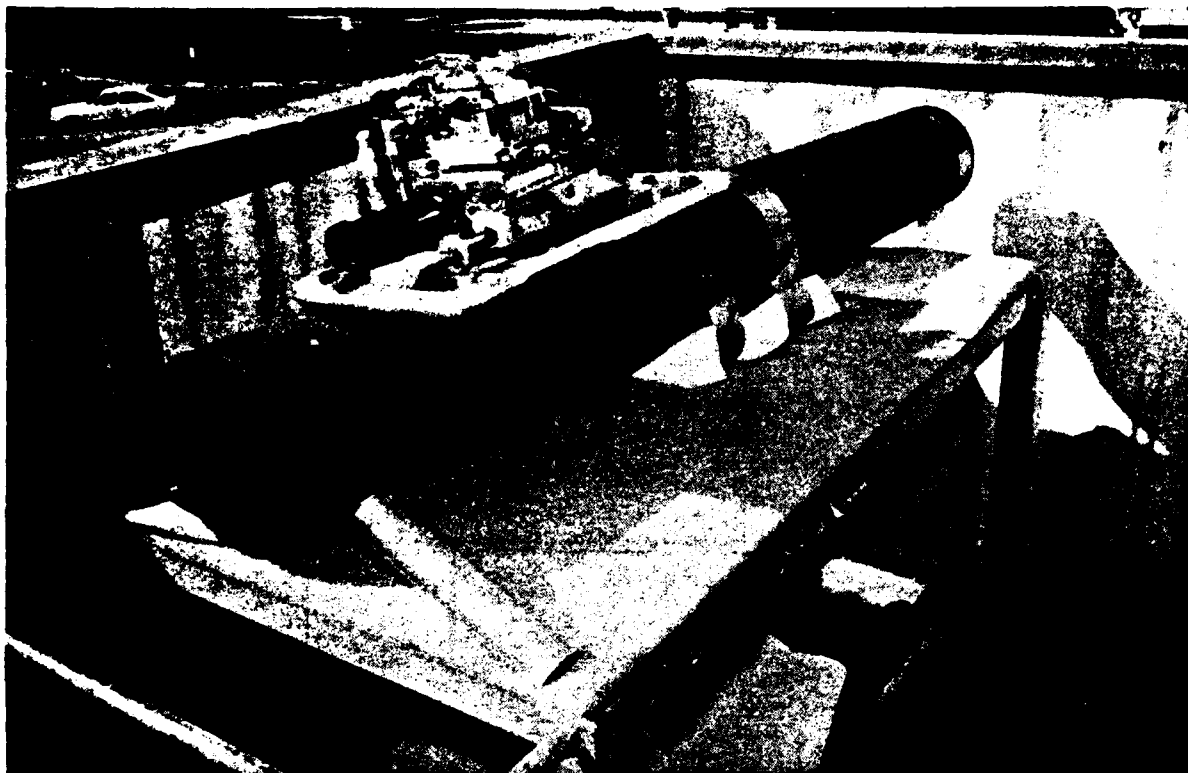


Figure 3.0-1. System Schematic



**Figure 3.1-1. Launcher Module**



### 3.1.2 Gyro

The Incosym Mod V is a two degree-of-freedom dynamically tuned gyro. The rotor is driven by a hysteresis synchronous spin motor. The rotor suspension system is mechanically tuned to the spin speed to torsionally decouple the rotor from the case-fixed shaft, thus, enabling the rotor to operate as a free body about any axis perpendicular to the spin axis. Electrical pick-offs are provided to sense relative motion between the rotor and the case. Electro-magnetic torquers are included to provide a capability of torquing the rotor.

This unit weighs 180 gms (6.3 oz) and is  $\sim 1\frac{3}{8}$ " long and  $\sim 1$ " in diameter (see Figure 3.1.2-1). Spin speed is 9600 rpm, with spinup time of about 10 seconds, and 1.5 watts maximum are consumed to maintain speed. The unit has a maximum capability of 400 degrees per second. One sigma drift rates are 50 deg/hr g-insensitive, and 50 deg/hr/g g-sensitive. One unit has been tested to a 200g shock level with no degradation in performance.

The caging loop design employed in this application provided an instrument bandwidth of 80 Hz at 45° phase lag.

### 3.1.3 Torquers

The two gimbal torquers, for control of the stabilized platform azimuth and elevation angles, are Aeroflex model TQ25-2 brushless wide angle DC torque motors. Peak torque capability is 80 oz-in, with a continuous torque rating of 25 oz-in. Driving voltage for a 25 oz-in output is 14.8 VDC into 16 ohms, and back EMF is 0.19 v/rad/sec. Each unit weighs 12 oz and is 2.5 inches in diameter and 1 inch long. The torque sensitivity versus angular excursion is shown by Figure 3.1.3-1. The angular excursion utilized in this application is  $\pm 5$  degrees.

### 3.1.4 Gimbal Angle Sensors

The platform gimbal angle pickoffs, one for each axis, are Schaevitz model 100 MHR Linear Variable Differential Transformer (LVDT) type position transducers. They produce a phase sensitive ac voltage output proportional to linear displacement of the core within the coil housing. The core rod is connected to a crank arm at each gimbal pivot, the arm being of length sufficient to insure good angular linearity of the LVDT output over the  $\pm 5^\circ$



Figure 3.1.2-1. Incoosym Mod V Gyro

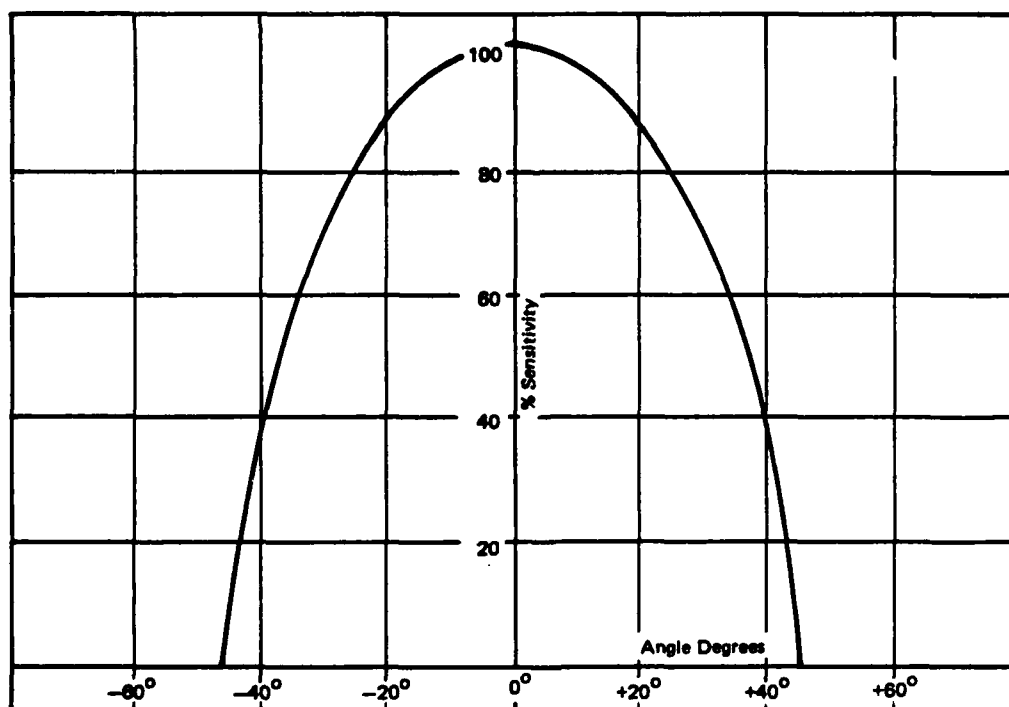


Figure 3.1.3-1. Aeroflex TQ25-2 Torquer Performance Curve



gimbal travel.

### 3.1.5 Eyepiece Display

The viewfinder for the Hitachi GP-7 self-contained color TV camera is being used for the eyepiece monitor. Designated as Model VM-151A, it has a 1.5" diagonal CRT screen and weighs under 2 lbs. A 1 volt peak-to-peak composite video signal is the input requirement. The unit consumes 1.3 watts of power at 9 volts d.c.

### 3.2 Electronics Module

Figure 3.2-1 shows the electronics cabinet housing the controls, displays, and power supplies for the tracker system. The various components of this module are described in the following paragraphs. In the tactical weapon, the tracker, servoamps, control logic, gyro loop, and reticle generators would be miniaturized and housed in the guidance unit on the launcher. The TV monitors, test-oriented controls, and most of the power supply elements are, of course, unique to the test and development environment.

#### 3.2.1 Tracker

The DBA series 606 automatic television target tracker is a selectable edge or centroid tracking unit which will accept standard RS 170 video format, and is commercially available from DBA Systems, Inc. It has an adjustable track gate size, and produces azimuth and elevation error signals as well as an aimpoint cursor and reticles indicating video center (sensor boresight) and track gate outline. The unit employed in this test is 19-inch rack mounted with controls on the front panel. Table 3.2.1-1 shows some of the pertinent specifications.

This tracker requires a high contrast, uncluttered target in order to reliably maintain track, and would not be suitable for tracking motorized ground vehicles in typical background situations. For this reason, field tests of the autotrack mode were not attempted.

#### 3.2.2 Servoamplifiers

The gimbal torquers are driven in push-pull by Opamp Labs Model 440KR 50 watt differential operational power amplifiers. These amplifiers were utilized in a current feedback mode in order to minimize back EMF torques on the gimbals. Each amplifier is capable of driving 1.9 amps into the 16 ohm torquer load at frequencies ranging from d.c. to over 50 KHz.



Figure 3.2-1. Electronics Module

Table 3.2.1-1. TV Tracker DBA 606A

Specifications

Input Signals:

Video Input:

Composite video level, 1.5 Vpp nominal  
Compatible with TV or FLIR of 200 to 1250 lines per frame  
Scan, interlaced 2:1 or sequential

Auxiliary Input:

Allows externally generated signals to be mixed with the output composite video for display on a TV monitor, such as external reticles, timing signals, video character generators, etc.

Target Contrast:

Selectable white, black or mixed target referenced to average, TV signal

Target Tracking Specifications:

Minimum Resolvable Target Displacement  
Edge - 1 TV line  
Centroid - 1 TV line

Minimum Target Size:

1 TV line/field - Correlator out  
2 TV lines/field - Correlator in

Minimum Target Signal/Noise Ratio:

(Peak Signal to RMS Noise)

Edge - 4:1  
Centroid - 2:1

Tracking Gate Performance:

Tracking Gate Position:

Manual - Fixed to the center or manually positioned to any point within the field of view.  
Automatic - Automatically follows the field of view.

Tracking Gate Modes:

Centroid - Center of mass of the target.  
Edge - Operator selectable, Right, Left, Top or Bottom of the target.

Tracking Gate Size:

Manually adjustable from 1% to 100% of the field of view.

Output Signals:

Video Output:

Composite video mixed with artificial video, defining gate area, track point indicator, etc.

Error Output:

DC voltage proportional to target position in the field of view, nominally +5 to -5 VDC at 1 K  $\Omega$  impedance. The maximum linearity error is dictated by the video chain which is nominally  $\pm 2\%$ .

Azimuth/Elevation Indicator:

A Digital Panel Meter (DVM) indicator which gives displays of the Az/EI output error signals.

Test Reticle:

An artificially created signal which is visible on the monitor as a crosshair describing the Az/EI null points.

### 3.2.3 Control Panel

The control panel for stabilization contains switches and circuits for:

- Gyro Turnon (Spinup)
- Gyro Cage
- Gimbal Torquers Enable
- Mode (Track/Cage)
- Gain Change
- Input/Output Test Jacks

### 3.2.4 Gyro Electronics

The gyro is operated as an angular rate indicator by operating it in a closed loop or "strapdown" mode. The electrical pickoff signals are demodulated, shaped, current amplified, then fed back to the gyro's internal torquers in such a way as to bring the gyro back to null. The torquer current, proportional to angular rate, is used as the input rate signal to the control boards.

### 3.2.5 Circle Generator

Gimbal angle queueing is provided within the sight unit (CRT display) by a circle. The distance between the center of the circle and the crosshairs is proportional to the gimbal angle. When the sight is in the autotrack mode, the gunner's duty is to keep the circle around the target which is centered in the display. This action will keep the gimbal angle near zero and away from the gimbal limits.

### 3.2.6 Sync Stripper

The Colorado Video 302-2 sync stripper is used to provide synchronization for the circular reticle. The unit derives these synchronizing signals from the DBA tracker's composite video signal. Hence, the circle may be superimposed onto the target scene on the CRT display.

### 3.2.7 Buffer Amps

The buffer amps provides buffering in two locations in the video path:

1. Between vidicon output and DBA tracker input;
2. Between DBA output and circle generator inputs.

### 3.2.8 Control Board

The control board is an analog circuit utilizing operational amplifiers which perform the control logic necessary to stabilize the platform in either cage or track mode.

### 3.3 System Design

The Phase I results of this effort indicated a clear superiority for the common gimbal tracking and stabilization configuration. The design of this configuration for Phase II testing included two operating modes:

1. An automatic tracking and stabilization mode (T/S)
2. A soft cage (SC) mode.

The tracking and stabilization mode is the primary mode which would be used to guide the missile to the target. The soft cage mode would be used to aid in initial acquisition and recognition by providing the gunner with the capability to voluntarily maneuver the sight while attenuating his involuntary and undesirable psycho-motor reflexes (jitter).

The implementation of this configuration for Phase II testing was heavily influenced by funding and schedule constraints. These constraints were the primary factors in many design decisions; key among these were:

1. The selection of an analog system
2. The use of an existing, off-the-shelf DBA tracker
3. The use of a standard TV vidicon camera as the imaging sensor

These selections minimized cost, schedule and technical risks but had a significant impact on system performance, design flexibility and operational flexibility when compared with other design alternatives. The vidicon camera and DBA tracker combination resulted in a tracking resolution that was an order of magnitude coarser than comparable focal plane array and correlation tracker combination. Very high contrast targets were also required to obtain stable tracking performance with the DBA tracker which was specifically designed to track high contrast targets. In selecting analog circuitry, design and development simplicity was traded for the flexibility inherent in a digital system using a microprocessor. Mode switching, non-linear design features and design changes were therefore limited.

In the primary mode (Tracking and Stabilization) the system must provide the two separate and distinct functions of target Tracking and line-of-sight stabilization. The system has been configured so that the stabilization and tracking functions are uncoupled allowing both functions to be treated independently. With this approach the two functions can be addressed separately to achieve the best overall performance within program constraints. This functional separation is achieved in a straightforward manner by using tracker and gyro outputs with the state estimator shown in Figure 3.3-1. As the figure shows, the transfer functions of the state estimator outputs to gimbal angle motion are unity. The response of the system to gimbal angle disturbances such as gunner jitter, is the stabilization function. Since the transfer functions are unity, the state estimator has no effect on the bandwidth of the stabilization system.

The tracker signal bandwidth is affected by the state estimator as the tracker transfer functions indicate. The state estimator provides a first-order filter for the tracker signal only and, therefore, this design parameter can be used to provide additional filtering for the tracking function without influencing the stabilization function.

Figure 3.3-2 shows an additional state that is the estimate of target line-of-sight rate. This estimate is a rate aiding signal that is used to track a constant velocity target with no steady state error. This signal can also be used to provide the Coriolis acceleration command required in line-of-sight guidance to minimize miss distance in crossing target engagements.

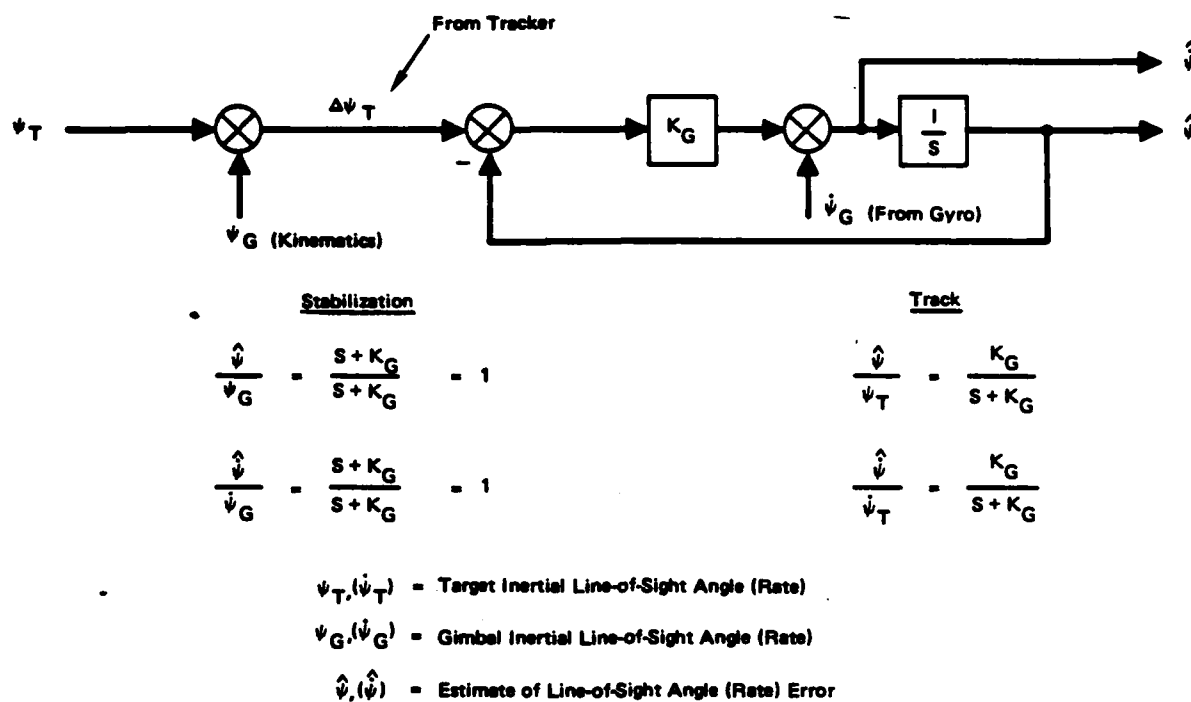


Figure 3.3-1. State Estimator

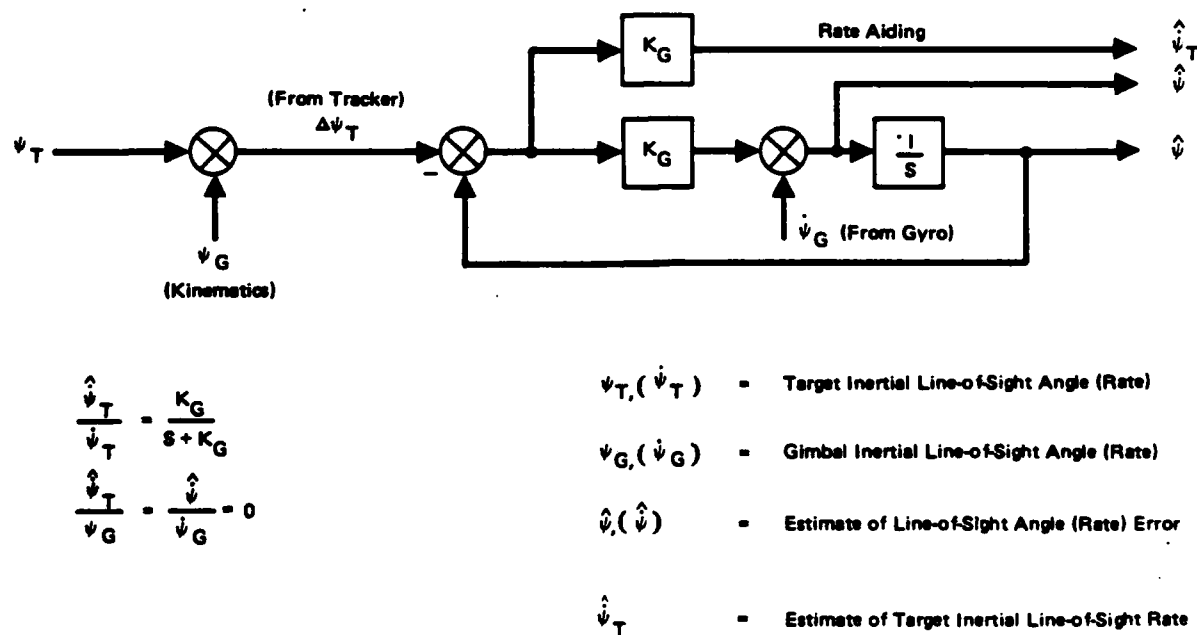


Figure 3.3-2. Rate Aiding



Closing the loops about the state estimator results in the tracking and stabilization system shown in Figure 3.3-3. Brushless DC torquers were used as the actuation mechanism for this system because they minimize the friction coupling to the stable gimbal platform. Gunner jitter is the main disturbing input to the stabilization system which enters through non ideal hardware characteristics such as friction and magnetic drag. Most of the isolation is provided by the natural inertia of the gimbal system. The other principal error sources are tracker noise and tracker resolution.

The design parameters  $K_A$ ,  $K_R$  and  $K_G$  are selected to optimize system performance for two conflicting trends. High bandwidth decreases errors due to gunner motion and low bandwidth decreases errors due to sensor noise. Analysis and simulation have shown that a stabilization loop undamped natural frequency of 5 to 10 hertz is optimum depending on assumptions made concerning gunner motion. A typical simulation result is shown in Figure 3.3-4. A stabilization loop frequency of 7.5 hertz was selected for the Phase II design. Similarly, a state estimator bandwidth of 1.0 hertz was selected based on the simulation results shown in Figure 3.3-5.

The same design approach is used for the soft cage mode shown in figure 3.3-6. In this mode, the gimbal angle sensors have replaced the scene tracker. The state estimator gain,  $K_G$ , is mechanized as a variable parameter so that the handling quality of the soft cage mode can be evaluated.

The gain,  $K_G$ , determines the amount of stabilization or isolation that the unit will provide from the gunner motion. At one extreme, with the gain set to zero and the rate aiding signal out, the unit will be inertially stabilized and will not respond to any gunner motion. This is not a useful condition since it is desirable to respond to the deliberate motion of the gunner so that he can voluntarily change his viewing area or aimpoint for target acquisition. By increasing the gain, the low frequency motion will be transmitted through the system to respond to voluntary movement of the line-of-sight while high frequency, involuntary motion will be attenuated.



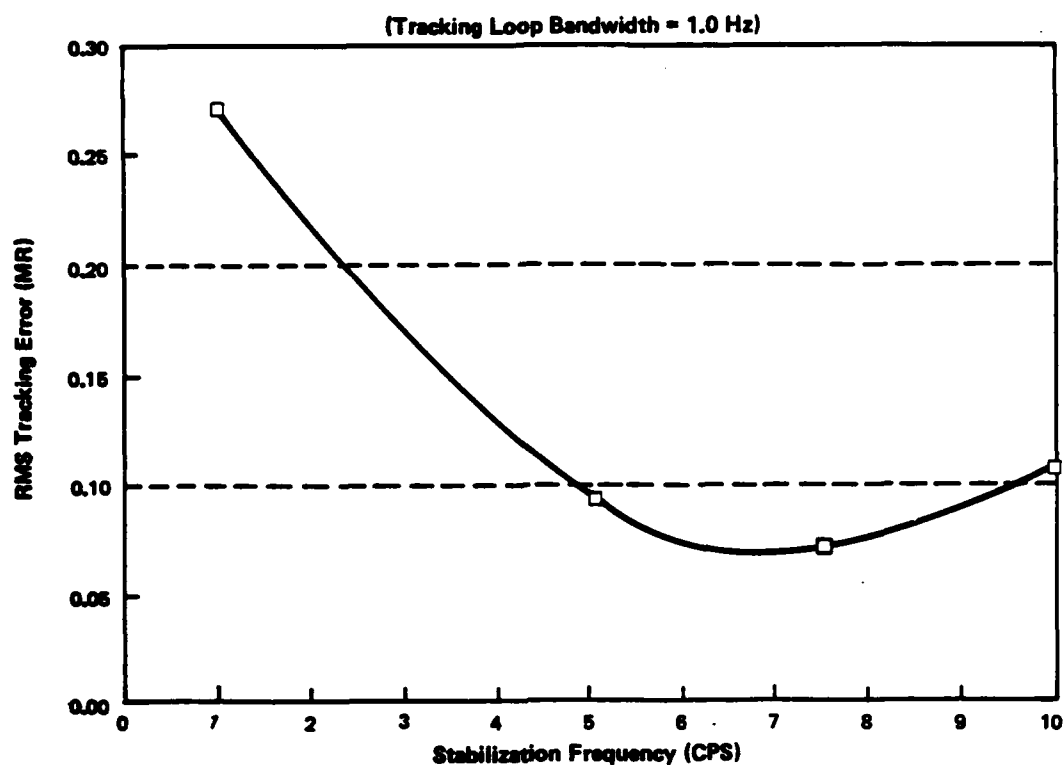


Figure 3.3-4. Stabilization Loop Optimization

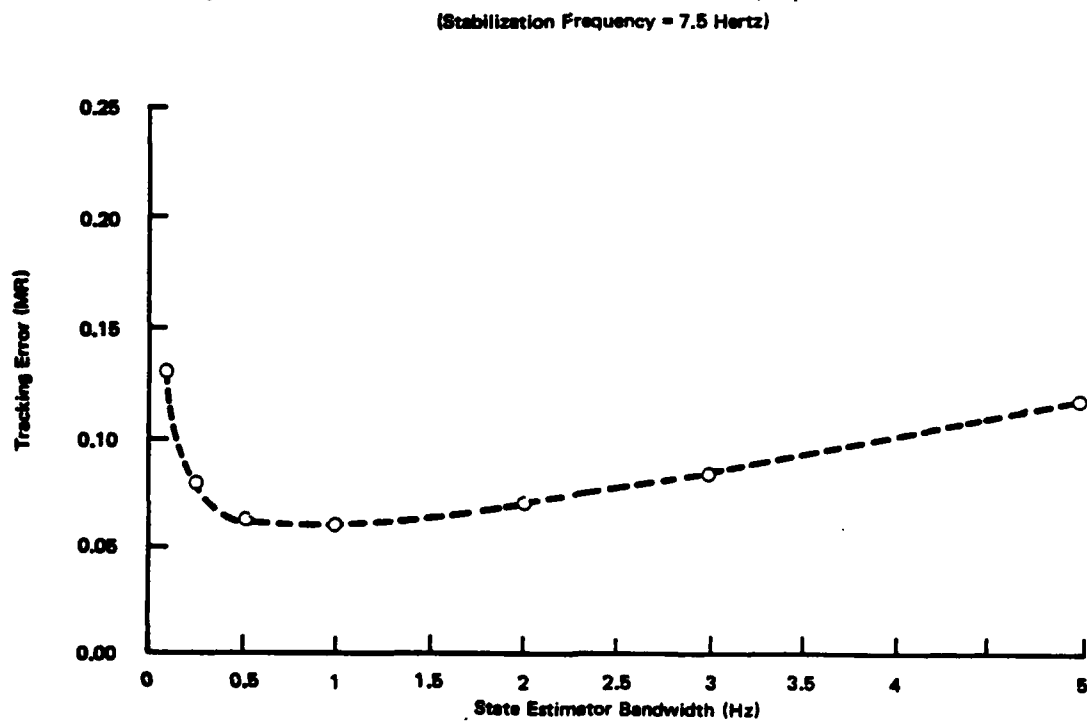
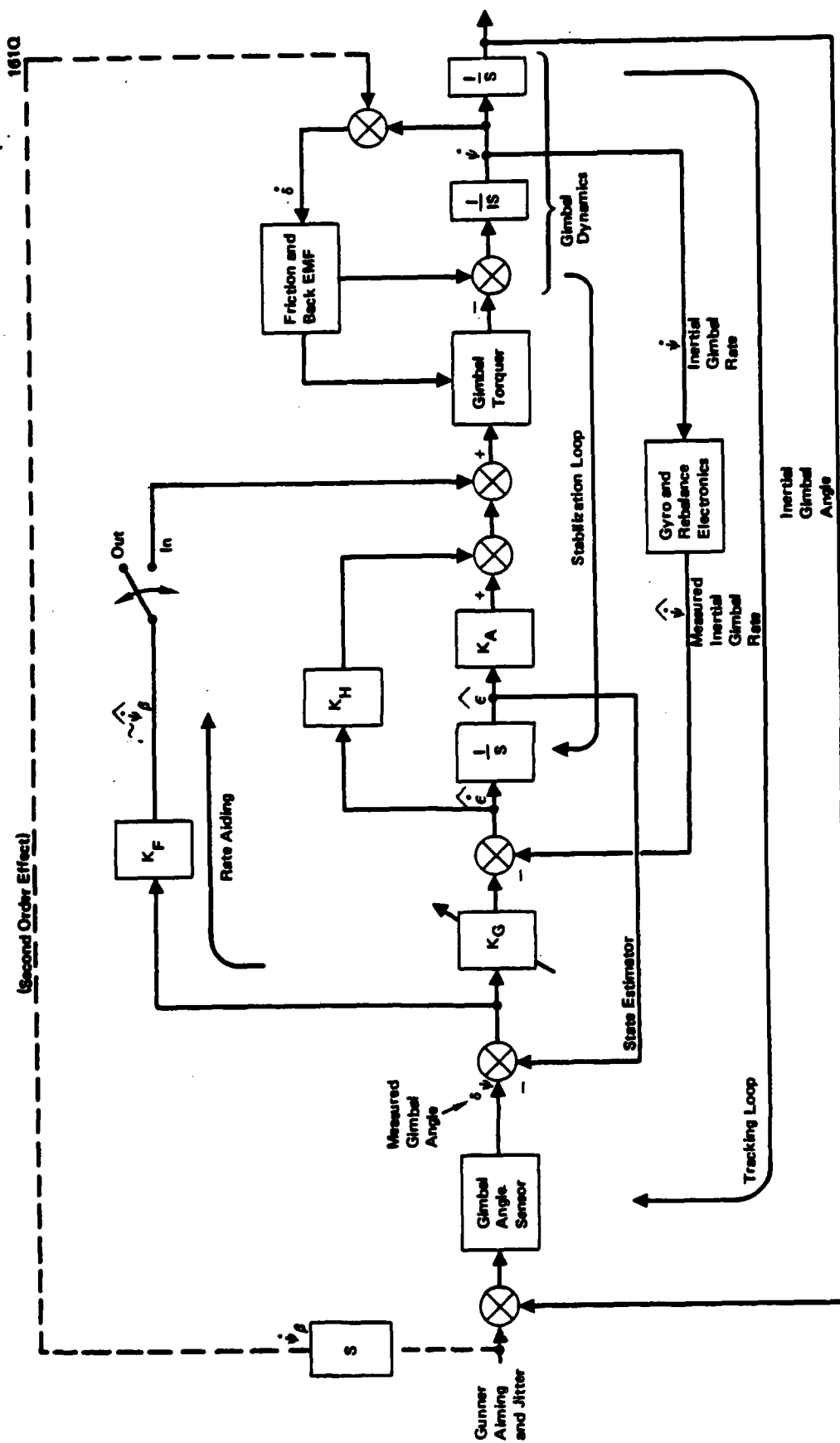


Figure 3.3-5. State Estimator Bandwidth Optimization



**Figure 3.3-8: Soft Cage**

#### 4.0 Test Equipment Description

Two types of tests were performed: Table mounted tests and shoulder mounted tests. The table mounted tests were performed to obtain quantitative data to determine the tracking and stabilization performance under controlled conditions. The shoulder mounted tests were qualitative, to determine handling qualities of the unit in the soft cage mode.

The table mounted test equipment consisted of:

- o Servo Table
- o Noise Generator
- o Theodolite
- o Brush Recorder

#### 4.1 Servo Table

The Aeroflex ARVG-121 consists of a 2 degree-of-freedom pedestal and a servo electronics unit. Pertinent physical, mechanical and electrical features of the pedestal are shown in Figure 4.0-1. The table was operated in a closed loop mode using a position pot as the angle transducer. A tachometer provides the angular rate signal for damping and a direct coupled DC torquer provides the actuation in each axis.

The control board schematics for the electronics unit are shown in Figures 4.0-2 and 4.0-3. The frequency response of the closed loop system was tested and modeled for simulated gunner noise tests. These results are summarized in Figures 4.0-4 and through 4.0-7.

#### 4.2 Noise Generator

The Hewlett-Packard 3722A is a low-frequency broadband noise generator designed primarily for use in control systems evaluation and applications requiring the simulation of random disturbances. The specific feature of the HP3722A that was used in the test phase was the GAUSSIAN output, a random noise output of a continuous waveform nature with approximately Gaussian amplitude distribution. If the spectrum of the GAUSSIAN output is assumed to be rectangular, then Total Power = equivalent bandwidth x power density, with the equivalent bandwidth normally exceeding the stated GAUSSIAN NOISE BANDWIDTH (fo) by about 5%.

Degrees of Freedom

Az:  $\pm 120^\circ$   
Elev:  $\pm 75^\circ$

Direct Drive Torque Motors

Az: 18 Ft-Lbs  
Elev: 9 Ft-Lbs

Acceleration With 0.04 Slug Ft<sup>2</sup> Load

Az:  $850^\circ/\text{Sec}^2$   
Elev:  $850^\circ/\text{Sec}^2$

Gimbal Opening

9 in. W X 12 in. H

Tachometer:

Inland Type TG-4011  
10V Per Rad/Sec  
Max Velocity  $300^\circ/\text{Sec}$   
Linearity: 1% of Actual  
Ripple: 4.5% of Actual

Power Amplifier:

Solid State Non-Switching DC Amplifier

Load Capacity:

300 Lbs With 15g Shock

Stops

Adjustable Cushion Type, Fluid Filled

Stow

Mechanical and Electrical Caging

Pickoff

Provision for  $2^{18}$  Encoder (CFE)

Orthogonality

1 Arc Min

Wobble

30 Arc Sec

Weight

150 Lbs

Power

5 Amps at 115V-60 Hz

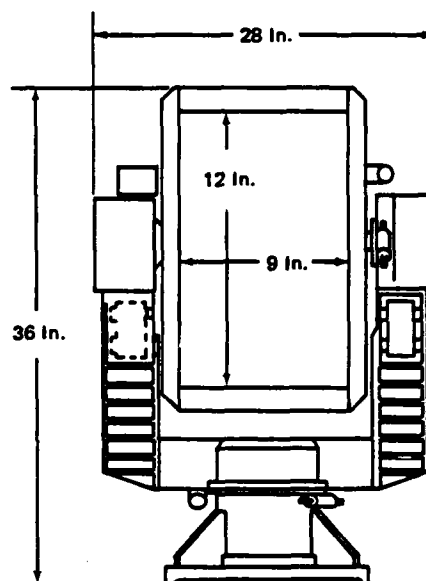


Figure 4.0-1. Aeroflex ARVG-121 Servo Table

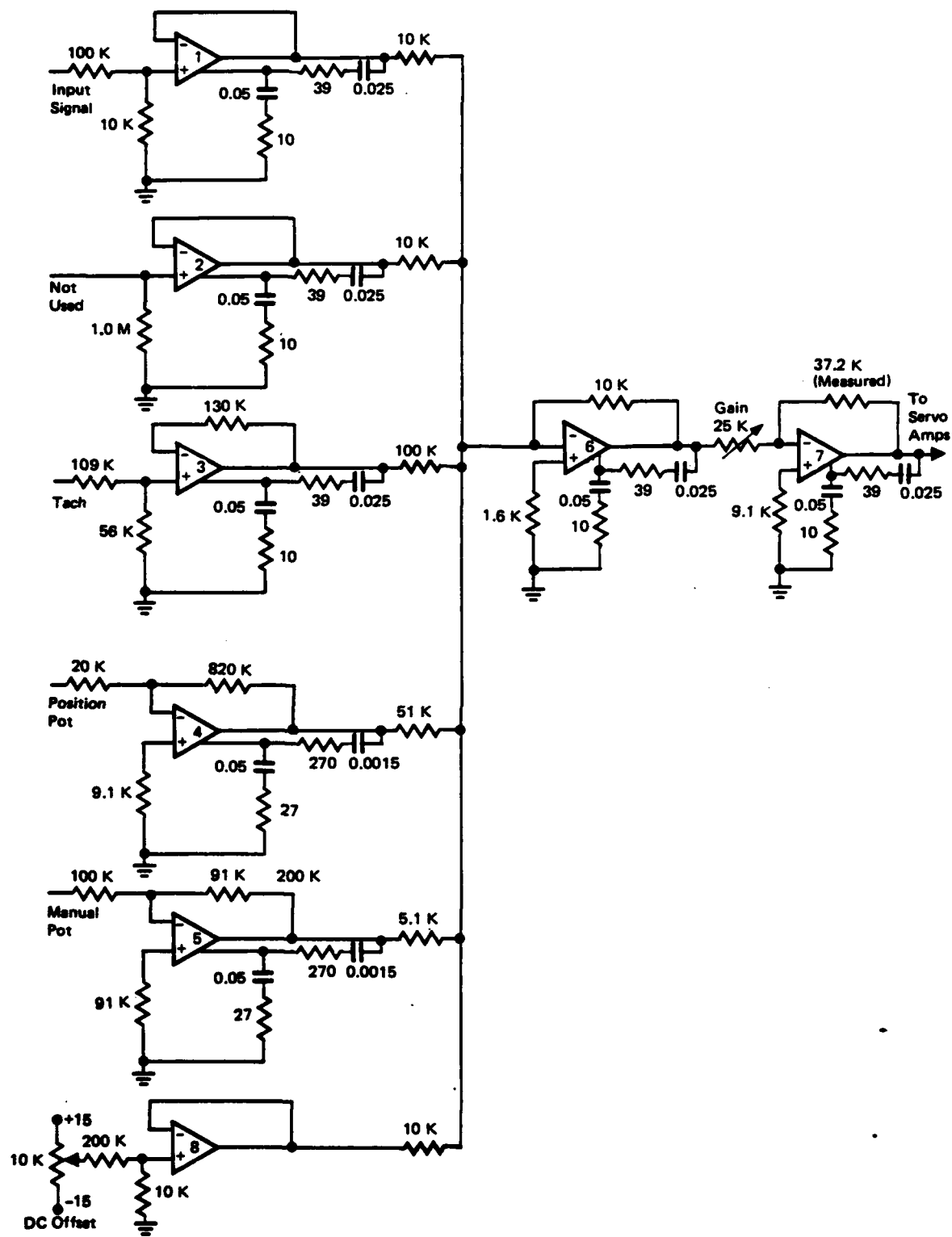


Figure 4.0-2. Aeroflex Control Electronics – Azimuth

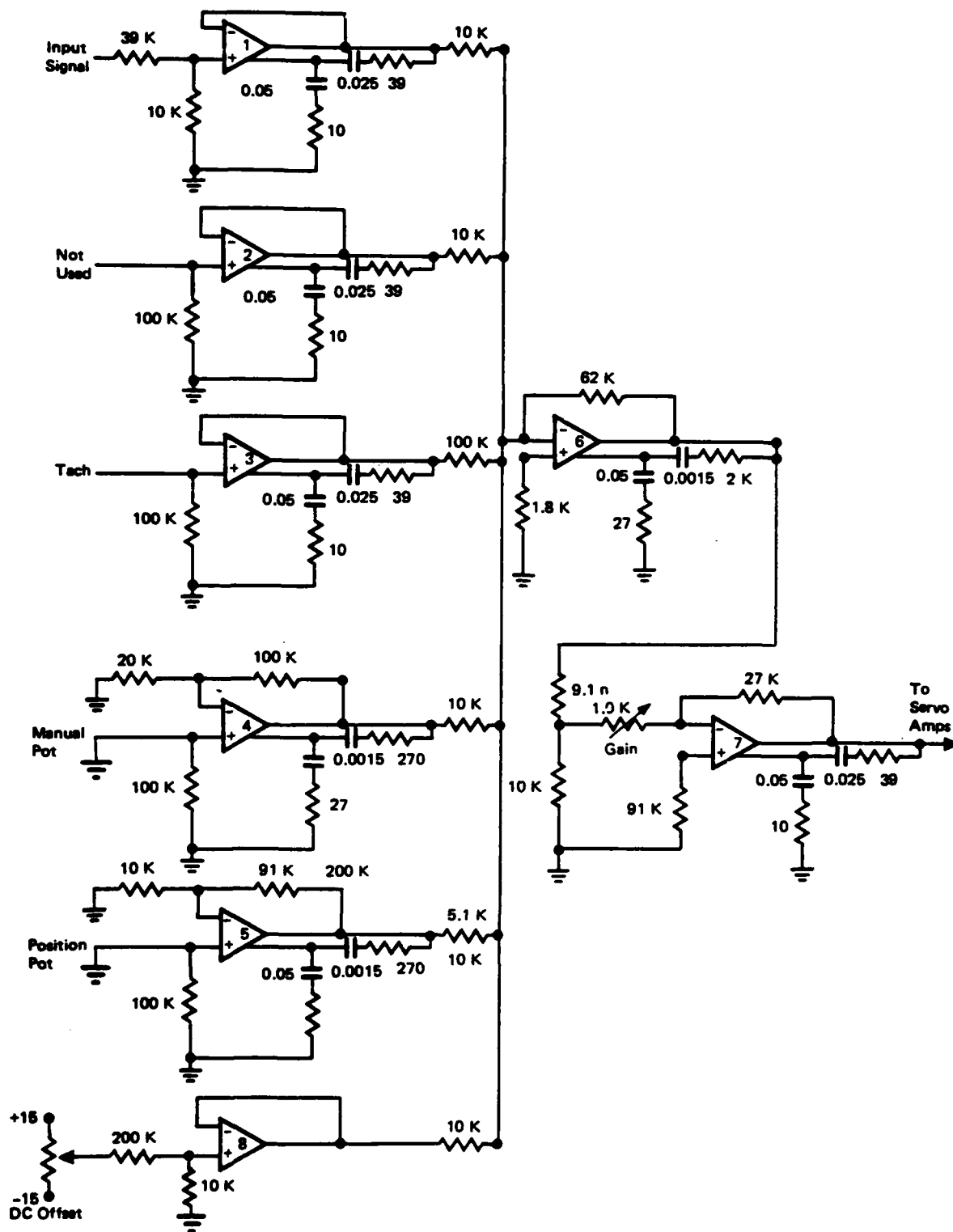


Figure 4.0-3. Aeroflex Control Electronics - Elevation



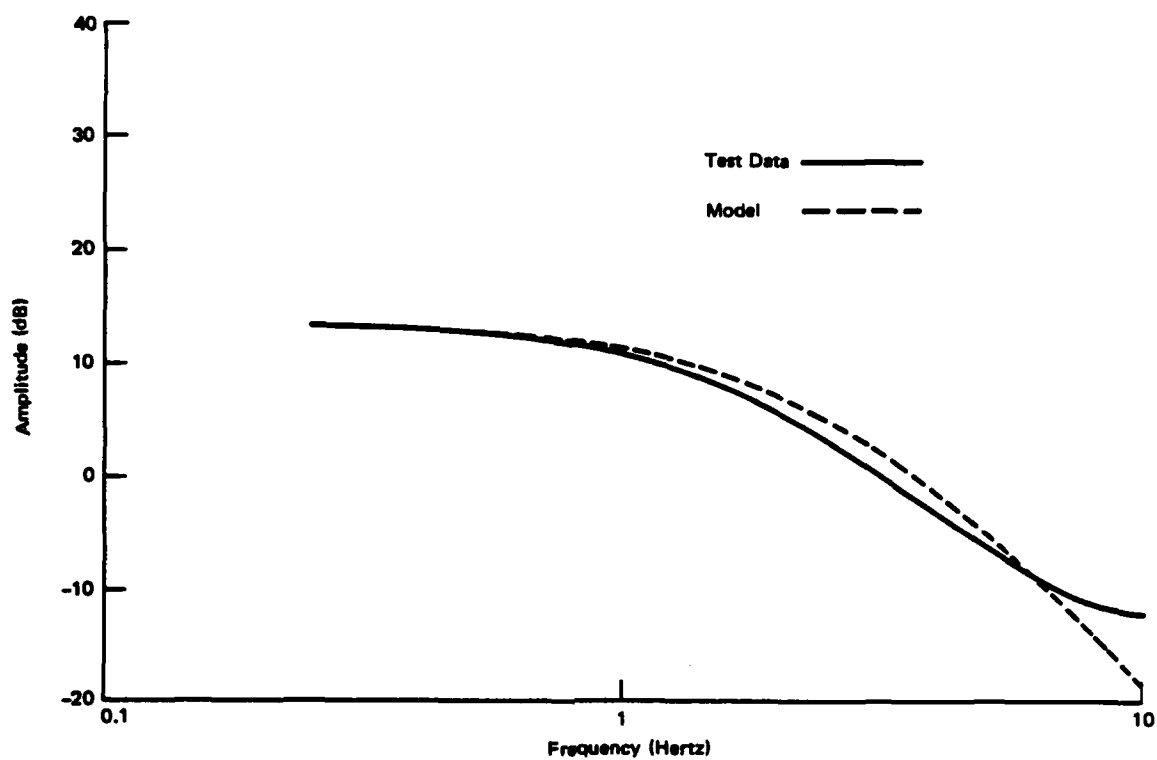


Figure 4.0-4. Aeroflex Frequency Response - Azimuth

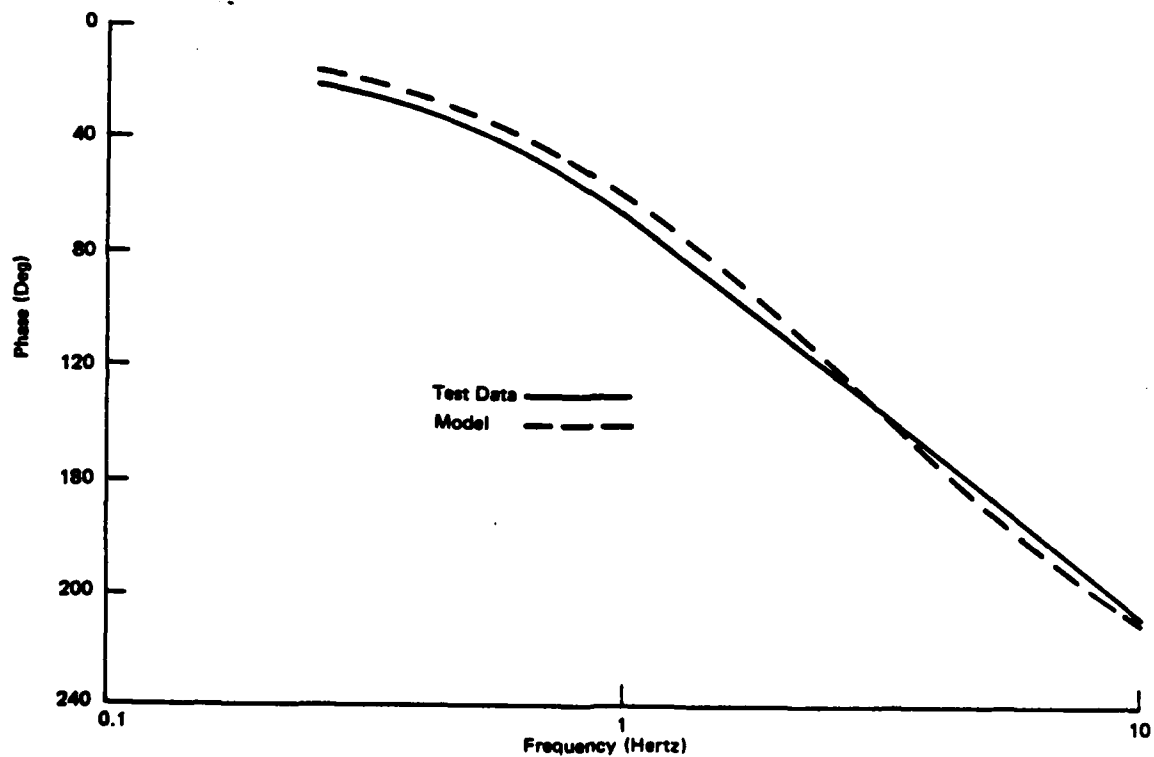


Figure 4.0-5. Aeroflex Frequency Response - Azimuth

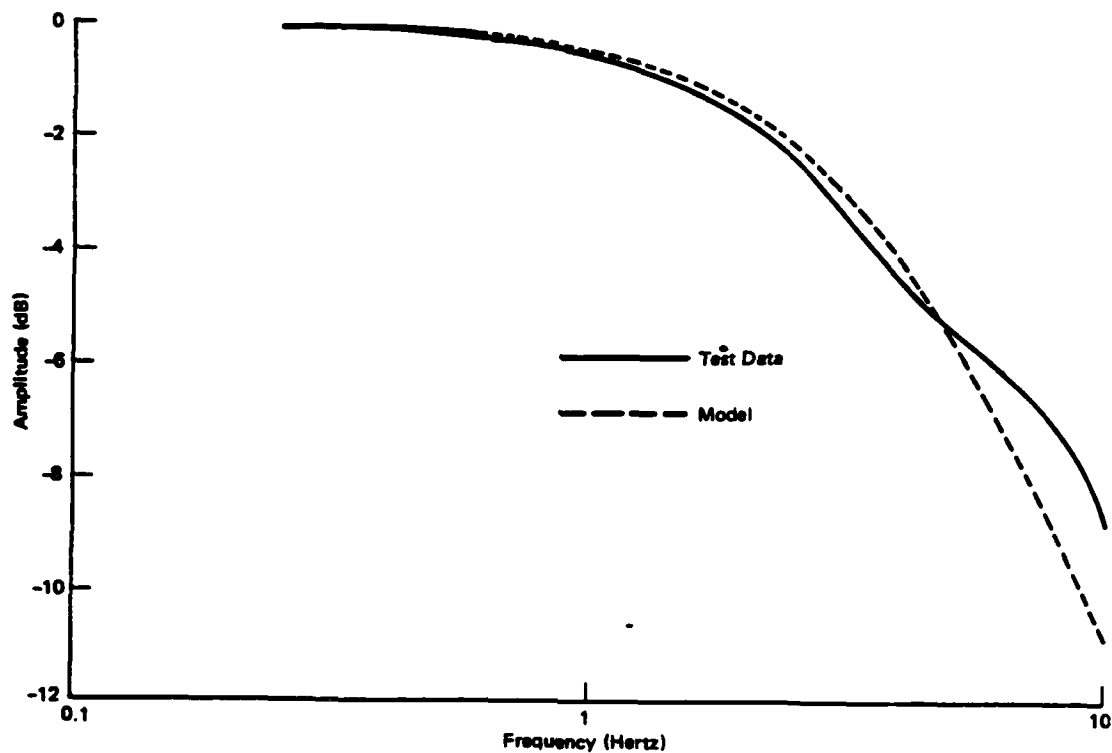


Figure 4.0-6. Aeroflex Frequency Response - Elevation

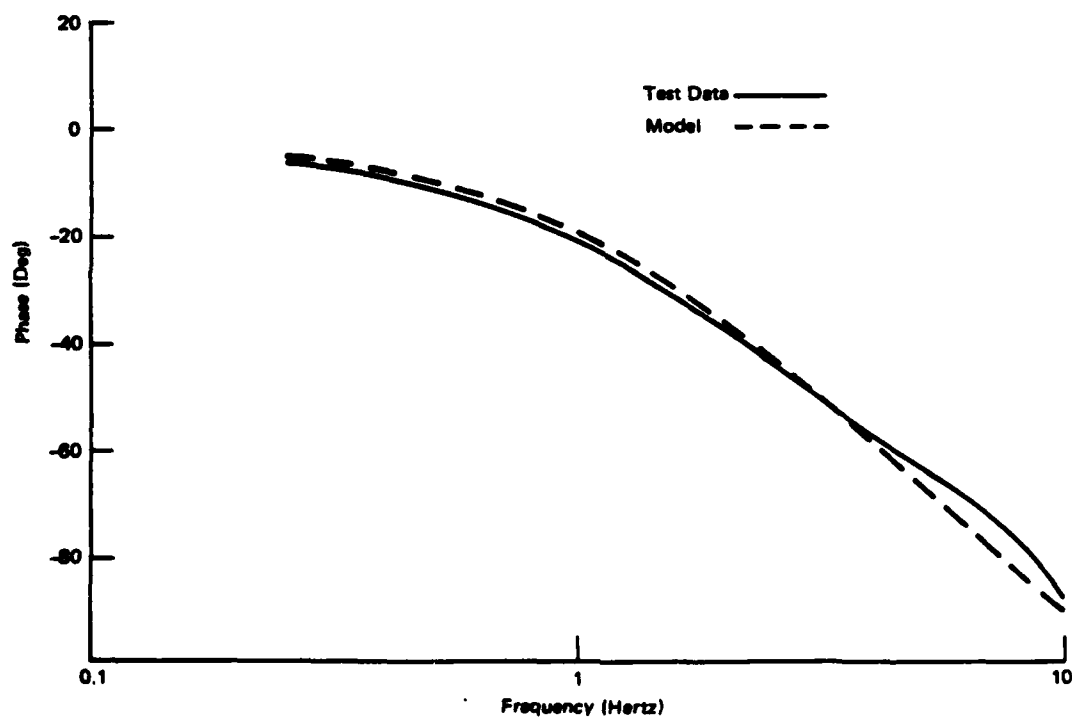


Figure 4.0-7. Aeroflex Frequency Response - Elevation

#### 4.3 Theodolite

The Kern DKM2 is a double-circle triangulation theodolite with an optical micrometer. It has a telescopic magnification of 30X, with an objective aperture of 45mm. Readings are accurate to within 0.1 seconds of arc.

#### 4.4 Brush Recorder

A 4-channel Brush recorder model 2400 was used to record the test data.

No test equipment was required for the shoulder mounted tests.

### 5.0 Table Mounted Tests

The table mounted tests were conducted to determine the performance of the T/S unit. The gimbaled portion of the unit was mounted on the Aeroflex table as shown in Figure 5.0-1. Because of the geometry of this configuration, the azimuth axis of the table and the T/S unit were separated by 0.25 inch. The elevation axes were co-linear.

The dynamic characteristics of the tracking and stabilization unit are similar to the MDAC proposed tactical system for IMAAWS. The pertinent parameters are summarized below:

	<u>PHASE II TRACKER</u>	<u>IMAAWS TACTICAL</u>
Moment of Inertia (oz-in-sec <sup>2</sup> )		
Azimuth	1.3	1.4
Elevation	1.4	1.75
Maximum Torque (oz-in)	43*	30

\*The Phase II system torquers have a maximum output capability of 80 oz-in but were limited to 43 oz-in in the brassboard configuration.

The table-mounted tests were conducted in three groups. In the first group the Aeroflex table was driven with sinusoidal inputs of known amplitude and frequency to obtain parametric data on the stabilization performance of the unit. In the second group of tests, a noise generator was used to drive the table with random inputs that were representative of typical gunner aiming error motion under various conditions. The third test involved tracking of a simulated crossing target.

The test geometry is shown in Figure 5.0-2. The nonmoving target was a plastic tank model that was about 1/50 of full scale, so that the tank image size was equivalent to that of a full-size tank at 211 meters. The model was sprayed with light gray paint and was set against a dark background to provide sufficient contrast for good operation of the DBA tracker. A moving target was simulated by using a Helium Neon laser that was projected onto the wall via the galvanometer-operated mirror.

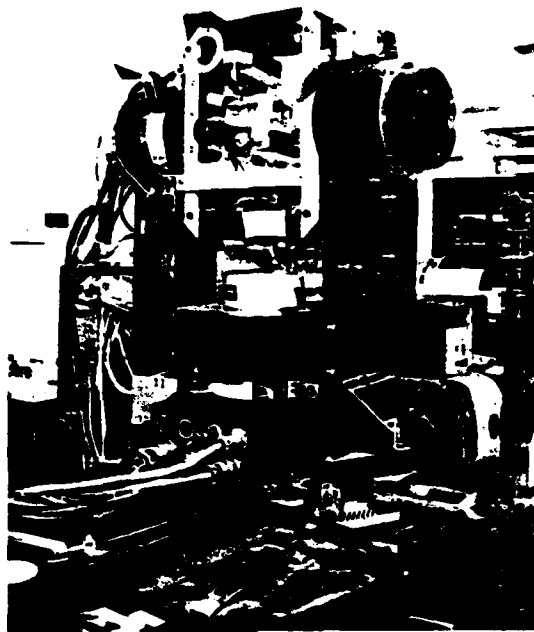


Figure 5.0-1. Table Mounted Test Fixture

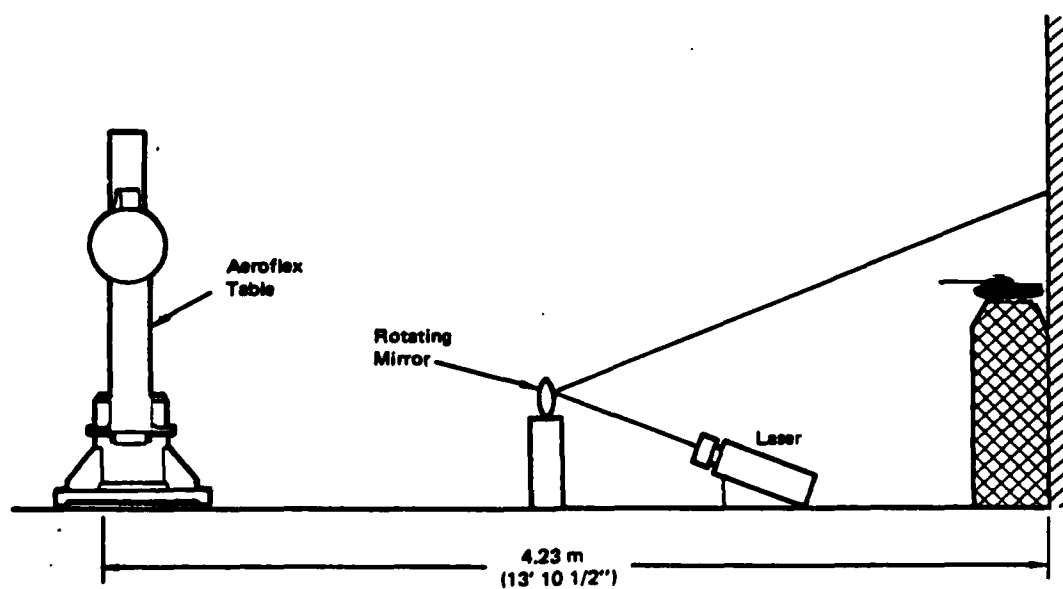


Figure 5.0-2. Table Mounted Test Geometry

### 5.1 Sinusoidal Tests

The test parameters for the sinusoidal tests are summarized in Table 5.1-1. Two types of measurements were made to estimate system performance. First a theodolite was used to measure the line-of-sight jitter. Four different measurements were made for each azimuth test and the results were averaged. The maximum deviation of the theodolite measurements in any single test was 29  $\mu$ radians (6  $\widehat{\text{sec}}$ ).

The state estimator output from the control board circuits was used as a second estimate of system performance. This output was recorded on the Brush recorder for each test. A sample of this output is shown in Figure 5.1-1 for the 2.5 hertz, 15 milliradian peak-to-peak run. The state estimator output has a varying amplitude. The median amplitude of this output was used as a measure of system performance.

The digital simulation was used as another verification of performance. The simulation results matched very well with the test results in the azimuth axis. Comparisons of the test and simulation results are shown in Figures 5.1-2 through 5.1-4 for the high frequency (2.5 cps) base motion inputs of 5, 10 and 15 milliradians respectively. The true tracking error from the simulation is also shown in the figures. The true tracking error is larger than that indicated by the state estimator by 20 to 30 percent. The low frequency (0.25 cps) results are shown in Figures 5.1-5 through 5.1-7.

An advantage of using simulation results is that performance measures can be reduced to standard statistical quantities. The RMS value of the true tracking error was determined from the simulation results. A comparison of the three performance estimates: theodolite, state estimator and simulation are shown in Figures 5.1-8 through 5.1-11 for the four input frequencies. The median of the state estimator and the RMS of the true tracking error from the simulation show similar performance capability of the tracking and stabilization unit, especially at the higher frequencies.

The T/S performance is summarized in Figure 5.1-12 for the azimuth axis. The attenuation ratio is the ratio of the base motion amplitude to the tracking error amplitude. For the simulation data the RMS input amplitude was used instead of

Table 5.1-1. Sinusoidal Test Schedule

Test No.	Frequency (Hertz)	Amplitude (MR)
1	N/A	0
2	0.25	5
3	0.25	10
4	0.25	15
5	0.50	5
6	0.50	10
7	0.50	15
8	1.0	5
9	1.0	10
10	1.0	15
11	2.5	5
12	2.5	10
13	2.5	15

the peak-to-peak amplitude so that a consistent comparison could be made. This accounts, in part, for the lower attenuation ratio of the simulation data.

Performance in the elevation axis was analyzed in a similar manner. The theodolite data was not recorded for the elevation test due to the length of time required to take these measurements. Theodolite measurements were taken periodically during the tests to verify that the state estimator and theodolite measurements were similar in magnitude. These "spot checks" showed that the state estimator and theodolite measurements were within the accuracy with which the theodolite data could be consistently read ( $\sim 30 \mu\text{rad}$ ).

Duplication of the test data by simulation was not as successful as it was in the azimuth axis. The magnitudes were similar but the shape could not be duplicated. The apparent reason is the synergism or coupling between the line-of-sight jitter and the DBA tracker, which could not be duplicated with the simulation model. A higher fidelity tracker model seems to be necessary to achieve a better match between the test data and the simulation results. The poor resolution capability of the DBA tracker in the elevation axis ( $\pm 0.32 \text{ mr}$ ) is a principal contributor to the analysis problem. The method of processing of the interlaced horizontal lines in the two T-V fields that make up a single picture needs to be better understood to increase the fidelity of the simulation model.

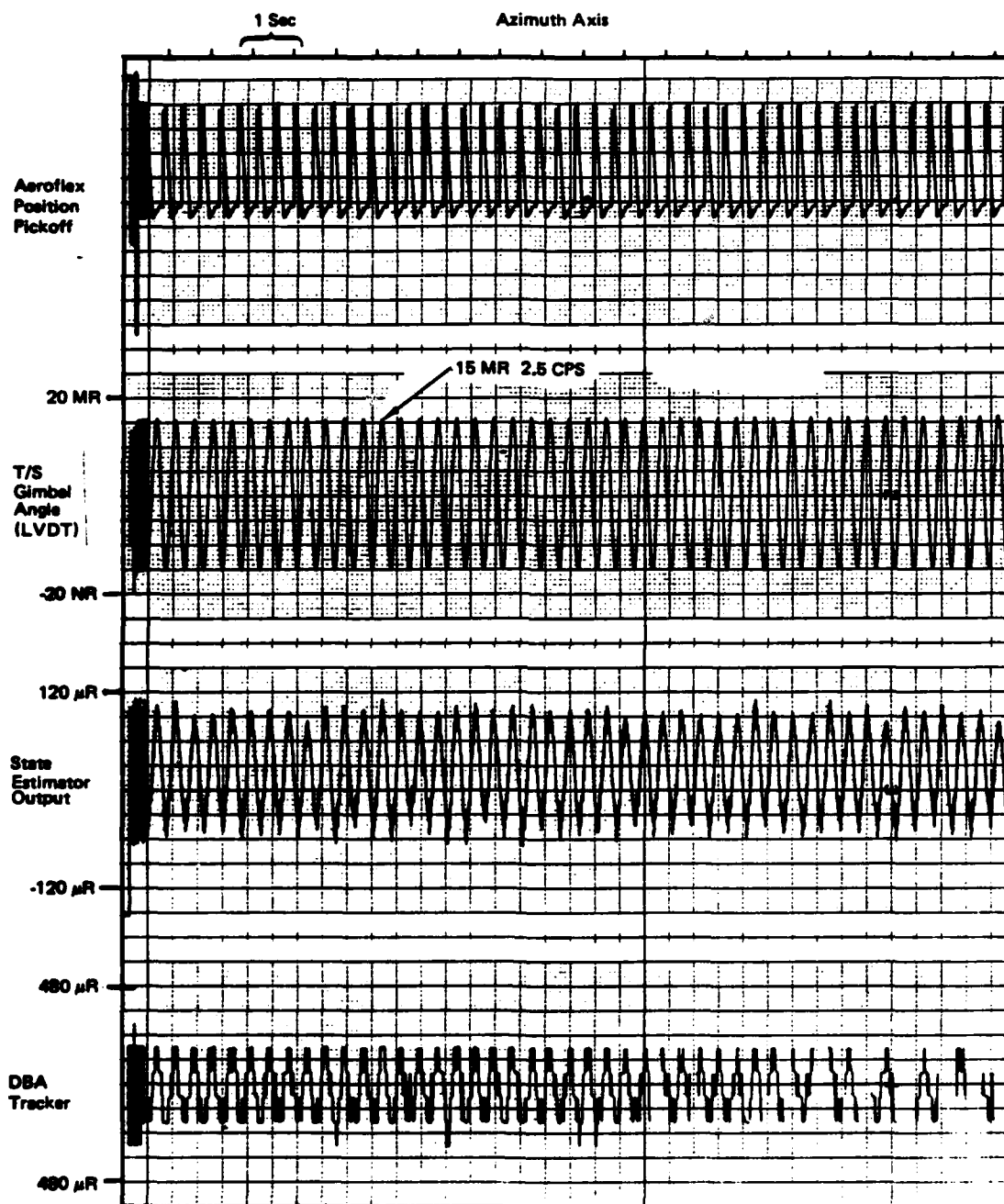


Figure 5.1-1. 15 MR 2.5 CPS Test



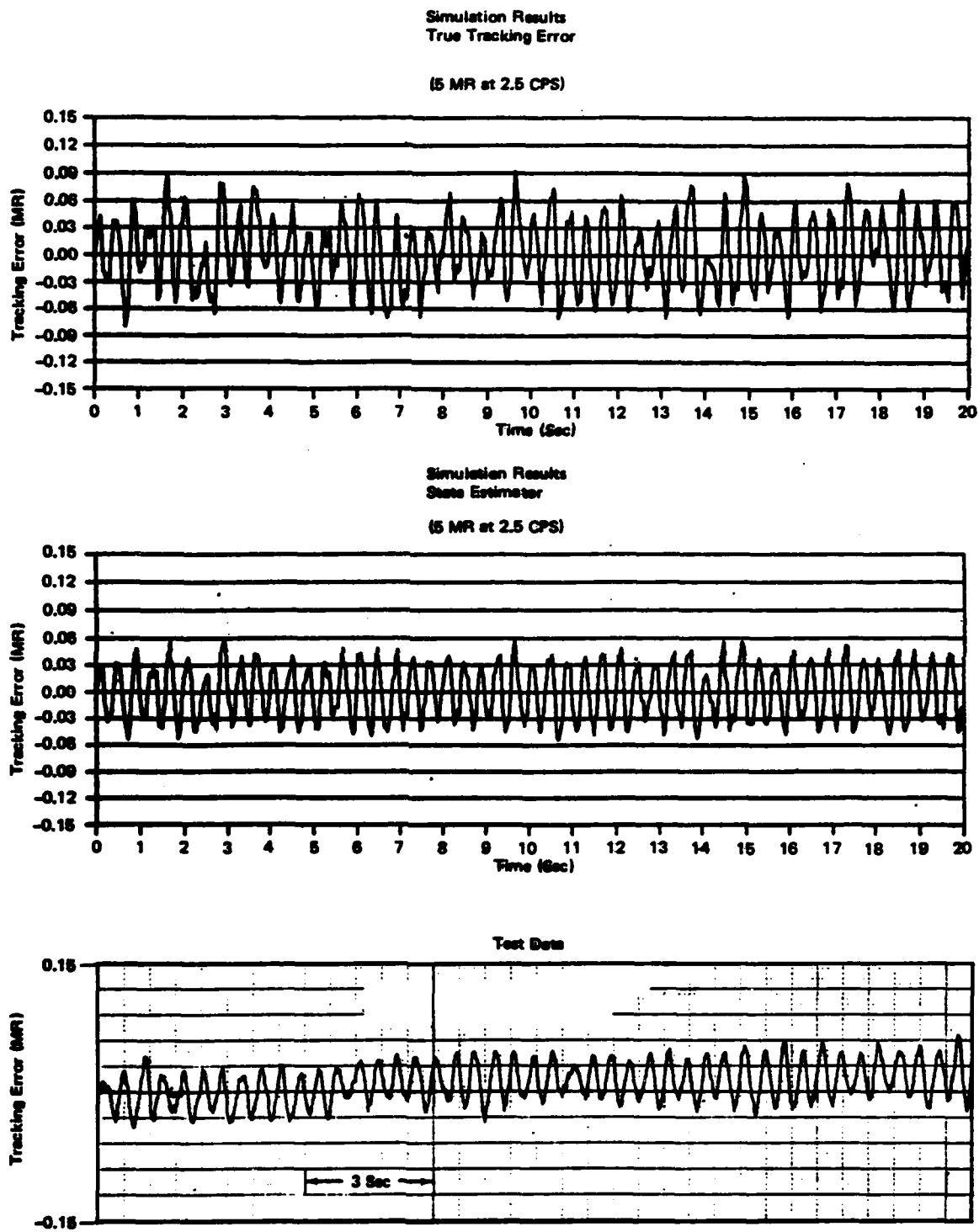


Figure 5.1-2. Test/Simulation Comparison - Azimuth

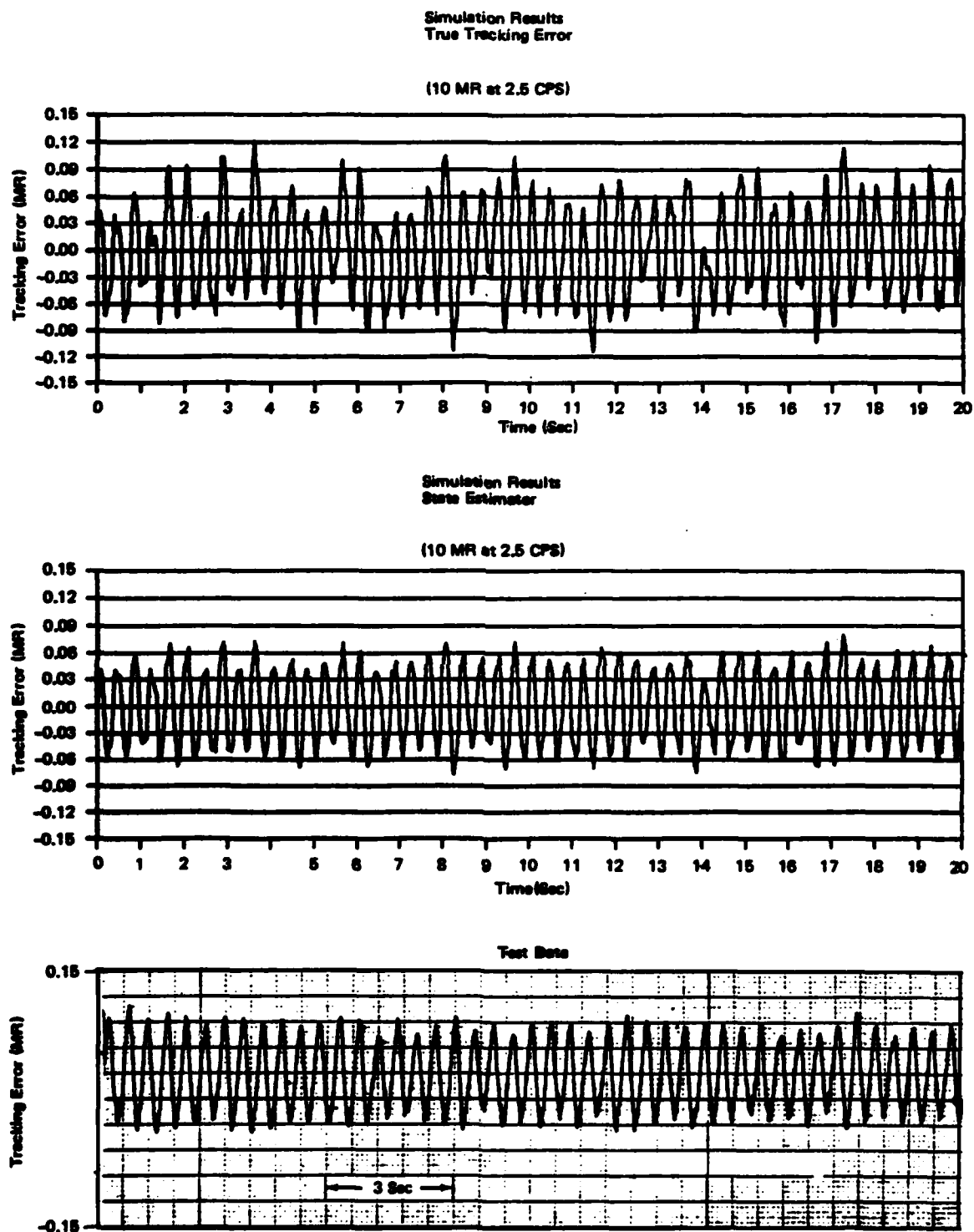


Figure S.1-3. Test/Simulation Comparison - Azimuth

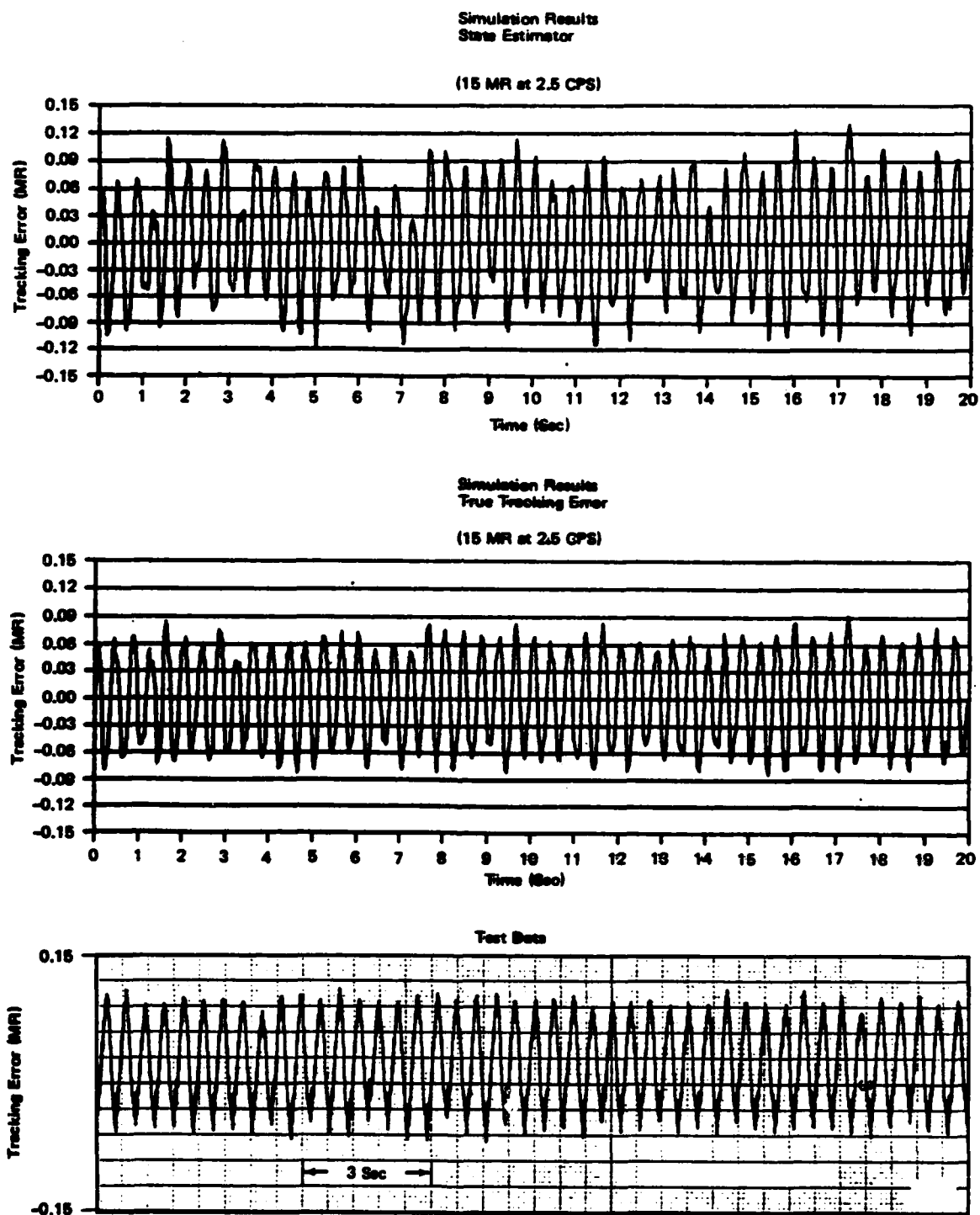


Figure 5.14. Test/Simulation Comparison - Azimuth

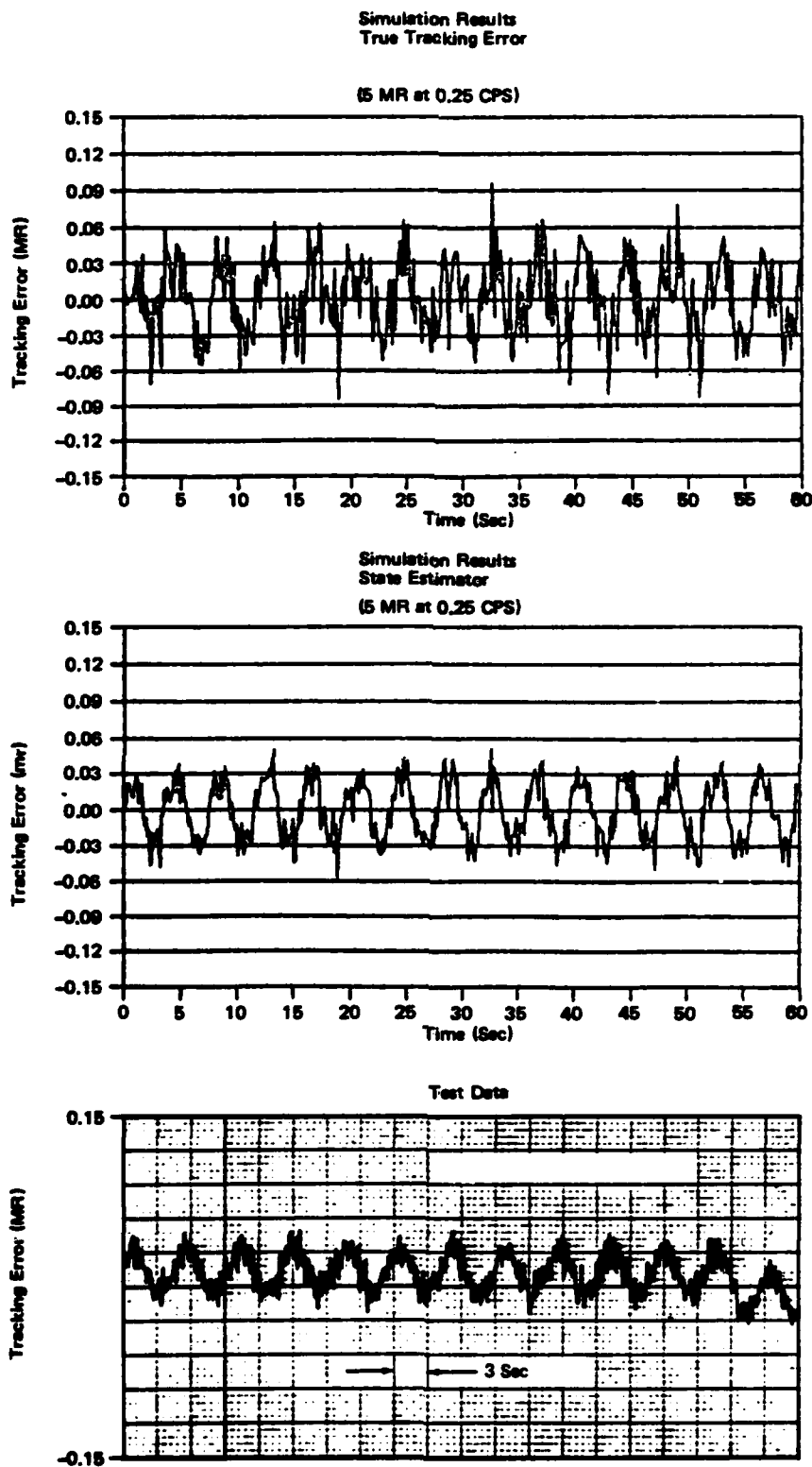


Figure 5.1-5. Test/Simulation Comparison - Azimuth

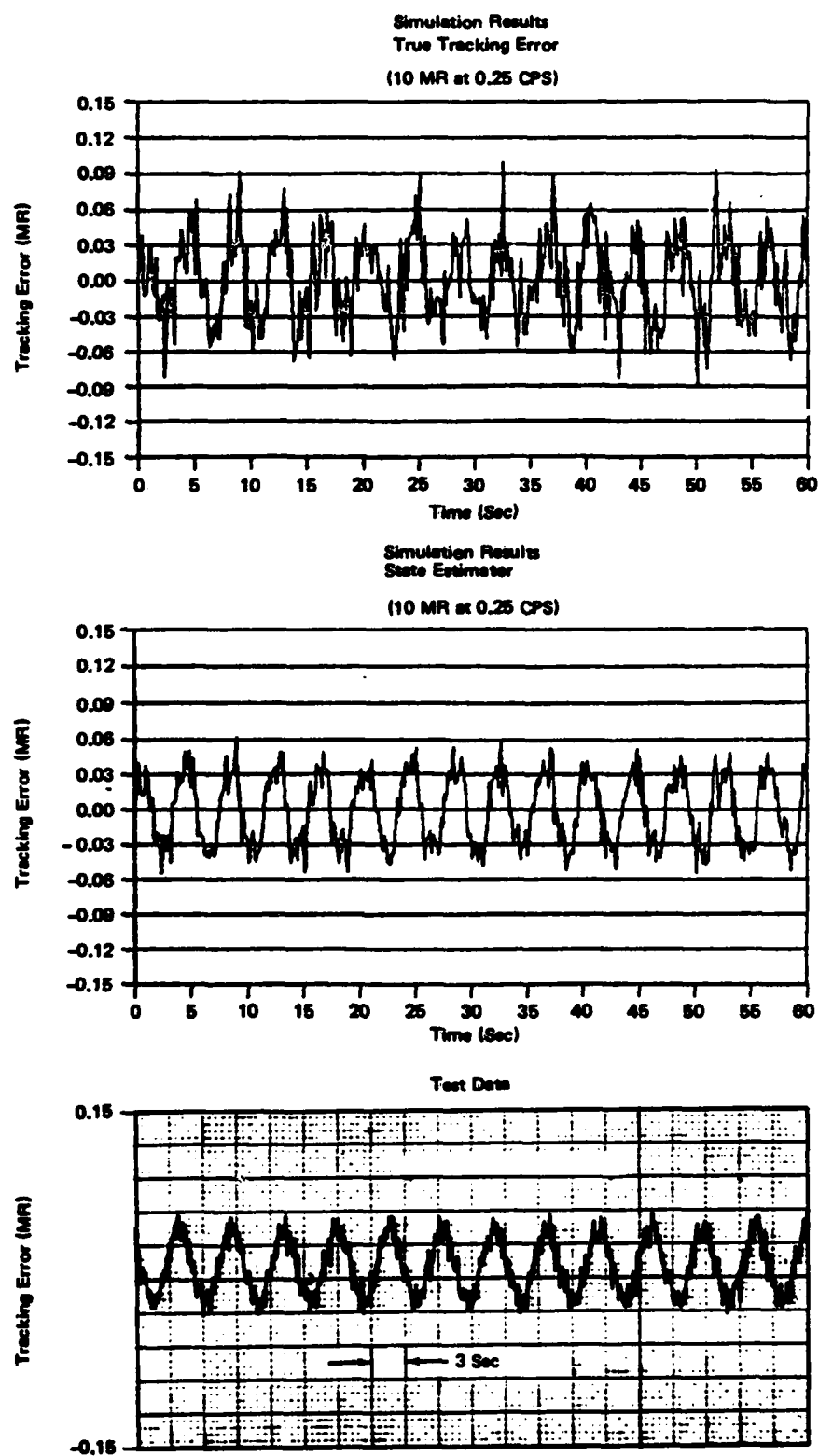


Figure 5.1-6. Test/Simulation Comparison - Azimuth

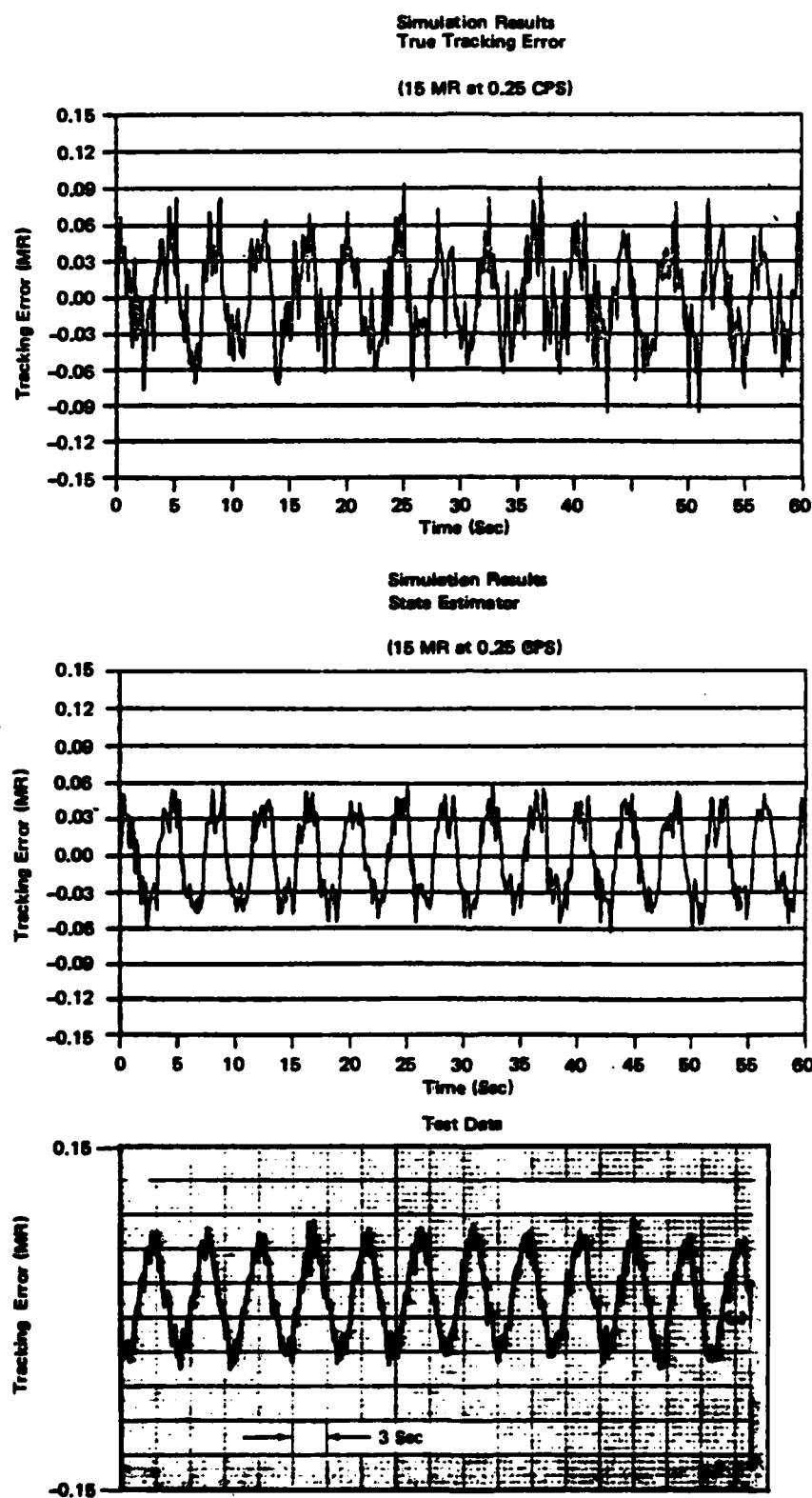
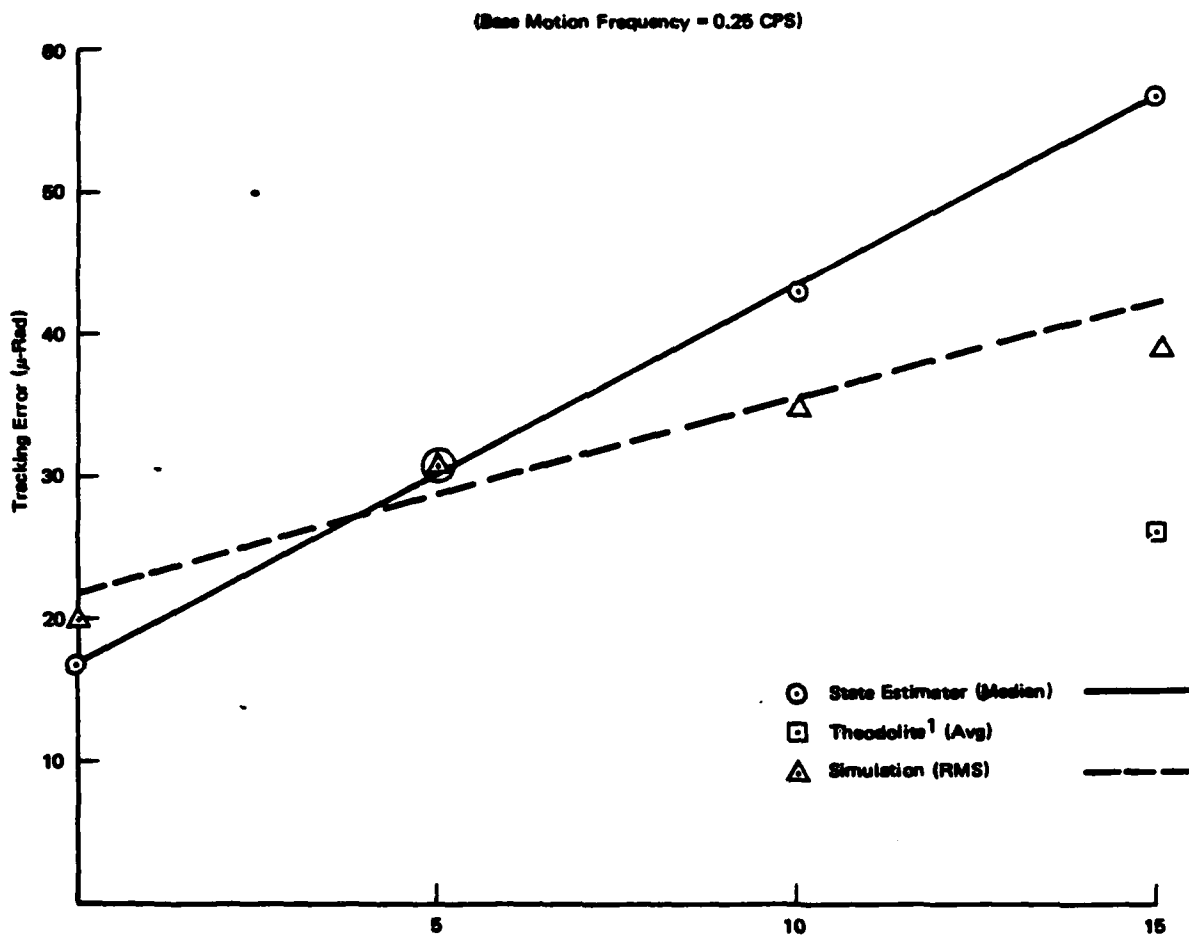


Figure 5.1-7. Test/Simulation Comparison - Azimuth



1 Theodolite Data For 5 & 10 MR Not Available Due to Measurement Error

Figure 5.1-8. Comparison of Alternate Performance Measures - Azimuth

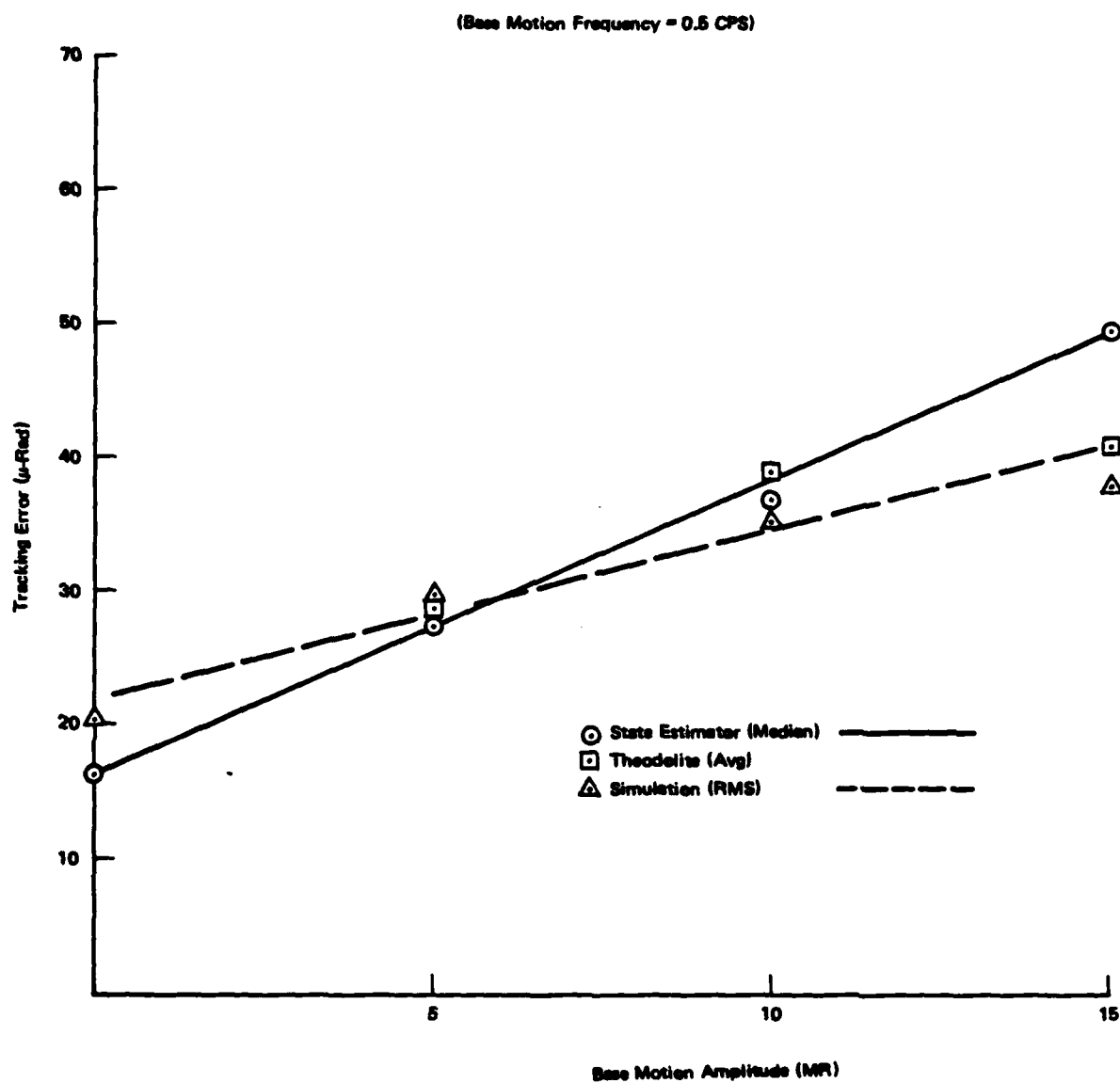


Figure 5.1-9. Comparison of Alternate Performance Measures - Azimuth



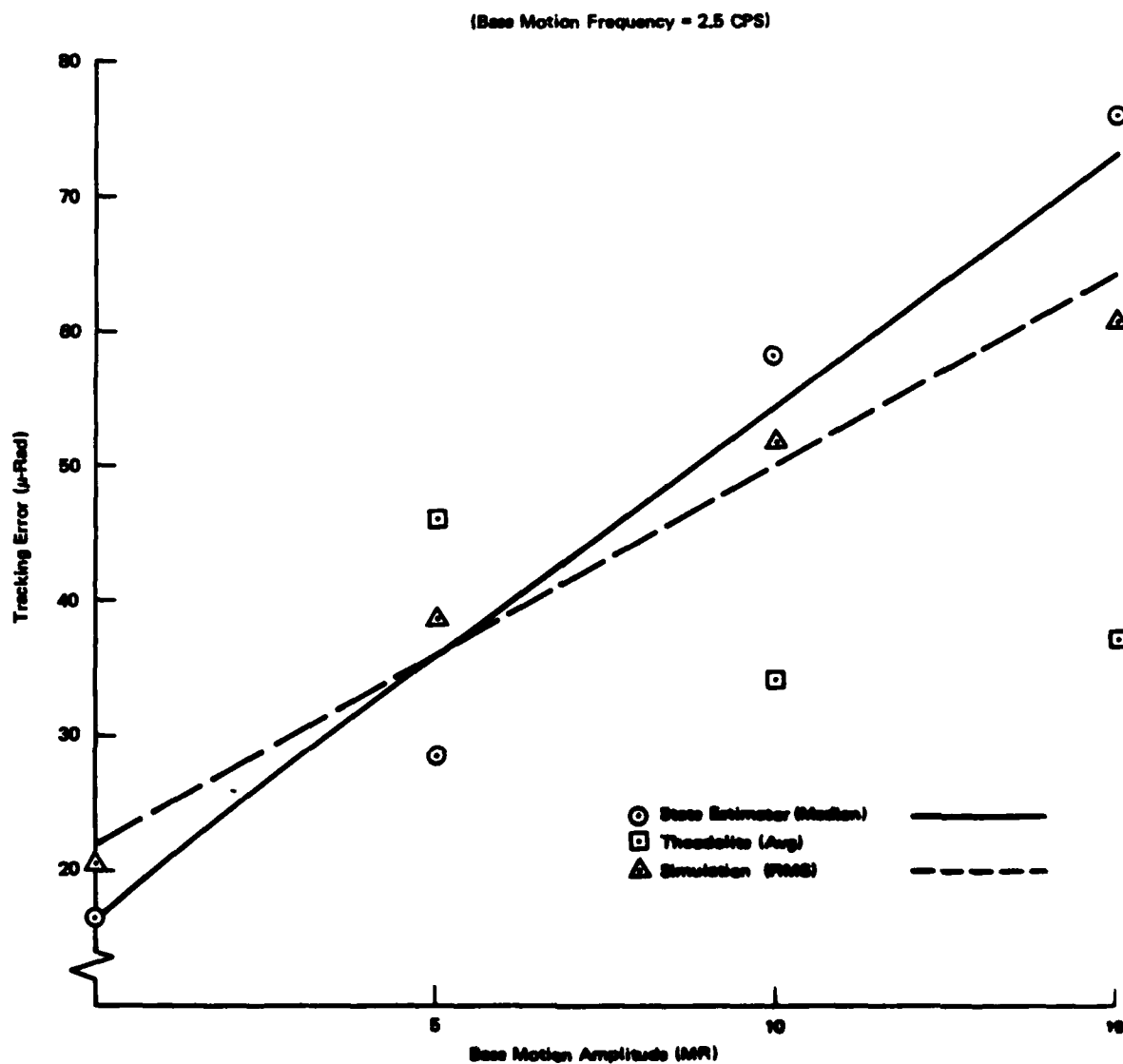


Figure 5.1-10. Comparison of Alternate Performance Measures - Azimuth

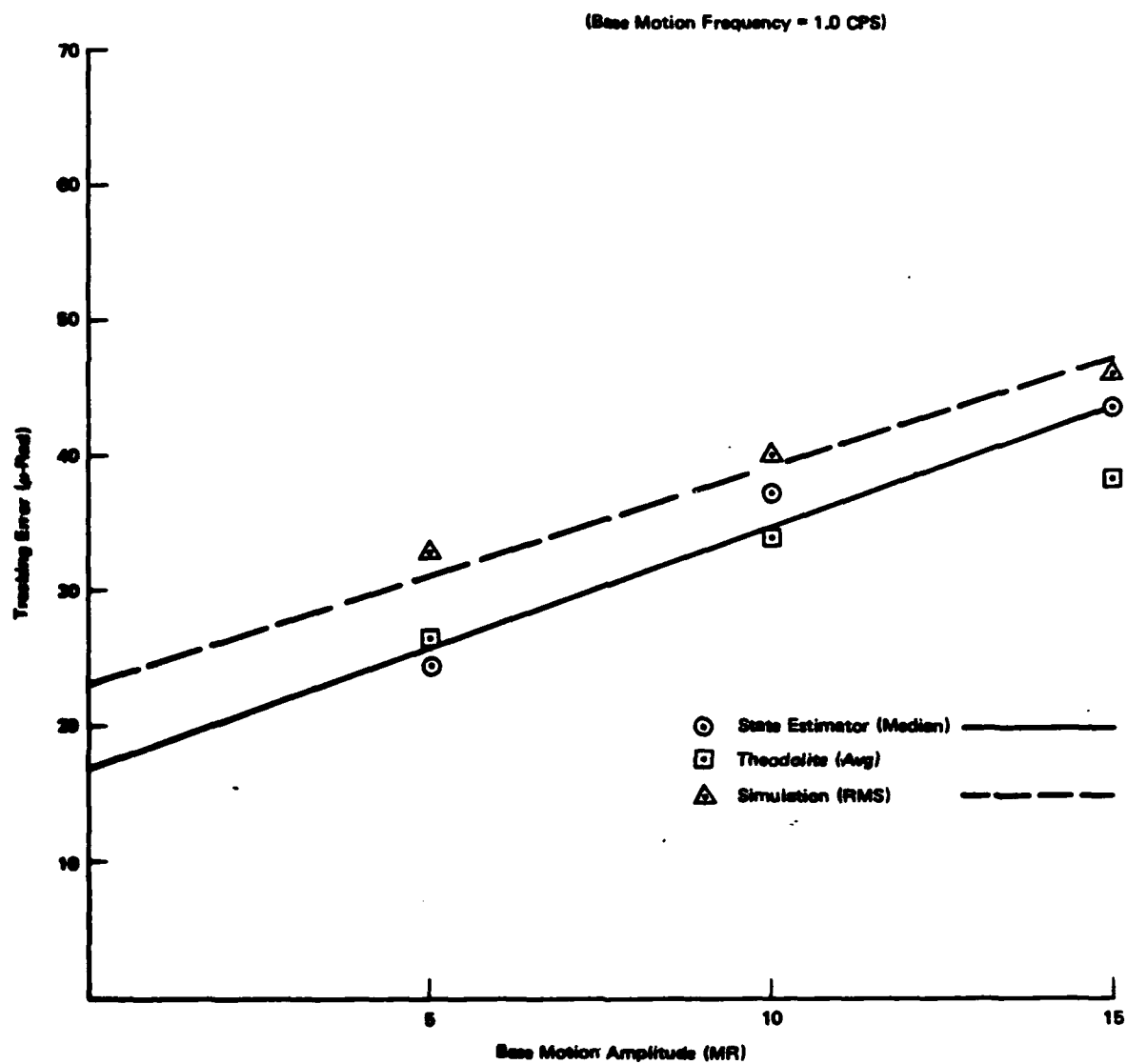


Figure S.1-11. Comparison of Alternate Performance Measures - Azimuth

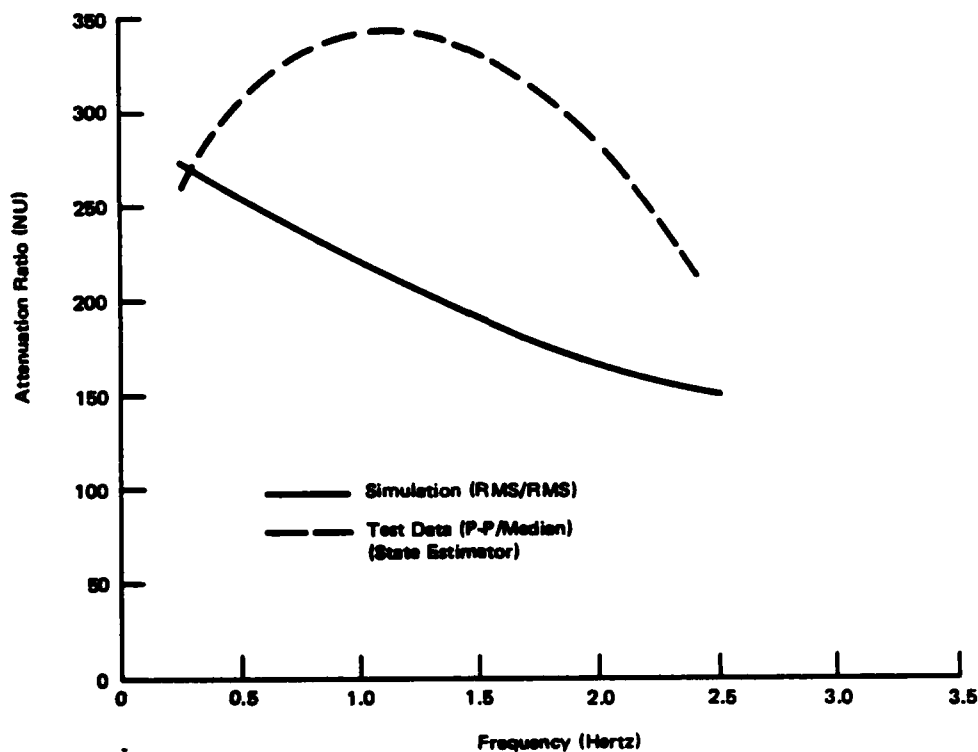


Figure 5.1-12. Base Motion Attenuation - Azimuth

The dynamic interaction of the DBA and the T/S unit is evident in Figures 5.1-13 through 5.1-16. The shape of tracking error response with the various frequencies indicates that there is some interaction. The differing response of the DBA tracker is also an indication of the same phenomenon. The bias in the state estimator data is due to mass unbalance. In the tactical system this error would be removed by integral compensation. Time and funding constraints did not permit this feature to be incorporated in the Phase II system.

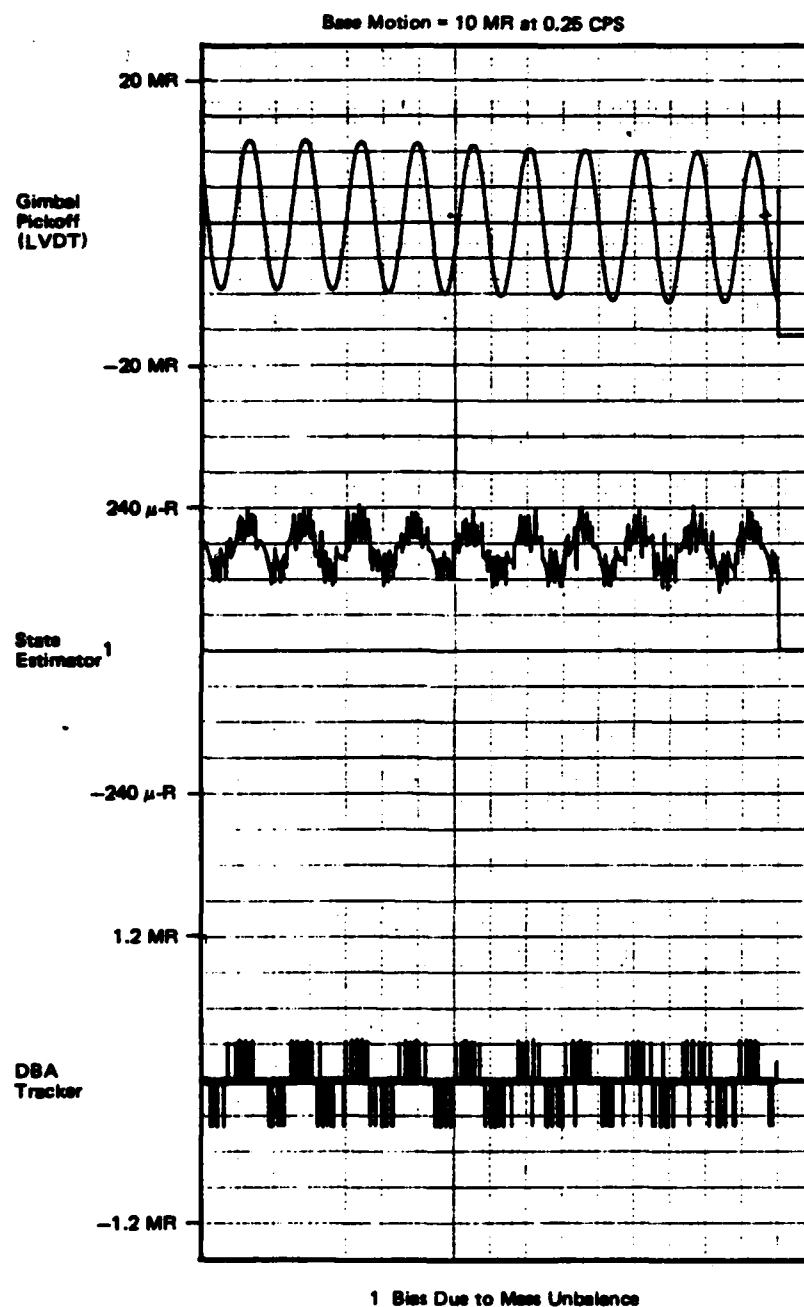


Figure 5.1-13. Test Data - Azimuth

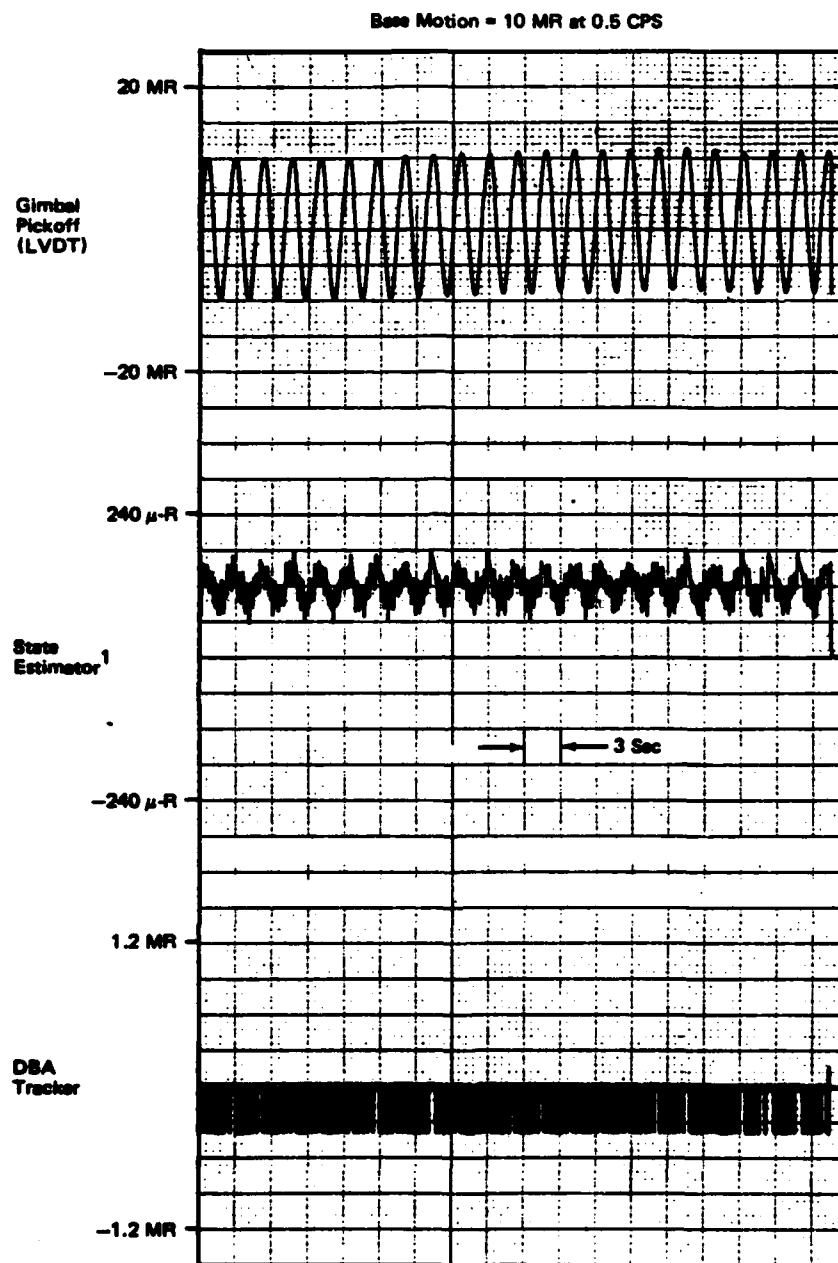
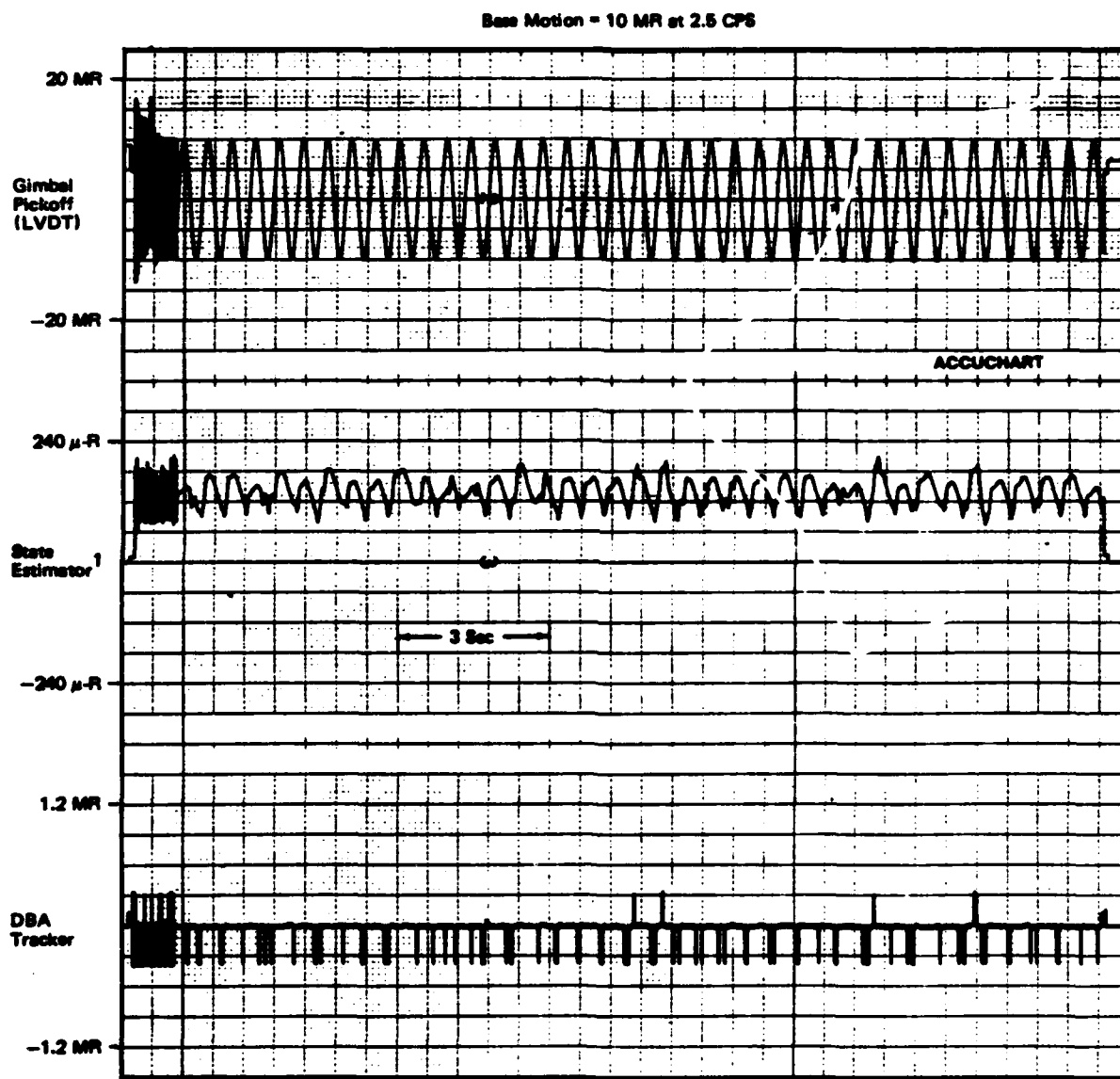
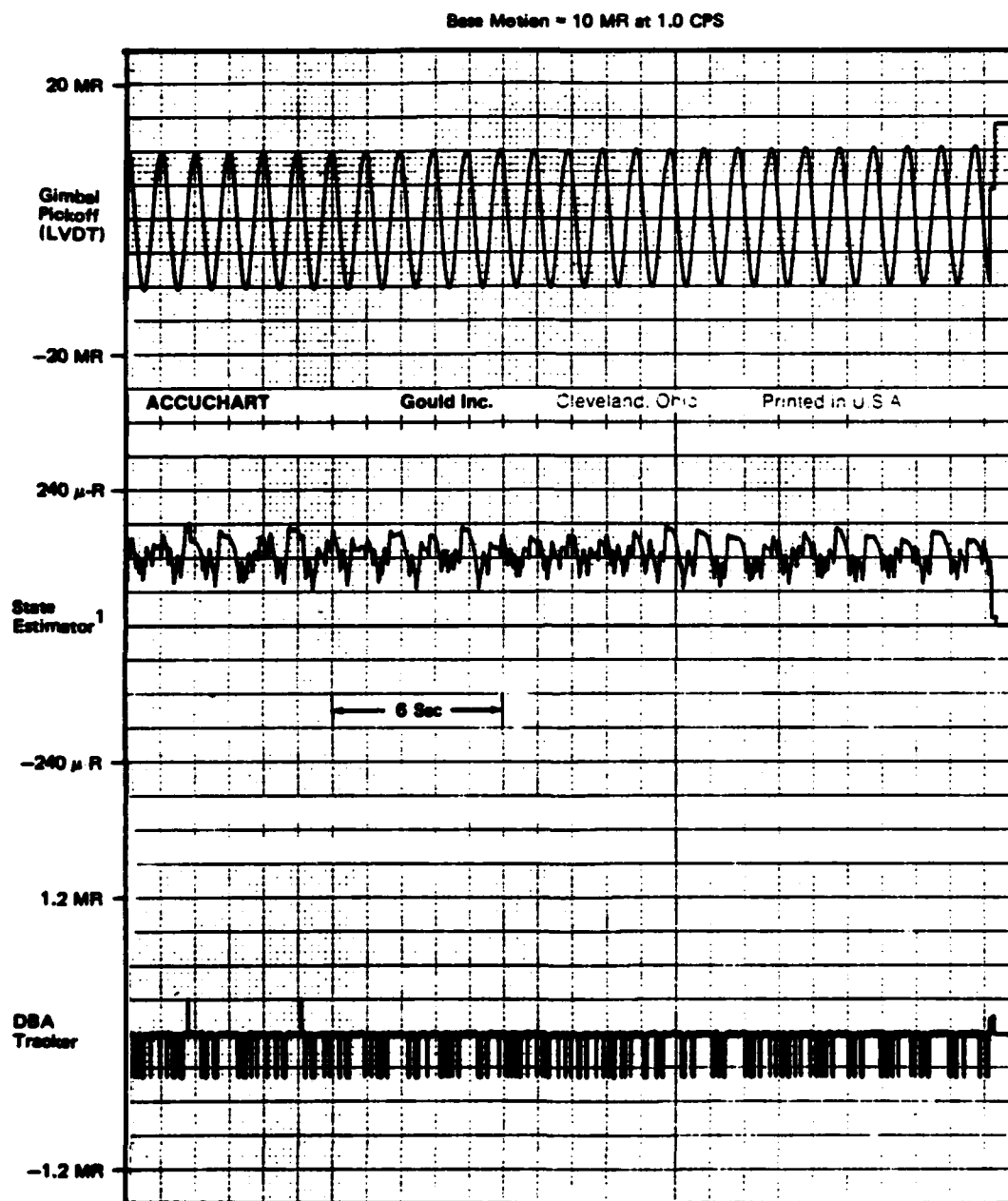


Figure 5.1-14. Test Data - Azimuth



1 Bias Is Due to Mass Unbalance

Figure 6.1-15. Test Data - Elevation Axis



1 Bias Is Due to Mass Unbalance

Figure 5.1-16. Test Data - Elevation Axis

The quantitative data shows some similarity between the simulation and test results as shown in Figures 5.1-17 through 5.1-20. It is also apparent that the low frequency test data indicates a higher error than the simulation. The opposite is true at the higher frequencies. The performance estimates are summarized in Figure 5.1-21 for the elevation axis.

The minimum performance estimates of both the elevation and azimuth axes indicate that the tracking and stabilization unit has a base motion attenuation capability of at least 150 to 1. This capability will be further enhanced by the type of tracker envisioned for an anti-tank weapon system such as IMAAWS. The use of a digital processor will also add to the system's capability by utilizing more sophisticated processing techniques than were possible with the analog system used in the Phase II device.

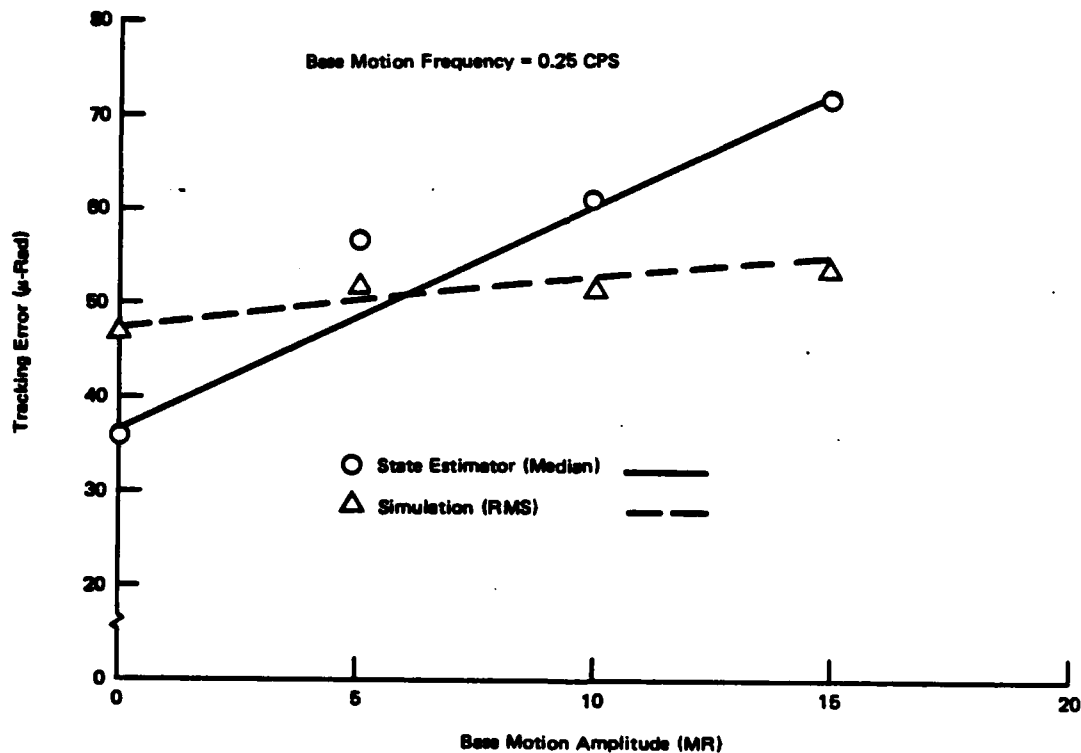


Figure 5.1-17. Comparison of Alternate Performance Measures — Elevation



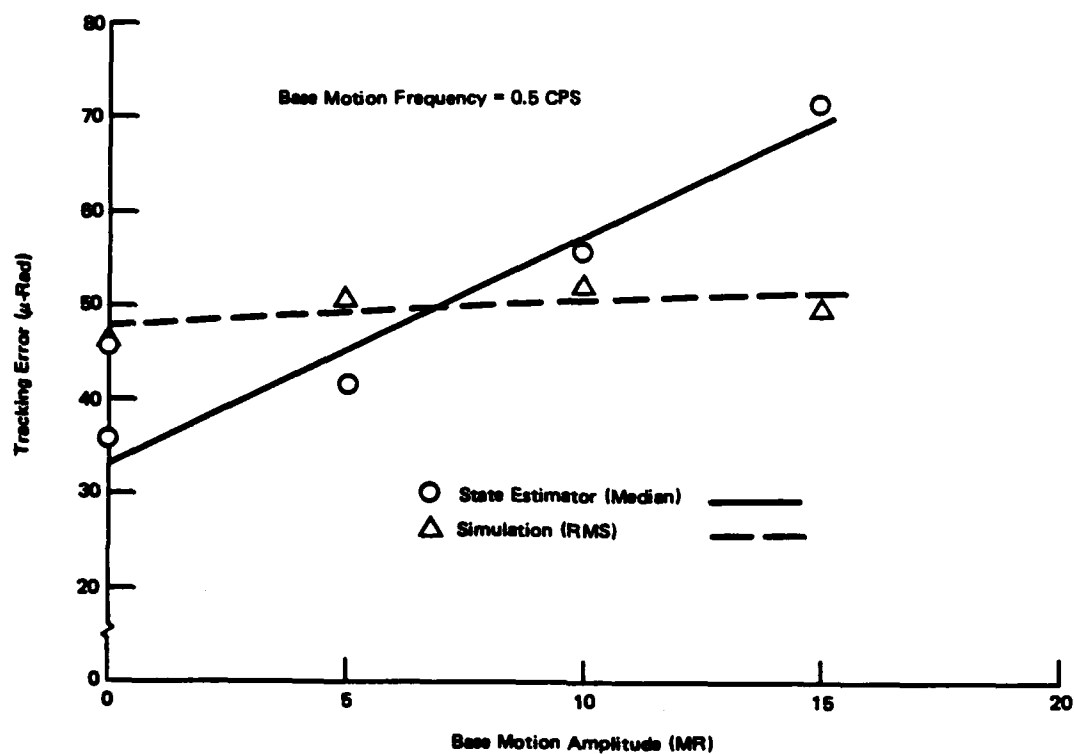


Figure 5.1-18. Comparison of Alternate Performance Measures – Elevation

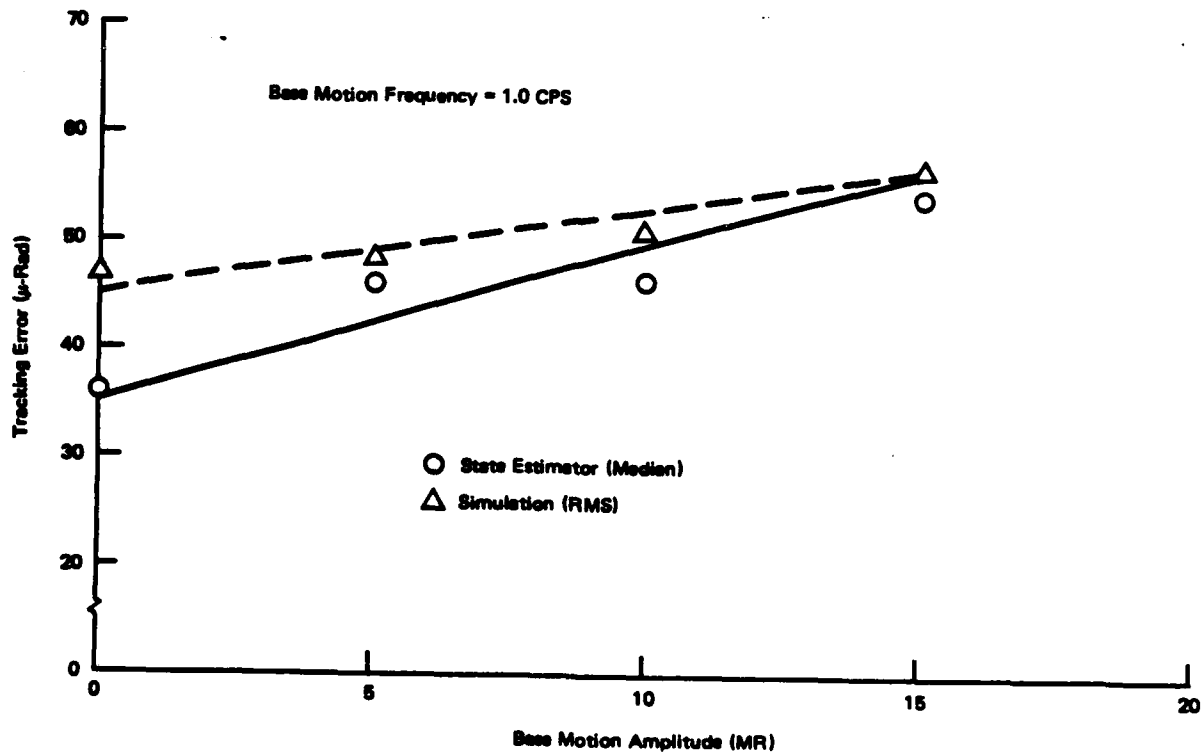


Figure 5.1-19. Comparison of Alternate Performance Measures – Elevation

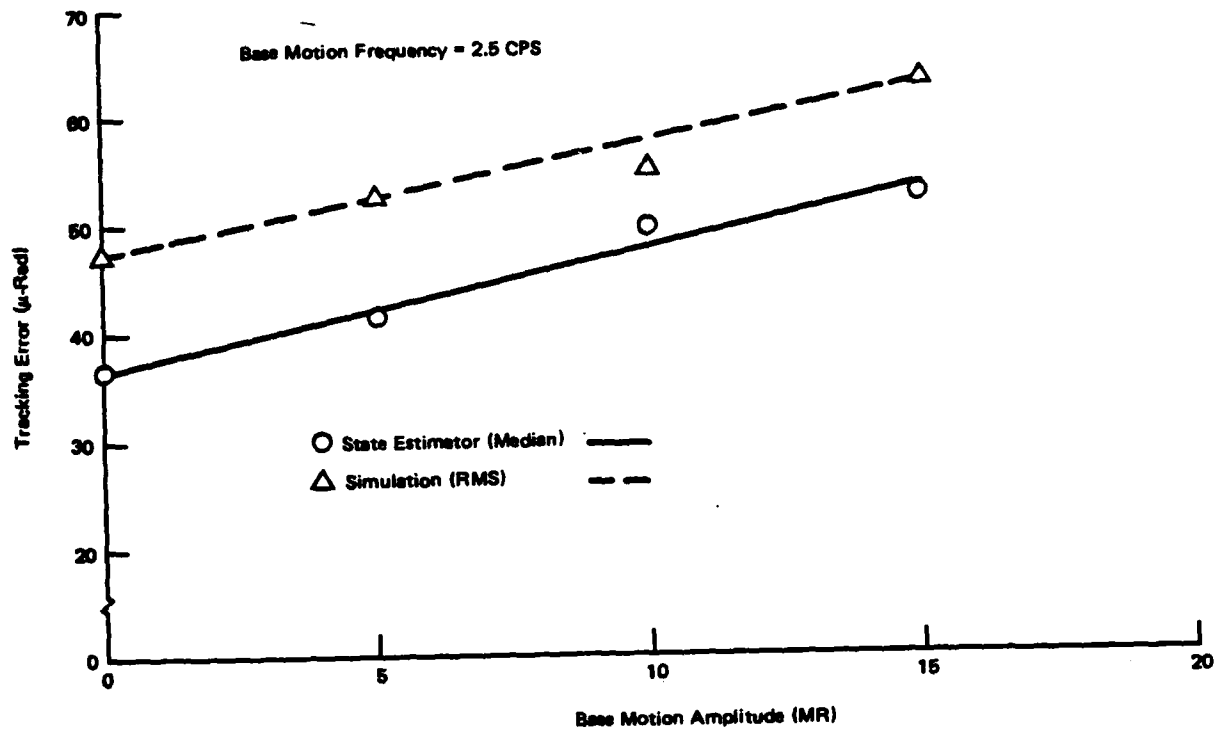


Figure 5.1-20. Comparison of Alternate Performance Measures – Elevation

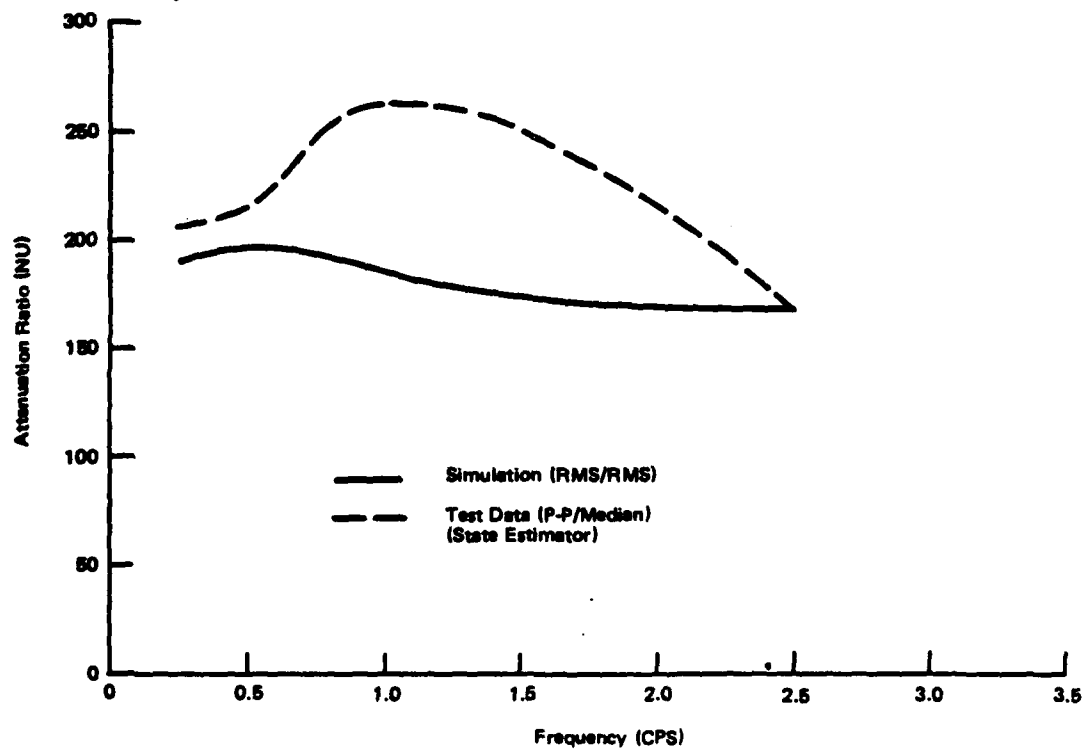


Figure 5.1-21. Base Motion Attenuation

## 5.2 Random Base Motion Tests

A literature search was made to determine gunner aiming capability with manportable weapon systems. A few reports were found which described gunner aiming capability in statistical terms that were quantitative, but no information was found describing the frequency content of the aiming error. The error amplitude varied with the amount of training and the type of support provided to the gunner. A summary of the RMS aiming error for various conditions is summarized in Table 5.2-1.

Frequency content of gunner aiming errors was available from aiming error tests made during the Dragon Phase IIC test program, and recent tests made at Fort Benning by MDC-Titusville. Two generic types of power spectral densities resulted from these tests. One type is illustrated in Figure 5.2-1. The histogram represents a statistical average of 10 tests performed at Fort Benning. The solid curve is the power spectral density (PSD) of the Aeroflex azimuth axis in response to white noise. A Hewlett-Packard model 3722A noise generator was used to reproduce this power spectrum. This noise generator is capable of producing a rectangular power spectrum to within 5% of the theoretical RMS value. This device was used to generate a 5-cycle per second rectangular power spectrum. The amplitude was adjusted so that the Aeroflex output RMS values were 5, 10, 15 and 20 milliradians. These three values more than cover the anticipated levels shown in Table 5.2-1. This generic type of PSD usually results when the target aimpoint is not well defined, and consequently the low frequency aimpoint wandering tends to predominate the power spectrum. This type of response may very well occur with a stabilized sight since the gunner's required task, keeping the gimbals away from the stops, does not have a sharply defined visual objective.

The second type of spectrum, shown in the histogram of Figure 5.2-2, occurs when the aimpoint is well defined. Painting crosshairs on a target, for example, will produce this type of response. In this case, the predominant response is shifted toward the higher frequencies and usually occurs around 2 hertz. The solid line in the figure represents the Aeroflex elevation response to white noise. Approximately twenty percent of the energy of the histogram is contained in a narrow frequency band near

Table 5.2-1. Gunner Aiming Error — Amplitude

Error Classification	RMS Error	Representation
Low	1 to 2 Milliradians	Trained Gunner with Support (Bipod, Etc)
Medium	3 to 4 Milliradians	Trained Gunner W/O Support or Untrained Gunner With Support
High	6 to 8 Milliradians	Untrained Gunners W/O Support Poor Gunners

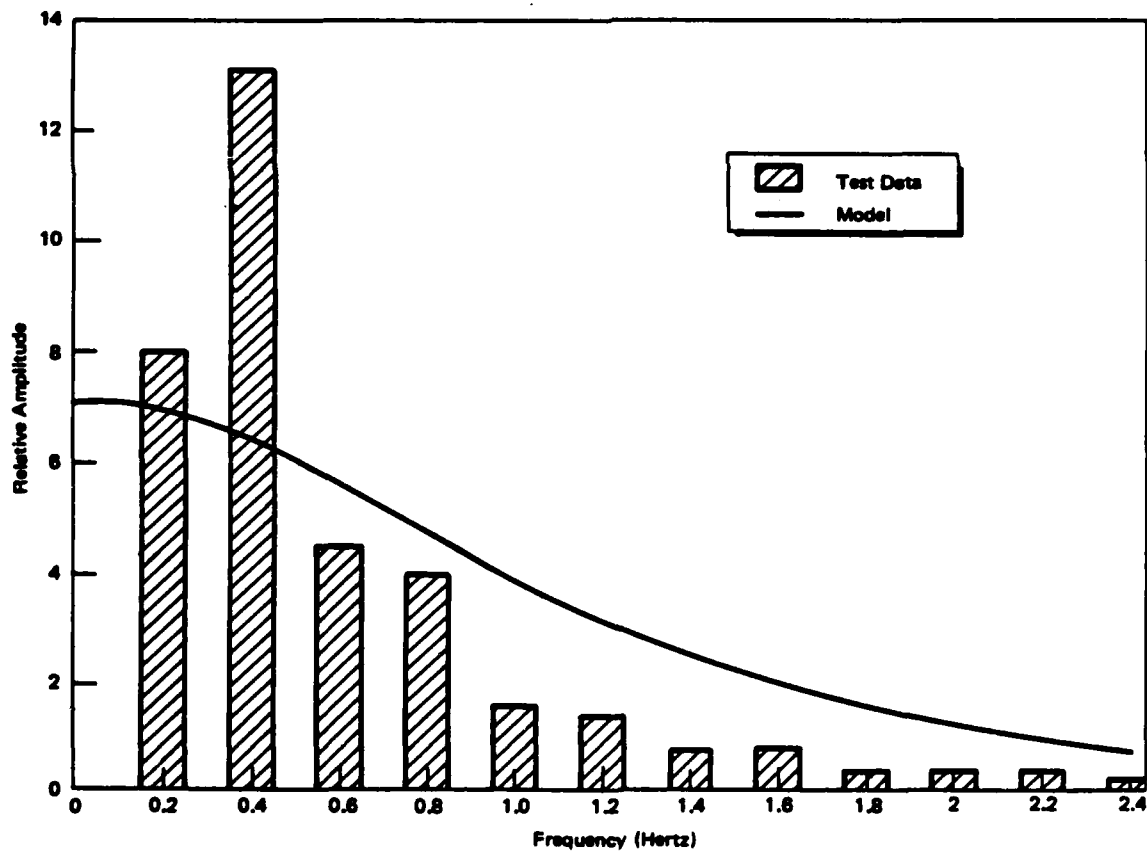


Figure 5.2-1. Fort Benning Gunner Test

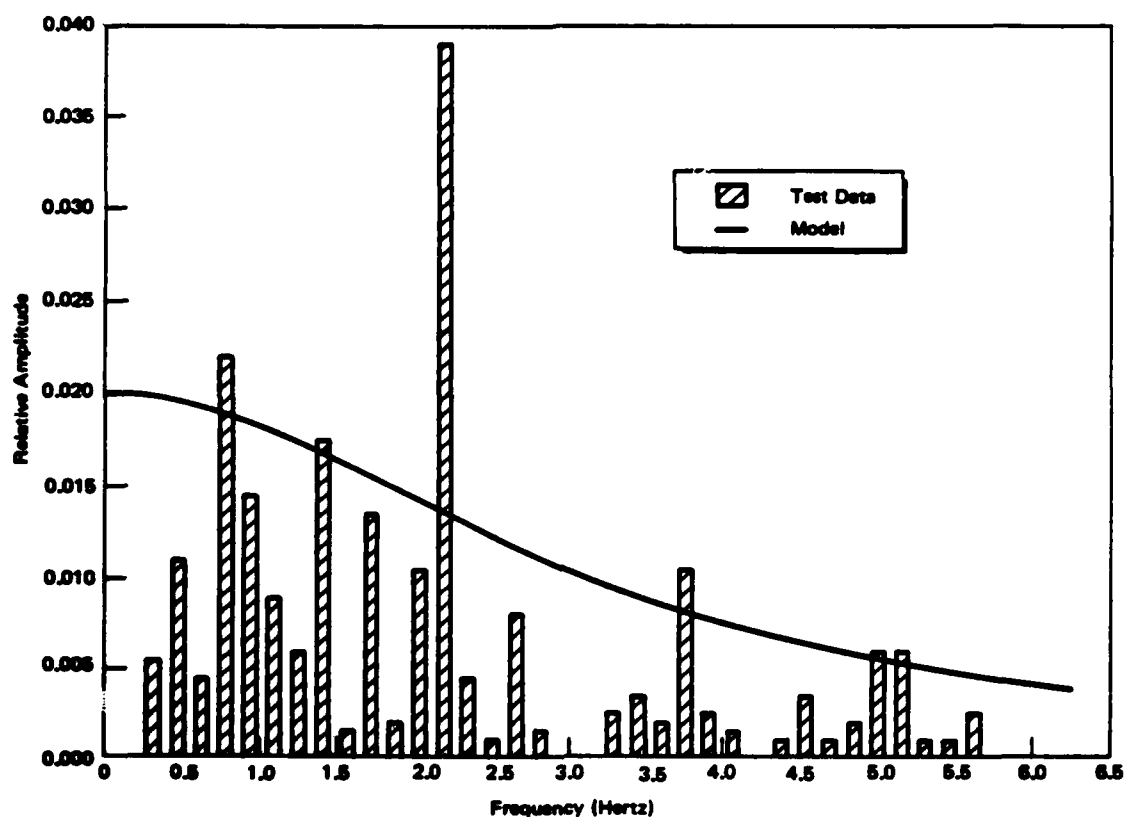


Figure 5.2-2. Phase II C Gunner Tests

2 hertz. To approximate this power spectrum, the noise generator was used to drive the elevation axis of the Aeroflex table. The amplitude was set so that the RMS output of the Aeroflex table was 80 percent of the total RMS value desired. The other 20 percent was added by superimposing a 2 hertz sinusoidal input of the proper magnitude so that the Aeroflex output RMS value was 20 percent of the desired total. Total output RMS values of 5, 10, and 15 milliradians were used in these tests. Because of a calibration error, the tests were actually run at 4.2, 8.4, and 12.6 milliradians.

The results of the random base motion tests are shown in Figure 5.2-3. These results are based on the state estimator output as discussed in the previous section. The automatic tracking system provides a line-of-sight stabilization error of approximately 40 microradians with the base motion representing a poor or untrained gunner. Allowing for a possible 30 percent error in the state estimator output, as discussed in the previous section,

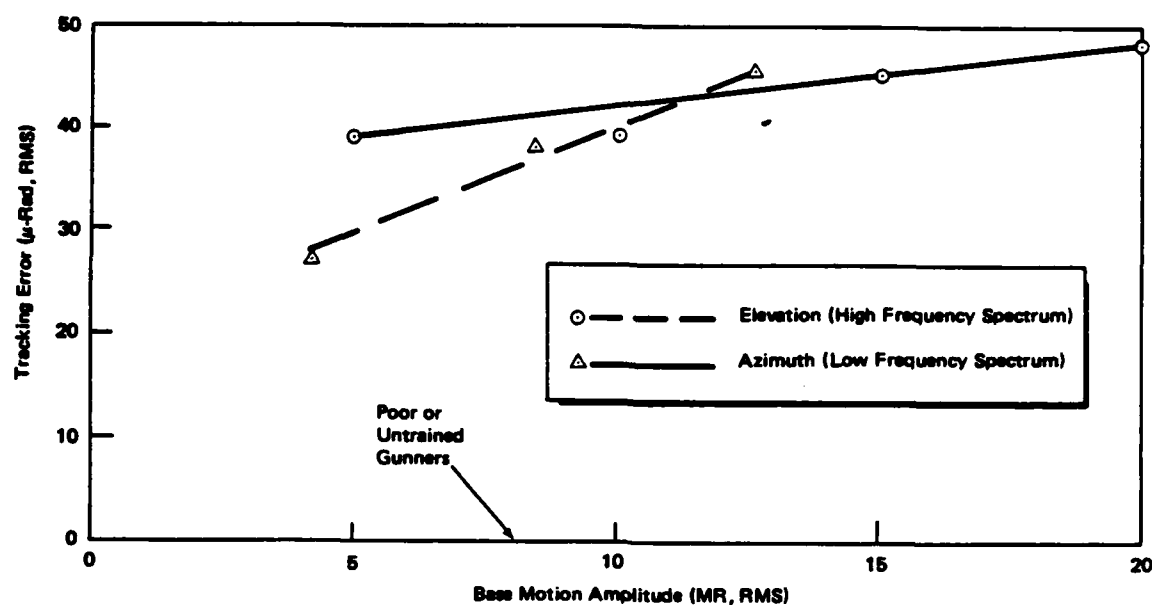


Figure 5.2-3. Test Results – Random Base Motion

the line-of-sight stabilization error would be less than 55 microradians which is within the range of accuracy desired for manportable antitank weapons.

### 5.3 Crossing Target Tracking Test

The target tracking test was performed by projecting a Helium Neon laser onto a galvanometer operated rotating mirror and reflecting it onto the wall as shown in Figure 5.0-2. The mirror was driven from a signal generator with a triangular wave so that the mirror would rotate at a constant angular velocity during each half cycle. The angular rate was adjusted so that it represented a 10 meter-per-second target at 100 meters range as seen from the T/S unit. Neither a theodolite nor the state estimator could be used to measure performance for this test. The theodolite could not be used because it does not measure error relative to a moving line-of-sight. The output of the state estimator that included the compensation term for moving targets (rate aiding) was not accessible with the present circuit design. Modifications of the design to provide this signal, although technically simple, was not possible to accomplish within the Phase II schedule.

The only measure of performance available was the output of the DBA tracker. The T/S unit was able to track the moving target to within the resolution of the DBA tracker which is  $\pm 120$  microradians in azimuth. The tracking performance was, therefore, equal to or better than 120 microradians.

## 6.0 Shoulder Mounted Tests

The shoulder mounted tests were conducted to test the handling quality of the stabilized sight in the soft cage mode and in particular to determine the degree of "stiffness" or responsiveness that provides the best compromise between the desire for scene stabilization and the ability of the system to follow the gunner's voluntary pointing movements. Both moving and still targets were used for these tests.

The launcher module described in Section 3.1 and shown in Figure 6.0-1 was used for the hand held shoulder mounted tests. The unit weighted 24.5 lbs. and was balanced about the shoulder support point. The tube was 48 inches long and had a moment of inertia of approximately 1 slug-ft<sup>2</sup>.

The "stiffness" of the soft cage mode can be adjusted by changing the gain, KG, in the state estimator shown in the block diagram of Figure 6.0-2. A higher gain results in more responsiveness and less scene stabilization. A lower gain results in less responsiveness and more stabilization. The gain was adjustable in ten discrete steps as shown in Table 6.0-1. Four of these gains, switch positions 1, 4, 7 and 9 were used in the test.



Figure 6.0-1. Shoulder Mounted Test Fixture

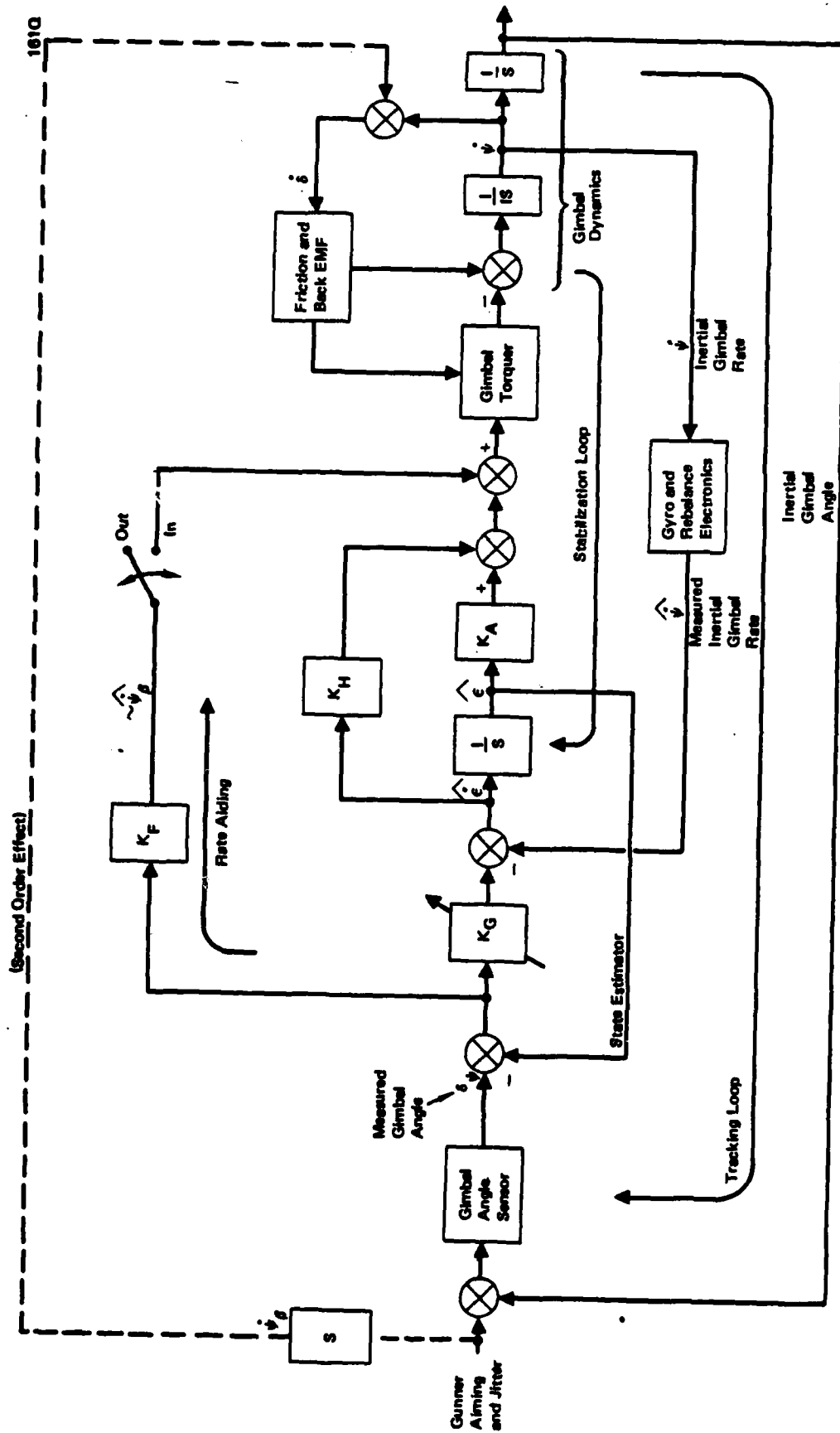


Figure 6.0-2. Soft Cage



Table 6.0-1. Variable Gains for the Soft Cage

Switch Position	Gain, $K_G$ ( $\text{Sec}^{-1}$ )	Time Constant (Sec)	Bandwidth (Hertz)
0	6.3	0.16	1.0
1	4.7	0.21	0.75
2	3.7	0.27	0.59
3	3.0	0.33	0.48
4	2.5	0.40	0.40
5	2.1	0.48	0.34
6	1.7	0.56	0.28
7	1.4	0.71	0.22
8	1.0	1.0	0.16
9	0.44	2.3	0.07

☐ Used in Shoulder Mounted Test

### 6.1 Test Description

The test geometry for the moving target tests is shown in Figure 6.0-3. The speed of traffic on this road (Bolsa Chica) varies from 45 to 60 miles per hour, so that the maximum angular rate at nadir varies from 8.4 to 11.2 degrees per second. Five subjects were used in the tests. Pertinent data for these subjects is summarized in Table 6.0-2. Each subject was asked to track targets of opportunity from the traffic light or beyond to nader or slightly beyond. The trees shown in the figure prevented tracking beyond this point. The subjects were instructed to track the right front wheel of each vehicle. Each subject tracked two cars at each of the four gain settings from the "stiffest" to the "softest". They were asked to state which gain felt better. The subjects were then asked to track a still target. The still target was a water tower that was 4.3 kilometers (2.7 miles) away. The tower subtended a total angle of 0.88 milliradians in azimuth. The rate aiding signal was removed for the still target tests. The moving target test was then repeated by reversing the gain sequence. Two cars were tracked with each gain starting with the softest and proceeding toward the stiffest gain.

The rate aiding signal was removed for the still target tests when it became evident that the error in this signal was a dominant factor with still targets. With the rate aiding signal in, it was difficult to see any difference in performance in the various gain settings. The error in

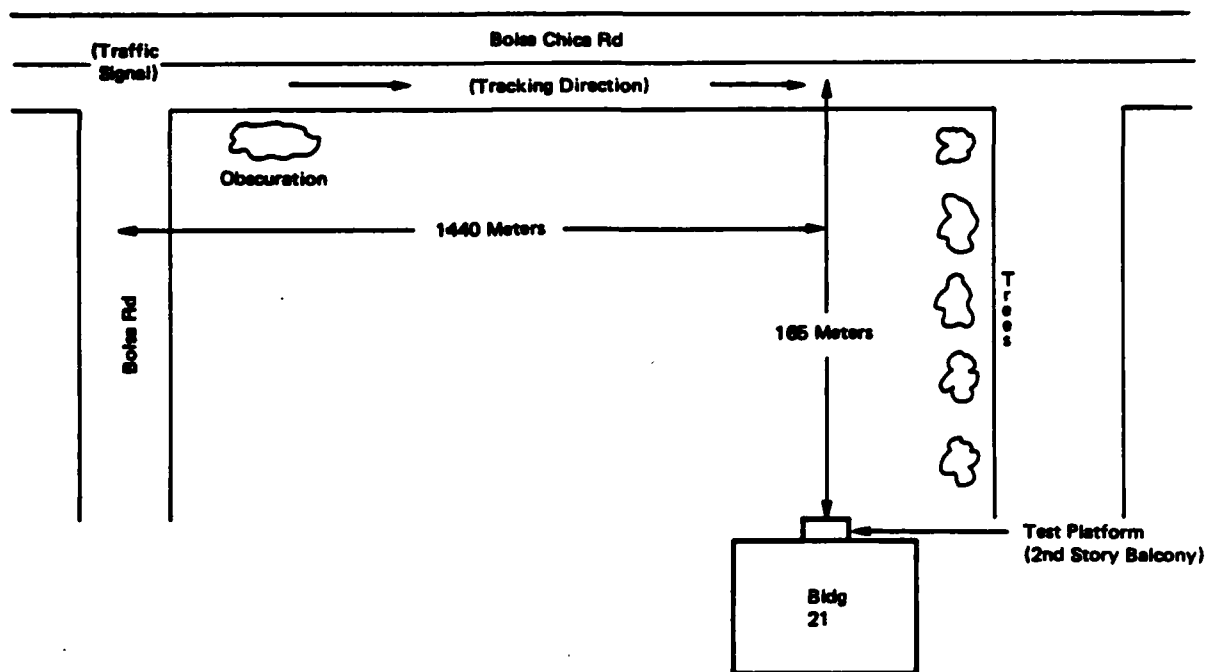


Figure 6.0-3. Shoulder Mounted Test Geometry

Table 6.0-2. Pertinent Gunner Data

Gunner	Height	Weight	Age	Comment
A	6'1"	165	46	Good Gunner
B	5'8"	155	30	Med Gunner
C	6'2"	190	25	Poor Gunner
D	5'8"	152	24	Med Gunner (Left Handed)
E	5'8"	155	43	Good Gunner

this signal at zero target rate seems to be due to a mismatch in the two sensors, gyro and gimbal pickoff, near null. It is these two signals that are differenced to obtain the rate aiding signal.

With the crossing targets, the rate aiding signal provided a definite improvement in performance and handing quality. Future designs will need to consider this problem. One solution might be to use a threshold for the rate aiding signal. Below a certain threshold, the signal would be out of the system and above the threshold, the signal would be included. Other non-linear compensations should also be considered.

## 6.2 Test Results

All subjects agreed that gain setting number 7 was the best gain for tracking moving targets. Some were more definite about this than others. The better gunners were able to be more definite in their selection than the poorer gunners. All gunners were more definite of their selection after the second set of tests, after they had become more familiar with the device. Gunner A, one of the best commented, "gain 7 is by far the best." Medium gunner B said, "no difficulty in tracking (with gain 7)". The poorest gunner could make a selection only after he made a direct comparison with gain setting 1 and 7. His comment: "This is pretty nice, doing better with this one".

All subjects had the same difficulty with gain setting 9 on the moving targets. They were able to track the targets well initially when the line-of-sight rate and acceleration were low. As they approached the nadir, the high angular acceleration caused the system to lag and eventually hit the gimbal stops. In some cases, the subjects mentioned as they began tracking, that this was the best setting but revised their opinion after they completed the full tracking sweep.

All subjects also agreed that gain setting 9 was best for the still target. With this setting all subjects were able to keep the cross hair within the profile of the target which subtended a total angle of 0.88 milliradians. Their tracking performance was therefore  $\pm 0.44$  milliradians. With the higher gain settings, tracking errors of  $\pm 3$  milliradians were not unusual.

Two of the better gunners were later asked to make a comparison of the performance with the gimbals hard caged and the soft cage with gain number 7. There was no mechanical caging device so a piece of foam was placed between the gimbal and the base of the sight to hold it in place. Oddly enough, neither subject could decide which was better. The responsiveness of the hard cage had a better feel to it when it was needed, during the high acceleration portion at nadir or after the gunner lagged behind the target. He could swiftly compensate by moving the aimpoint forward and the unit responded as he expected. The visual and physiological feel of the unit were in synch. It was not unusual for the gunners to lag behind the target after they had been tracking it well for a distance. This was caused by either a relaxing of concentration or a

shifting of one part of his body (feet or shoulders) to make the large angular sweep necessary to track the target throughout the test range. The initial setup of feet position could easily affect his performance. The body orientation was an important factor just as it is in skeet shooting where high angular maneuverability without changing foot position is necessary.

It appears as though the optimum stiffness of the caging system is a function of target acceleration at least, and may be a function of velocity. The inability of the two best gunners to choose between soft and hard cage is probably due to the fact that at the lower acceleration and velocity of the initial tracking test, the soft cage has a better feel while later during high angular acceleration and rate, the quicker responsiveness has a better feel. This happened earlier with gain setting number 9, initially the subject said that this was the best but was unable to avoid hitting the stops later as the acceleration increased.

### 6.3 Summary

A soft cage mode is a definite aid in tracking and identifying still targets. Scene stabilization and tracking accuracy improvements of an order of magnitude are achievable with the soft cage implementation. This is also probably true with slow line of sight rate targets that occur either because of long distance or slow moving targets.

Tracking improvement against close in, high speed targets was not as dramatic although all gunners showed a definite preference for a particular tracking bandwidth. It is evident from the test that target geometries that result in a high angular acceleration require additional compensation to achieve a significant improvement in tracking performance. Non-linear or adaptive techniques should be investigated. High order aiding, such as acceleration aiding should also be investigated. The gain selected for the non-moving target was 0.44/seconds. This corresponds to a bandwidth of 0.07 hertz and a time constant of 2.27 seconds. This was the lowest gain mechanized so a lower gain may be optimum. However, the performance improvement from the next higher gain (7) to this one was not as noticeable as the change in performance from gain 4 to gain 7. There appears to be a diminishing return for lower gains and, therefore, a lower setting is probably unwarranted.

The gain selected for moving targets was 1.4/seconds corresponding to a time constant of 0.7 seconds and a bandwidth of 0.221 hertz. Gain number 8 was not used in this test. It has a time constant of approximately 1.0 which is the time constant used by Stinger alternate (Ref 4.). The gains selected for the non-moving and moving targets, therefore, bracket the Stinger alternate gain which implies that similar results were obtained in that program.

## 7.0 Results and Conclusions

Phase II testing has demonstrated the ability of the Tracking and Stabilization unit to attenuate gunner motion by over two orders of magnitude in the auto-track mode. This translates into a line-of-sight stability of better than 55 micro-radians with a poor or untrained gunner, which is within the level of accuracy required for a man portable anti-tank weapon system. The system was also able to track a 0.1 radian per second crossing target to within the resolution of the DBA tracker ( $120\mu\text{-rad}$ ).

Scene stabilization can be provided in the soft cage mode for target acquisition and recognition. The soft cage mode provides maximum stabilization at low line-of-sight acceleration and velocities. This is precisely the condition that occurs at the long ranges envisioned for man portable weapons. The soft cage mode therefore provides maximum gunner jitter attenuation when it is most needed for target recognition. Gunner jitter can be reduced by an order of magnitude in this mode.

For close in-moving targets, some manual tracking relief can be provided but further work is necessary to provide the varying "stiffness" required to cope with the high line-of-sight acceleration that occurs with high speed crossing targets. Non-linear or adaptive approaches are possible candidates.

## Section IV RECOMMENDATIONS

The results of the tradeoff study indicate a clear superiority for a configuration which provides for the 2-axis gimbal mounting of a miniaturized FLIR and laser projector, with a 2-axis gyro mounted on the stabilized platform. This configuration of elements can readily form the basis for a lightweight, rugged, accurate pointer-tracker, of very low technical risk. For maximum effectiveness on the battlefield, it should be developed into a design having the following operational features:

1. A sensor which provides both day and night imaging
2. Stabilized scene display for all aiming and tracking modes
3. Three pointing-tracking modes:
  - a) acquisition mode, where the aiming reticle follows manually directed guidance unit pointing.
  - b) auto-track mode, after missile launch command, where the aiming reticle and laser beam follow an IR image process defined target aimpoint, and a steering reticle provided in the display to aid gross guidance unit pointing.
  - c) manual track mode, after missile launch command, where the aiming reticle and laser beam follow manually directed guidance unit pointing

The addition of the manual tracking mode (with stabilized scene display) provides a capability against bunkers and other poor thermal image targets, with almost no increase in weight and very little increase in mechanical complexity. A default hierarchy of modes might be provided such that low gunner training and proficiency levels do not degrade the basic system anti-tank capabilities.

Some provision should be made for a guidance (beam) lead feature to compensate for hangoff errors when the target line-of-sight is rotating. This should not be accomplished by independent steering of the projected beam, by steering mirror or separate gimbal, if some other method proves feasible.

The results of the testing phase indicate that the configuration recommended in the tradeoff study is a practical, workable approach, and would present no significant technical risks in terms of the functional concept. The ability to readily package the electronics into a small, lightweight, rugged guidance unit was not addressed by this study, and therefore the technical risks in that area will not be commented upon.

It is recommended that additional testing and analysis be carried out in the area of the acquisition mode design and optimization. It became apparent during the testing that the construction of the control electronics in this experiment, as well as cost and schedule constraints, did not allow for full exploration of the expected potential for a stabilization aided manual aiming mode. A microprocessor should be added to the system to provide the flexibility, including non-linear control policies, to explore a variety of target/scene situations.

Some other questions which should be explored are:

1. What are the effects of platform mass unbalances, and, if the effects are significant, how should they be dealt with?
2. How can weight and electrical power usage be driven to a minimum? This involves the evaluation of minimum sizes of components such as torquers, and the possibility of eliminating the gyro.



APPENDIX  
Bibliography

1. Atmospheric Effect on Image Quality Appendix II, Advanced Target Tracking Techniques Study, Air Force Weapons Laboratory AFWL-TR-72-87  
13 Sept 1972 (Secret Report)
2. Concept Development Report - Advanced Heavy Anti-Tank Missile System, Vol. III Technical Tradeoffs Considerations, Final Report MDC G7393,  
30 May 1978 (Confidential Report)
3. Stinger Alternate Advanced Development Program ITR-1  
Philco-Ford Corp DI-S-1800-1  
Defense Documentation CTR AD-530 249L  
Jun 1974
4. Stinger Alternate Advanced Development Program  
Philco-Ford Corp DI-S-1800-2  
Defense Documentation for AD-C000 216  
Dec 1974
5. Imaging IR Guidance Unit Development and Captive Flight Test Program  
Final Report  
Air Force Avionics Lab, AFAL-TR-75-137  
Defense Documentation Ctr, AD-C005 628L  
Hughes Aircraft Co., MSG-65108R  
Mar 1976

6. Crispino, N.F./Reaves, C./Robbins, A.G.  
Night Gimbal Pointing and Stabilization (U) Final Report  
Air Force Avionics Lab, AFAL-TR-75-131  
Defense Documentation Ctr., AD-C005 803  
General Electric Co., ACS-10954  
Mar 1976
7. Schroeder, K.F.  
Parametric Analysis of Stereometric Tracker for Use in Tactical Aircraft  
Air Force Inst. of Tech., AFIT/GEP/PH/78D-11  
Defense Documentation Ctr.  
Oct 1978
8. Stinger Alternate Advanced Development Program ITR-3  
Philco-Ford Corp DI-S-1800-3  
Defense Documentation CTR AD-C002 263  
Jun 1975
9. Sonalkar, R.V./Dygert, R.L./Sanyal, P.K.  
Real Time Adaptive Tracking System for the Coelostat Optical Tracking Mount. Final Report  
Rome Air Dev Ctr, RADC-TR-77-67  
Defense Documentation CTR, AD-A038 134  
Pattern Analysis and Recognition Corp, PAR-76-32
10. Santiago, J.M., Jr  
Fundamental Limitation of Optical Trackers, Refs  
Air Force Inst of Tech, AFIT/GE0/EE/78-4  
Defense Documentation Ctr, AD-A064 737  
Dec 1978
11. Dougherty, L.S.  
New Techniques for Tracking Sequences of Digitized Images  
Air Force Inst of Tech, AFIT/DS/EE/78-4  
Defense Documentation Ctr, AD-A066 194  
Nov 1978

12. Dougherty, L.S.  
New Techniques for Tracking Sequences of Digitized Images, Final Report  
Air Force Avionics Lab, AFAL-TR-79-1015  
Defense Documentation Ctr, AD-A069 996  
Feb 1979
13. Munteanu, C.  
Digital Area Correlation Tracking by Sequential Similarity Detection  
Canada, Defense Res Estab, DREV-R-4097/77  
Defense Documentation Ctr  
Nov 1977
14. Flachs, G.M./Perez, P.I./Rogers, R.B./Srymanski, J.M./Taylor, J.M.  
Real-Time Video Tracking Concepts, Final Report  
Army Res Office, ARO-13857.4-EL  
Defense Documentation Ctr, AD-A071 792  
New Mexico State Univ, NMSU-TR-79-1  
Jun 1979
15. Peralta, E.J./Kay, R.E./Oogan, J.H./Fisher, F.F.  
Advanced Sensor Concepts  
Aeronutronic Ford Corp, U-6333  
Defense Documentation Ctr, AD-B019 836L  
Jun 1977
16. Feuchter, W.C./Lockwood, L.  
Electro-Optical (E/O) Dir Tor Tracker, Final Report  
Air Force Avionics Lab, AFAL-TR-77-137  
Defense Documentation Ctr, AD-B023 880L  
Bendix Corp., BASD-TM-6569  
Aug. 1977
17. Anti-Tank Weapon Systems  
Battelle Columbus Labs A-3986  
Defense Documentation Ctr. AD-527601L  
June 1973

18. Mast Mounted Sight Subsystem, Vol. 1, Book 2, Technical Proposal  
MDC G9307P  
Dec 1980
19. Aguilera, R.A./Call, C.A./Rode J.P./Vitols, V.A.  
Advanced Infrared Imaging Seeker Development Program, Final Report  
Rockwell Intl Corp, 078-87/034A  
Defense Tech Info Ctr, AD-C021 140L  
Feb 1980
20. Bohan, D.J.  
Tow Thermal Night Sight Evaluation (U), Final Report  
Army Electronics CMD, ECOM-7041  
Defense Documentation Ctr, AD-C005 839L  
Apr 1975
21. Johnson, F.J./Cottle, R./Gibbons, J.C./Ginther, K./Hickman, H.  
Infrared Imaging Seeker Development (U), Final Report  
Texas Instruments Inc., TI-C1-135449-F  
Defense Documentation Ctr, AD-C005 715L  
Jan 1976
22. Bockwoldt, W.H./Latt, H.  
Infrared Imaging Seeker (U), Final Report  
Hughes Aircraft Co, MSG-65214  
Defense Documentation Ctr, AD-C006 266L  
Hughes Aircraft Co, HAC-REF-D3652  
May 1976
23. Aguilera, R.A./Schumann, D.G./Rode, J. P./Vitols, V.A.  
Advanced Infrared Imaging Seeker (AI2S) Development Program Vol 1,  
Unpaged Illus  
Rockwell Intl Corp, C78-87.1/034A  
Defense Documentation Ctr, AD-C013 181  
Jan 1978

24. Navy Pointer/Tracker (NPT) Mount Servo Subsystem Critical Design Review. 011 1  
Hughes Aircraft Co  
Naval Ordnance Lab White Oak  
N60921  
May 1974
25. Wick, D.O./Ross, C.L./Jackson, D.B.  
Fire-and-Forget Missile Seeker Evaluation, Vol 1 (U), Final Report  
Honeywell Inc, 76SRC43  
Defense Documentation Ctr, AD-C008 222L  
DAAH01-76-C-0852-FR
26. Gilbert, A.L./Giles, M.K.  
Concepts in Real-Time Video Tracking, Final Report, OP 111us  
White Sands Missile Range, Stews-ID-78-1  
Defense Documentation Ctr, AD-A054 475  
May 1978
27. Rogers, J./Taylor, W.E.  
Solid-State Imaging Devices Parameter Study for Uses in Electro-Optic Tracking Systems, Final Report  
Air Force Office of Scientific Research, AFOSR-TR-78-0064  
Defense Documentation CTR, AD-A049 956  
Mississippi State Univ, MSSU-EIRS-78/2  
Sep 1977
28. Advanced Focal Plane Imaging Seeker (U)  
Texas Instruments Inc, TI-C1-8902-0-F  
Defense Documentation Ctr, AD-C015 75  
Oct 1978

29. Minor, L.G.  
Application of a Microprogrammed, Bit Slice Microprocessor to the  
Real Time Imaging Tracking Problem  
Army Missile Res and Deve, DRDMI-T-78-53  
Defense Documentation Ctr, AD-A071 638  
Sept 1978
30. Flight Demonstration Program for Infantry Manportable Anti Armor  
Assault Weapon System (IMAAWS), Vol. II - Technical  
MDC 68512P  
May 1980
31. Riedl, J. L., MDAC  
CCD Sensor Array and Microprocessor Application to Military Missile  
Tracking SPIE Vol. 95 Modern Utilization of Infrared Technology II  
1976
32. Honeywell Miniature FLIR Description Marketing Document  
01533, 1978
33. Forward Acquisition System (FAS) Final Report (U)  
Contract #DASG60-79-C-0029  
MDC G8141 Oct 1979 (Secret Report)
34. Pinson L.J., Auburn University  
"Atmospheric Effects on Imaging Seekers"  
U.S. Army Missile Research and Development Command  
Tech Report T-CR-79-2  
July 1978
35. Gagliardi and M. Sheikh  
Pointing Error Statistics in Optical Beam Tracking  
Department of Electrical Engineering  
University of Southern California  
Los Angeles, California

36. Mackin, R. J.  
Beamrider Guidance Technique Investigation - Final Report  
McDonnell Douglas Astronautics Co., MDC E1315  
Jul 1975
37. Tutt, G. E.  
Phase II Test Plan, Target Track and Stabilization for Man Portable  
Direct Fire Missiles  
McDonnell Douglas Astronautics Co., MDC G9296  
Nov 1980
38. "Tank Gunners' Aiming Performance Against Clear Versus Indistinct  
Targets"  
Thomas A. Garry  
Human Engineering Laboratory, July 1974
39. "Gunner Aiming Performance as a Function of Target Tank Shape, Size  
and Selection of Firing Positions"  
Thomas A. Garry  
U. S. Army Human Engineering Laboratory  
July 1977
40. "Gunner Aiming Errors with the MAC and DC Medium Antitank Weapon System"  
Robert R. Gschwind  
Human Engineering Laboratories  
August 1966
41. "Field Investigation of Gunner Aiming Error as a Function of Launcher  
Weight"  
Gerald Chaikin, et al  
U. S. Army Missile Command  
Redstone Arsenal  
Feb 1972

42. "Target Tracking Evaluation of the Stinger Alternate Stabilized Sight"

R. R. Mitchell

U. S. Army Missile Research and Development Command

5 Oct 1977



**END**

**FILMED**

**1-84**

**DTIC**